St. Petersburg University

A. K. Vlasnikov

NUCLEAR PHYSICS

Saint - Petersburg

2021

ABSTRACT

The undergraduate textbook covers the basics of nuclear and particle physics, including nuclear structure, nuclear forces, nuclear radiation, mechanisms of nuclear reactions, origin of elements, quark model and Higgs mechanism, It breaks down major present applications of nuclear physics: nuclear energy and nuclear medicine. The textbook is useful as introduction to nuclear physics for students who intend to pursue in the domain.

CONTENTS

INTRODUCTION

This textbook is devoted to nuclear physics, a branch of physics that studies the smallest particles of matter currently known: atomic nuclei and elementary particles. Science does not exist separately from human society and is an integral part of universal human culture. Science is inseparable from both the era and its creators - scientists. The emergence of nuclear physics became possible not only due to the development of technology and industry, but also due to the spiritual state of society and culture, which led to a radical change in the scientific picture of the world (scientific paradigm).

What are the reasons for the emergence of nuclear physics as a branch of knowledge precisely at the turn of the 19th and 20th centuries? To do this, we must first dwell on the state of culture in the most developed countries on the eve of the 20th century.

In the public mind, this era was presented as a triumph of the ideas of the Enlightenment[1], the golden age of progress. It seemed that human possibilities are endless, that society can be organized on a rational basis, that progress will solve all social problems, and education will create a perfect person. Wars should become a thing of the past, because the created weapons of destruction will cause unacceptable losses from the aggressor. The future looked predictable, bright and cloudless. And there was every reason for such a point of view. Airships took off, the first planes promised to become like birds. The oceans were plied by giant steamers that connected all continents and for the first time made the most distant parts of the planet accessible for everybody. On land, a dense network of railways opened access to the centers of civilization for the inhabitants of the most remote parts of Europe and North America. Methods of transmission for a long distance and registration of electromagnetic signals, developed at the turn of the 19th and 20th centuries in different countries of the world (including Russia, A.S. Popov, 1895), opened way for fast communication, which laid the foundations of modern information society. The conveyors at the giant factories carried an unprecedented abundance of available goods. Moreover, the conveyor produced great amount of cars, a fast, affordable and comfortable means of individual mobility. Cinema entered life, promising a new way of spending leisure time. Those dream about "bread and circuses", the ideal of Ancient Rome, became really accessible.

The physical picture of the world seemed to be mostly complete. Classical mechanics and the theory of gravitation (I. Newton), the theory of electromagnetism (J. Maxwell), statistical physics and thermodynamics (W. Kelvin, L. Boltzmann, J. Gibbs, J. Maxwell) explained practically all experiments.

[1] The Enlightenment - a philosophical trend that originated in Europe in the 17th century (René Descartes, France) and reached its peak in the 18th century. (the top is an encyclopedia published under the editorship of French philosophers Denis Diderot and Jean d'Alembert, among the authors of which were Francois Voltaire, Jean-Jacques Rousseau, etc.). The ideology of the Enlightenment is based on belief in the power of human reason and free thinking.

But along with the seemingly completely victorious ideas of the Enlightenment, in the culture of the turn of the 19th and 20th centuries, a directly opposite ideas are destroying a clear classical picture of the world. These ideas most clearly manifested themselves in the philosophy of irrationalism (F. Nietzsche, Germany, 1844-1900), which denied the very possibility of scientific understanding of the world in its entirety. Psychoanalysis has become popular - a branch of psychology that believes that human behavior is irrational and controlled by the unconscious (Z. Freud, Austria, 1856-1939). In the literature begins to spread absurdism, a prominent representative of which was the English writer and professor of mathematics at the University of Oxford L. Carroll (1832-1898). His books Alice in Wonderland (1864) and Alice Through the Looking Glass (1871) turned the incredible into the possible, and thus, from childhood, prepared the mind for revolutionary changes in ideas about the world around us. In the visual arts, as a reaction to the emergence of photography, avant-garde painting began to play an increasing role, decisively breaking with the centuries-old traditions of object painting, striving to reproduce the surrounding world as accurately as possible. Thus, the public consciousness was more and more ripe for the onset of revolutionary changes.

Was science ready for these changes? The patriarch of European physics, William Thomson, Baron Kelvin, in his famous speech "Clouds of the 19th century over the dynamic theory of heat and light", presented at the Royal Institution of Great Britain in 1900, summed up the development of physics and outlined problems that still remained unresolved by the beginning of the 20th century. Among those mentioned were two that led to radical changes in physics in the 20th century. One of them is the problem of the so-called elastic luminiferous ether. But if the ether has elasticity, then how can the Earth move through it? Already five years later, A. Einstein (1879–1955) answered this question by developing the Special Theory of Relativity, which did not need ether. The second problem was associated with the so-called "ultraviolet catastrophe" in the theory of thermal radiation from a heated black body. Such a body emits electromagnetic waves in the frequency range from 0 to ∞. According to the theory of radiation developed by J. Maxwell and L. Boltzmann (1844-1906), when the radiation frequency tends to infinity, the radiation energy also tends to ∞, but this effect was not observed experimentally. This problem was solved by Max Planck in the same year 1900 thanks to the hypothesis that energy is emitted by fractional portions proportional to the radiation frequency, called quanta. Maxwell and L. Boltzmann (1844-1906), when the radiation frequency tends to infinity, the radiation energy also tends to ∞, but this effect was not observed experimentally. This problem was solved by Max Planck in the same year 1900 thanks to the hypothesis that energy is emitted by fractional portions proportional to the radiation frequency, called quanta.

Despite all the scientific wisdom, William Thomson (Baron Kelvin) did not pay attention to the discovery that led to a radical change in the place of science in the life of society. Five years before his speech in Germany, the rector of the University of Würzburg, William Roentgen (1845 - 1923), conducted experiments with the so-called "cathode rays" (according to modern concepts - a stream of electrons emitted by a heated cathode and accelerated by an electric field between the cathode and anode in vacuum tube, which is called the "cathode tube"). Naturally, the electrons, colliding with the anode, stop and do not fly out of the cathode tube. However, V. Roentgen discovered that a mysterious penetrating radiation emanated from the tube, not visible to the eye, but capable of illuminating a photographic plate. He called this radiation X-rays. After that, Europe was swept by "rays-mania".

A wave of enthusiasm has reached France as well. In 1896, Henri Becquerel (1852–1908), head of the physics department at the National Museum of Natural History (Paris), conducted experiments to study phosphorescence[2] of uranium salts (potassium uranyl sulfate). He tried to find X-ray phosphorescence from these salts. But he discovered that uranium salts emitted rays that illuminated photographic plate through a black paper even without exposure to the sunlight! By placing uranium salts in external electric and magnetic fields, A. Becquerel discovered that mysterious rays were deflected. These were not X-rays, but new, unknown radiation containing charged particles. It arose without supplying any energy from the outside and did not weaken over time. It seemed that one of the unshakable laws was violated - the law of conservation of energy. Or were there unknown reserves of energy hidden in the depths of the substance? So, with an accidental discovery, a new era began in the development of not only physics, but a new era in the development of mankind. Radioactivity was discovered.

But nobody knew yet what is the structure of atom and why radioactive decay occurs. The decisive step was taken in 1909-1911 in the laboratory of E. Rutherford in the city of Manchester (UK). In order to study the structure of the atom, Rutherford's colleagues H. Geiger (1882-1945) and E. Marsden (1889-1970) bombarded thin gold films by alpha particles emitted as a result of alpha decay. To the surprise of the researchers, in 10^{-4} cases, alpha particles were scattered at an angle greater than 90°. On March 7, 1911, at a meeting of the Manchester Society of Literature and Philosophy, E. Rutherford hypothesized that the bulk of the atom is concentrated in a tiny volume in the center (since most of the alpha particles passed without deflection through thin films) and is positively charged, and electrons rotate around this nucleus in elliptical orbits (planetary model of the atom). Estimates showed that the radius of the nucleus is four orders of magnitude smaller than the radius of the atom. It was a revolutionary idea because it remained unclear why accelerated

[2]Phosphorescence is a long-term light emission emitted by crystals and organic molecules after they are illuminated. The light emitted as a result of phosphorescence, as a rule, differs in color from the color composition of the incident radiation.

electrons do not emit electromagnetic radiation. The answer was given in 1913 by N. Bohr's model of the atom, which has become one of the cornerstones of modern quantum physics.

The next question was about structure of atomic nucleus. E. Rutherford's experiments of alpha particles scattering by nitrogen atoms (1919) showed that in 1: 50,000 of the cases, nuclei of hydrogen atoms were born. This means that the atomic nucleus contains protons. The last step in determining the structure of the atomic nucleus was made in the experiments of the German physicist W. Bothe, the French researchers the Curies and the English physicist, collaborator of E. Rutherford J. Chadwick (1932). They studied the radiation produced in collision of He nuclei with the nuclei of Be. It did not deflect in electric and magnetic fields and possessed great penetrating power. The analysis of energies of protons and N nuclei knocked out by this radiation from paraffin target has led to the conclusion that it was a new type of particles with mass close to the mass of proton and with zero charge. These particles with spin 1/2 were called neutrons. The discoveries of protons and neutrons have led to the proton-neutron model of atomic nucleus, proposed by D. Ivanenko (USSR) and W. Heisenberg (Germany). In this model atomic nucleus consists of protons and neutrons. The number of protons is equal to atomic number of chemical element and the number of neutrons and protons is equal to mass number of nucleus.

The proton-neutron model of atomic nuclei raised the question of forces binding the nucleus. It would seem that the Coulomb forces should split the atomic nucleus apart. If this does not happen, then, consequently, forces that exceed the Coulomb ones act in atomic nuclei. Since the scattering of alpha particles by nuclei is rather satisfactorily described by the Coulomb interaction, it can be concluded that nuclear forces manifest themselves only at short distances of the order of the size of the nucleus (10^{-12} cm). The simplest theory of nuclear forces in 1935 was proposed by the Japanese physicist H. Yukawa. He suggested that the interaction between nucleons[3]occurs through the exchange of a hypothetical massive particle emitted by one nucleon and absorbed by another. The theoretical estimates have shown that a mass of such particle was approximately ten times smaller than a mass of proton. These particles were called mesons (from ancient Greek. μέσος - medium). They (so-called pi-mesons) were discovered experimentally in 1947 (charged, rest mass about 140 MeV) and in 1950 (neutral, rest mass about 135 MeV). To detect them, balloons were used that raised photographic plates to a great height into the stratosphere. The forces acting between nucleons due to the exchange of pi-mesons are very short but they greatly exceed electromagnetic forces between protons. It guarantees stability of atomic nuclei.

The discovery of pi-mesons completed the creation of the proton-neutron model of atomic nuclei, which is generally accepted until now.

[3]Nucleon is the generalized name for proton and neutron. These are particles close in mass (a neutron is slightly more massive than a proton), having the same spin ½, but differing in electromagnetic properties (charge, magnetic dipole moment).

E. Rutherford died in 1937. No scientist made such a noticeable contribution to the development of nuclear physics. Under his leadership, a brilliant galaxy of Nobel laureates has worked. E. Rutherford possessed a unique intuition that made it possible to find answers to the most difficult questions of science. It is all the more surprising that shortly before his death, E. Rutherford argued that nuclear physics is unlikely to find significant practical application. Only a few years remained until the discovery of the processes that changed the fate of nuclear physics and of all mankind. It is induced nuclear fission which permits to release huge amount of nuclear energy.

After this historic introduction let’s consider the main aspects of nuclear physics.

LECTURE 1

1.1. Symbols and Units in Nuclear Physics

There are known ~ 3500 nuclides. Accepted notations of a specific nuclide:

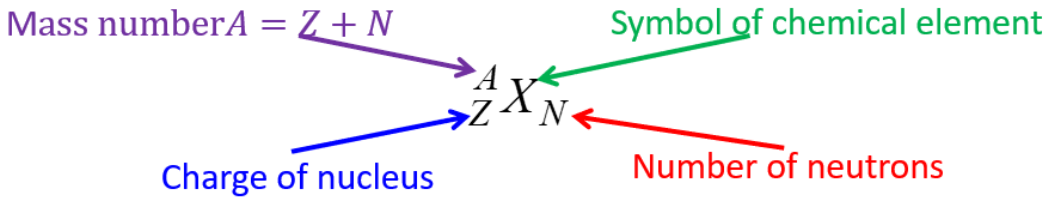

The values of number of protons (atomic number) Z, number of neutrons N, and number of neutrons and protons (mass number) A change in the limits:

- from Z=0 (neutron n) to Z=118 (Oganesson Og);
- from N=0 (proton p) to N=184 (Darmstadtium Ds);
- from A=1 (proton p and neutron n) to A=294 (Ds, Ts, Og).

Units of energy in nuclear physics.

Unit of energy in nuclear physics – electron-volt: 1 eV=1.6022·10^{-19} J.

Derived units are:

1 keV = 10^3 eV; 1 MeV = 10^6 eV; 1 GeV = 10^9 eV; 1 TeV = 10^{12} eV;

1 PeV = 10^{15} eV; 1 EeV = 10^{18} eV.

Binding energy of an electron in a hydrogen atom ~ 15 eV.

Comparison of sizes and energies in atomic and nuclear physics.

Atom (the dot denotes nucleus inside atom).

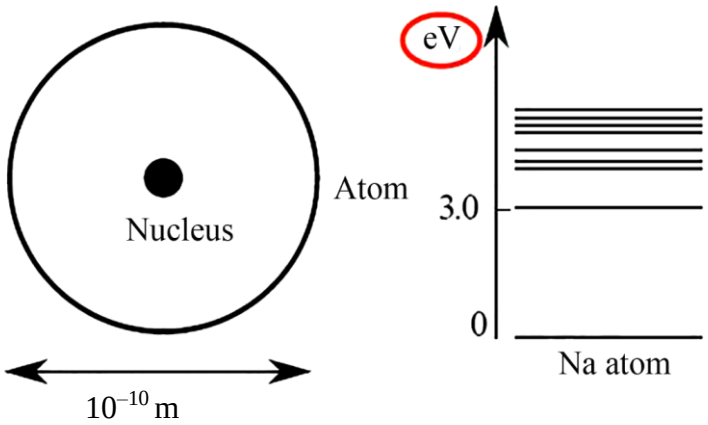

Atomic nucleus (the small circles denote protons and neutrons inside of the nucleus).

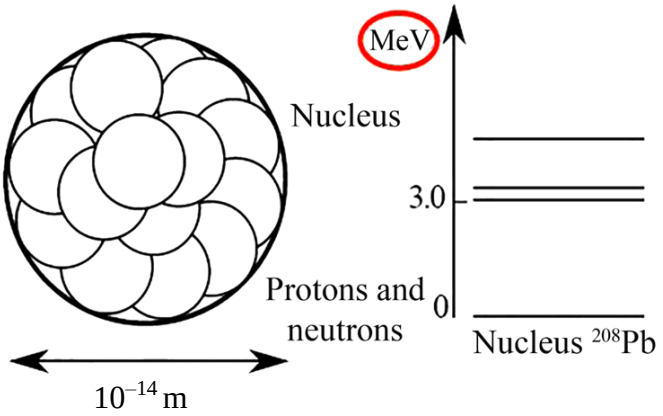

Proton (black circles denote quarks inside of the proton).

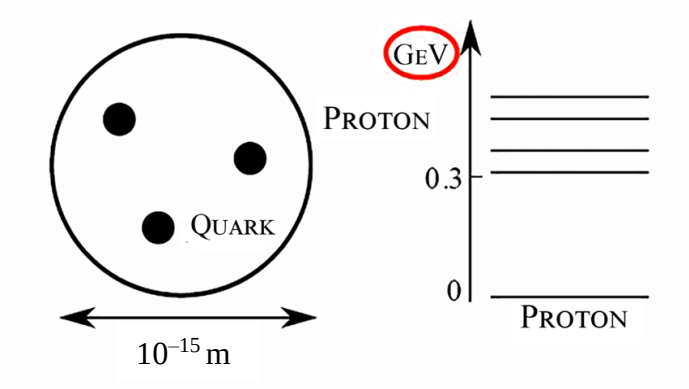

Units of mass in nuclear physics.

Traditionally the mass in nuclear physics is measured in the units of energy, corresponding to the rest energy of the nucleus.

- M_e= 0.511 MeV /c^2 = 9.1·10^{-28} g – mass of electron;
- M_p= 938.27 MeV /c^2= 1840 M_e – mass of proton;
- M_n= 939.56 MeV /c^2– mass of neutron.
- M_n– M_p > 2.5 M_e.

Another unit of mass in nuclear energy – *atomic mass unit* (a.m.u.):

1u = mass(atom ^{12}C)/12 = 931.502 MeV /c^2; 1u < M_p < M_n.

Atomic mass data center (China) gives evaluation of masses of atomic nuclei (http://amdc.impcas.ac.cn/).

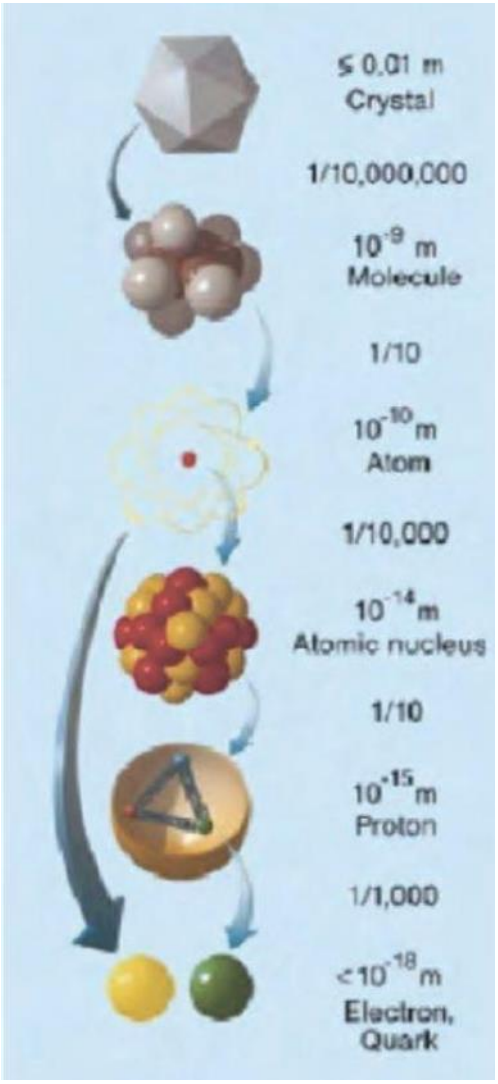

Units of length in nuclear physics.

Typical size of an atomic nucleus $R_N \sim 10^{-14}$ m.

10^{-15} m = 1 femtometer = 1 Fermi (1 fm); $R_N \sim 10$ fm

Units of area in nuclear physics.

$(R_N)^2 \sim 10^{-28}$ m^2= 100 fm^2= 1 barn.

Units of charge in nuclear physics.

Charge is measured in units of electron charge; $1e \approx 4.8\ 10^{-10}$ CGSE

Units of speed.

Speed is measured in β – fraction of the speed of light $c \approx 2.998 \cdot 10^{10}$ cm/c.

Useful constants.

Conversion constant $\hbar c \approx 197.3$ MeV · fm; Fine-structure constant $e^2/\hbar c \approx 1/137.04$

1.2. Isotopes, Isotones, Isobars

a) *Isotopes* is a set of nuclei with Z = const (A changes).

- Isotopes have the same chemical and similar physical properties (Fred. Soddy, 1913, radioelements are chemically inseparable).
- In nature, elements are a mixture of isotopes (J.J. Thomson, 1913, Ne-20,22).
- Isotopes with Z> 92 do not occur in nature.

.

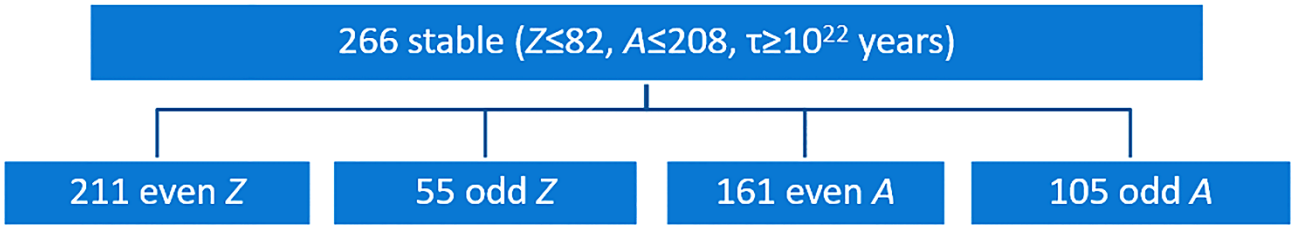

There are: 25 isotopes of $_{50}$Sn (among them 10 stable); 25 isotopes of $_{54}$Xe; 22 isotopes $_{82}$Pb.

Majority of stable isotopes are even-even, minority – odd-odd (^{2}H, ^{6}Li, ^{10}B, ^{14}N).

b) *Isobars* is a set of nuclides with *A*=const (*Z*, *N* change).

The study of isobar nuclei makes it possible to study the dependence of the interaction between nucleons on their charges.

Mirror nuclei– a pair of nuclei isobars ${}_ZX_N$ and ${}_NY_Z$.

Usually one nucleus of such a pair is radioactive. Such pairs have similar properties. Examples: ${}_1H_2$ and ${}_2He_1$; ${}_4Be_3$ and ${}_3Li_4$.

Among the *stable* nuclei, there are:

1 isobaric triad: ${}^{124}Sn$, ${}^{124}Te$, ${}^{124}Xe$;

48 isobaric pairs: 47 even-even with Z differing by 2;

One isobaric pair with odd *A* (*Z* differs by 1): ${}^{123}Sb$, ${}^{123}Te$.

c) *Isotones* is a set of nuclei with *N* = const (*Z*, *A* change).

1.3. Scattering cross section

v-speed

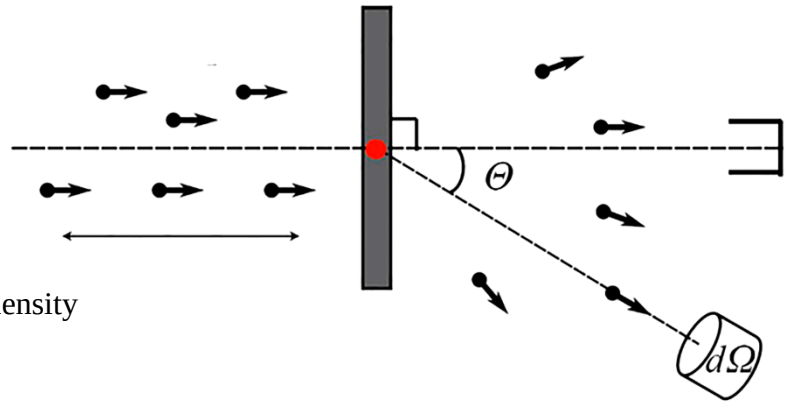

n-particle density

Φ is the flow of incident particles: the number of particles crossing a unit area per unit of time.

$$\Phi = n \cdot v$$

The number of particles scattered into a solid angle $d\Omega$ per unit time $d\Phi_{\text{scatt}} = \Phi \frac{d\sigma(\theta)}{d\Omega} d\Omega$.

$d\sigma(\theta)/d\Omega$ – differential effective scattering cross section.

$$[d\sigma(\theta)/d\Omega] = \text{ barn/steradian}$$

Rutherford formula.

Let's consider elastic scattering of two particles which are:

- Pointlike;
- Non-relativistic;
- With zero spin;
- Interacting by Coulomb potential.

Elastic scattering of a light particle with charge Z, mass m, energy E, and impact parameter b by a heavy nucleus with charge Z', mass M is shown in the figure below:

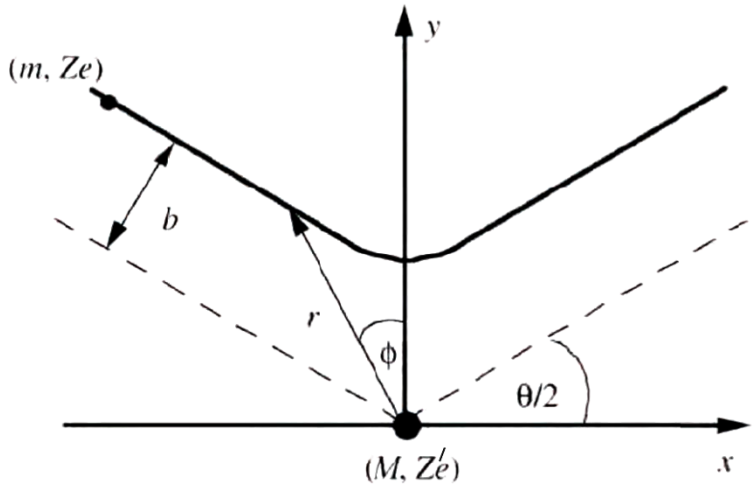

The differential effective cross section in the center-of-mass reference frame is given by the Rutherford formula:

$$\frac{d\sigma}{d\Omega}(\theta) = \left(\frac{ZZ'e^2}{4E}\right)^2 \frac{1}{\sin^4(\theta/2)},$$

where θ is scattering angle.

1.4. Charge and matter distributions, form factors, radii and masses of atomic nuclei

a) Charge and matter density distribution in atomic nuclei.

For medium and heavy nuclei charge or matter distribution is usually given by Woods-Saxon formula (figure below):

$$\rho(r) = \frac{\rho_0}{1+e^{(r-R)/a}},$$

where R is a half-density radius and $t = 4aln3$ is called the thickness of the surface layer.

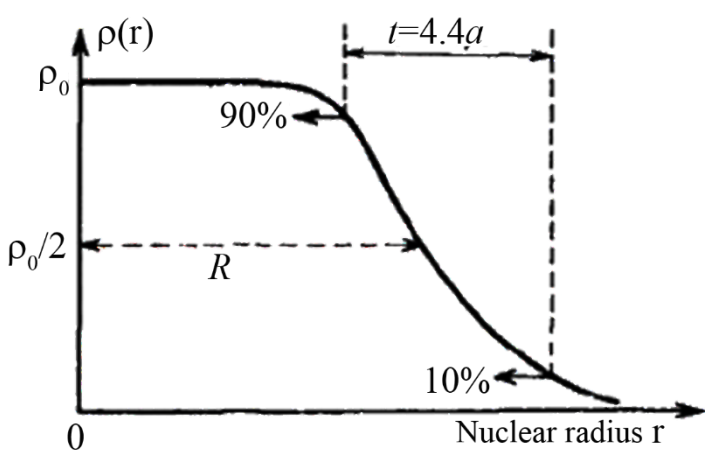

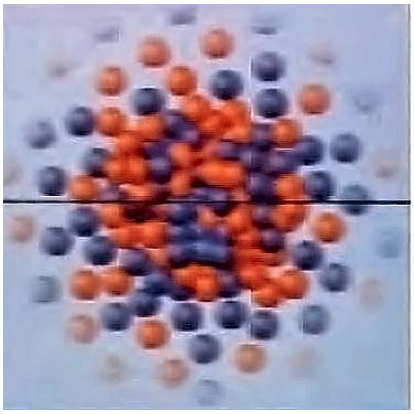

R is sometimes called the radius of the nucleus. $R \approx 1.2\ A^{1/3}$ фм (A>20, accuracy ≈ 20%).

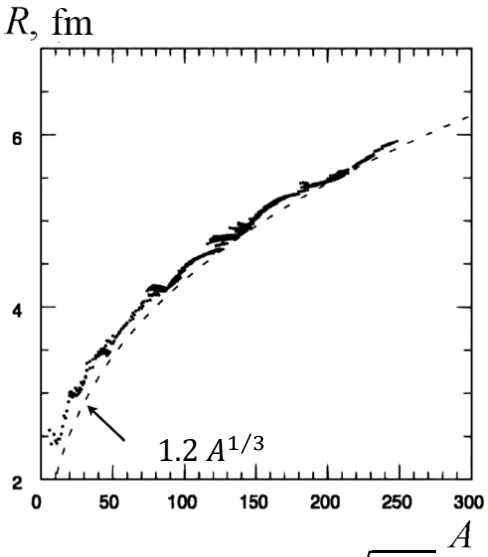

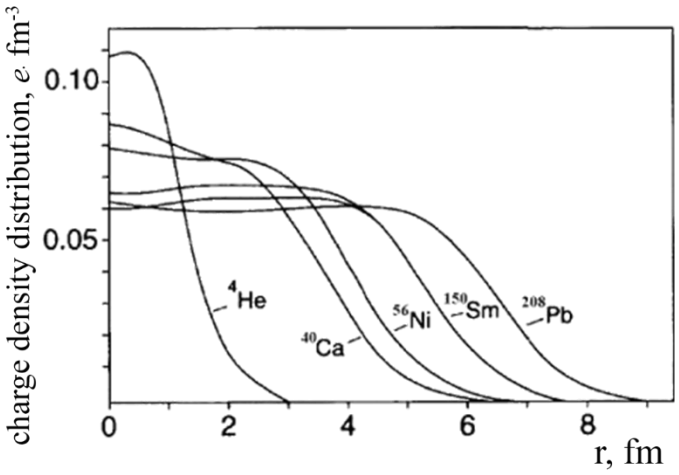

Root mean square radius: $\sqrt{\langle r^2 \rangle} \approx r_0 A^{1/3}$, $r_0 \sim 1$ фм.

But there are nuclei with charge and density distributions differing from the values given by Woods-Saxon formula.

For example: *halo nuclei*. In these nuclei one or two nucleons are far from the core.

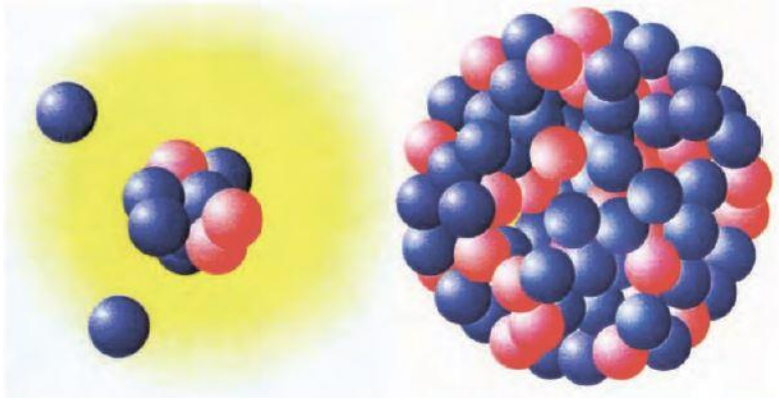

^{11}Li ($T_{1/2}$= 8.6 ms)−two neutrons outside the ^{9}Li core ^{208}Pb

Example of one-neutron halo nucleus is ^{11}Be ($T_{1/2}$=13.8 s):

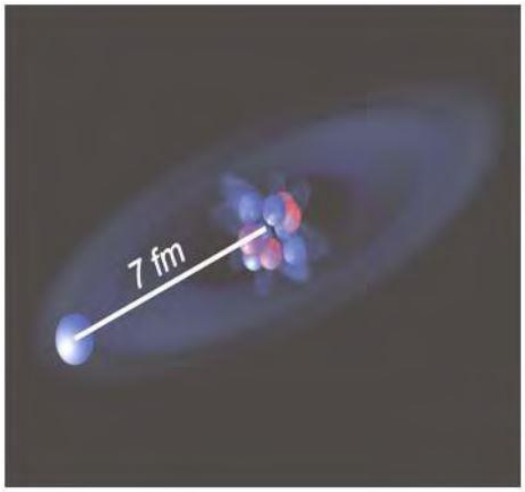

b) Form-factors.

The concept of form factor $F(q^2)$ (where q is momentum transferred) appears, when it is necessary to take into account the size of a nucleus. Then the differential cross-section of elastic scattering of point-like charged particle by the particle with charge density distribution $\rho(\vec{r})$ is given by:

$$\left(\frac{d\sigma}{d\Omega}\right) = \left(\frac{d\sigma}{d\Omega}\right)_{\text{Rutherford}} |F(\vec{q})|^2,$$

where $\left(\frac{d\sigma}{d\Omega}\right)_{\text{Rutherford}}$ is given by the Rutherford formula, and $F(\vec{q})$ is an elastic Coulomb form-factor:

$$F(\vec{q}) \sim \int \rho(\vec{r}) e^{i(\vec{q}\vec{r})/\hbar} d^3r.$$

For different charge distributions the q-dependence of form-factors is shown below:

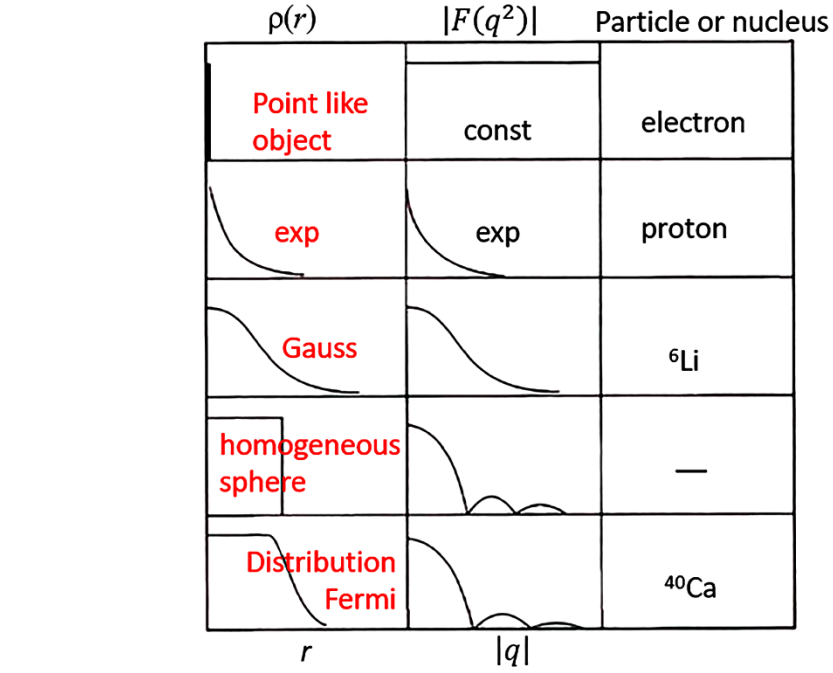

Connection between momentum transferred $\vec{q}$ and scattering angle θ:

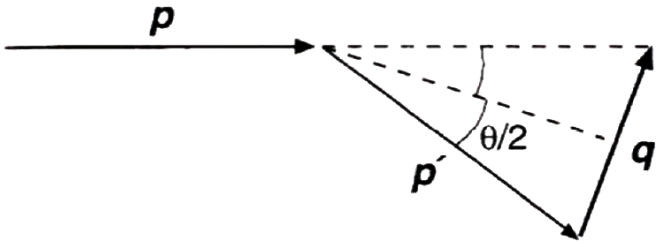

$$\vec{q} = \vec{p} - \vec{p}'$$

Here $\vec{\boldsymbol{p}}$ is momentum of the incident particle before collision and $\vec{\boldsymbol{p}}'$ − after collision.

Scattering in the approximation of an infinite mass of a scattering center gives a connection between scattering angle and momentum transferred:

$$|\vec{p}| = |\vec{p}'| \Rightarrow |\vec{q}| = 2|\vec{p}| \sin(\theta/2).$$

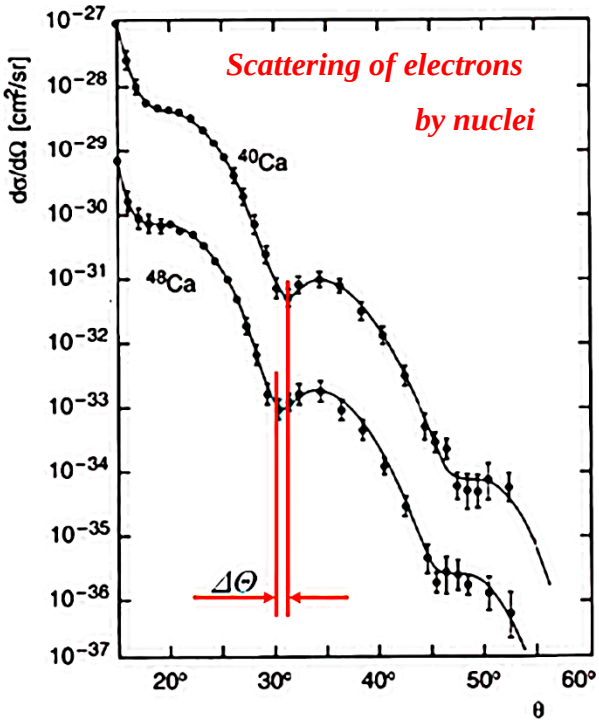

The maxima and minima in the experimental elastic cross section in the figure reflects a finite size of Ca nuclei. It is taken into account by the form-factor $F(\theta)$. The scattering of electrons by finite-size nuclei resembles the scattering of light by finite-size object. The reason is that microparticles are described by a wave function with a wave length given by de Broglie formula:

$$\lambda = h/p,$$

where p is a particle momentum and λ is its wave length.

When a particle is scattering on a sphere of radius R at $\lambda \leq R$, a diffraction pattern appears. Diffraction minima arise when particle is scattering at angles

$$\sin\theta_{min} = n\frac{0.61}{R}\lambda, \quad n = 1,2,3,\ldots$$

The greater the angle of diffraction minimum the lesser the radius of a sphere. It means that the charge radius of ^{40}Ca is less than the charge radius of ^{48}Ca.

c) Masses of atomic nuclei.

1) The mass of the nucleus is less than the sum of the masses of protons and neutrons. It is connected with energy of attraction between nucleons.

2) This difference is reflected in the *mass defect* $\Delta M(Z,A)$:

$$\Delta M(Z,A) \equiv Z\left(m_p + m_e\right) + Nm_N - M(Z,A)$$

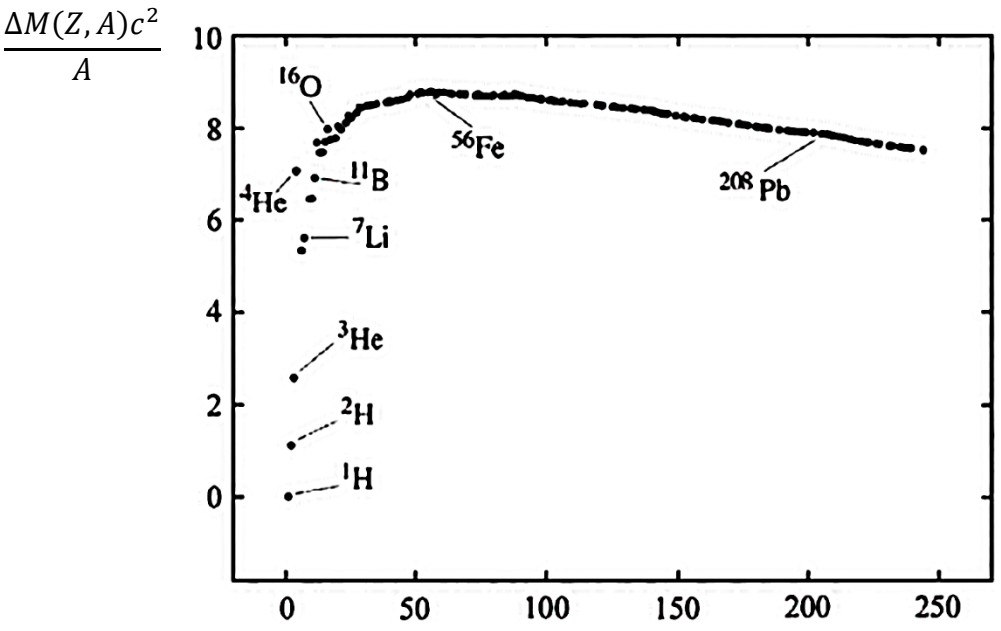

The mass defect per nucleon increases with increasing mass number for light nuclei ($A < 56$) and decreases with increasing mass number for medium and heavy nuclei.

1.5. Angular momenta, electric quadrupole momenta and magnetic dipole momenta of atomic nuclei

a) Angular moment.

The total angular moment J of a nucleus (or nuclear spin) includes orbital and spin moments of nucleons. It takes integer or semi-integer values:

$$J = 0, 1/2, 1, 3/2, 2 \ldots$$

The projection M of total angular moment takes negative and positive values:

$$M = -J, -J+1, \ldots, J-1, J.$$

The values of total angular moment and its projection are connected with eigenfunctions $\Psi_{JM}$the eigenvalues of corresponding operators of total angular moment $\hat{J}$ and its projection M by relations:

$$\hat{J}^2\Psi_{JM} = \hbar^2 J(J+1)\Psi_{JM};$$

$$\hat{J}_Z\Psi_{JM} = \hbar M\Psi_{JM}$$

b) Electric quadrupole moment (EQM).

- The electric quadrupole moment determines the interaction of the system with the gradient of the external electric field and is determined by the charge distribution in the nucleus.

- The electric quadrupole moment of the nucleus is given by the relation:

$$Q = \frac{1}{e}\int (3z^2 - r^2)\rho(r)\, d^3r,$$

where $\rho(r)$ charge density distribution in the nucleus. When calculating the internal (classical) EQM, the coordinate axes are directed along the axes of inertia of the nucleus.

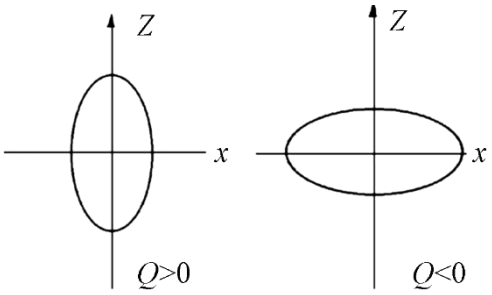

For a spherical nucleus, the EQM is zero, for a prolate nucleus it is positive, for an oblate nucleus it is negative.

- Quadrupole moment is measured in barns.
- Observed electromagnetic moments of nuclei are less than classical.
- Large quadrupole moments are characteristic of prolate nuclei.
- There are more prolate nuclei than oblate.

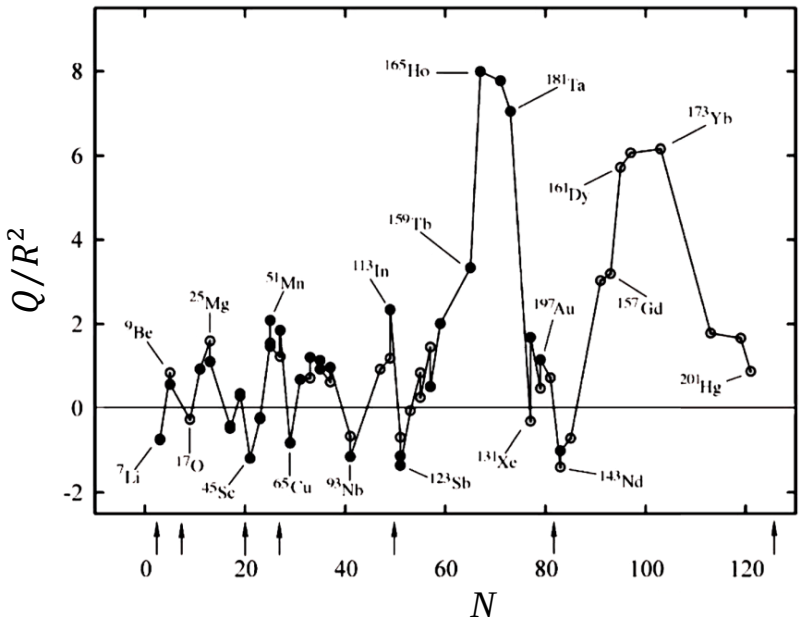

c) Magnetic dipole moment.

In classical electrodynamics, the magnetic dipole moment μ is:

$$\mu = (\text{current} \cdot \text{area})/c.$$

The magnetic dipole moment can be expressed in terms of the orbital angular momentum *L*:

$$\vec{\mu} = \frac{q}{2mc}\vec{L},$$

where *q* is charge of particle and *m* is mass of this particle.

In the transition to a quantum system, L is replaced by the spin J, q by e:

$$\vec{\mu} = g\frac{e}{2mc}\vec{J},$$

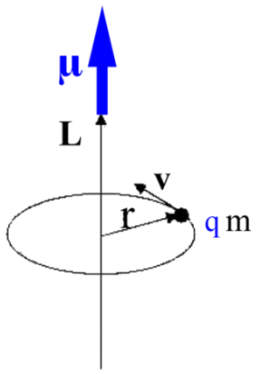

- In atomic physics, the Bohr magneton μ_B is used as a unit of magnetic moment:

$$\mu_B = g\frac{e\hbar}{2m_e c} = 0.5788 \cdot 10^{-14} \text{ MeV/G},$$

where m_e is a mass of electron.

- The magnetic moments of nucleons and nuclei are expressed in nuclear magnetons:

$$\mu_N = g\frac{e\hbar}{2m_p c} = 3.1525 \cdot 10^{-18} \text{ MeV/G},$$

where m_p is a mass of proton.

- Nuclear magneton in m_p/m_e = 1836 times smaller than Bohr magneton.
- For a proton and for a neutron, the experimental magnetic dipole moments are respectively:

$$\mu_p \approx 2.79\ \mu_N\ ; \quad \mu_n \approx -1.91\ \mu_N.$$

For a particle without internal structure $\mu_p \approx \mu_N$, $\mu_n \approx 0$. The experimental values of magnetic dipole moments of nucleons (so-called *anomalous magnetic dipole moments*) show, that nucleons are not point-like particles.

Methods of measurements of nuclear magnetic moments include:

- Stern-Gerlach method;
- Hyperfine splitting of atomic and molecular spectra;
- Nuclear spin flip effect in a strong external magnetic field upon absorption of a photon.

The measured values of magnetic dipole moments of some odd nuclei as a function of angular moment of odd nucleon (neutron or proton) are given by the dots in the figure below.

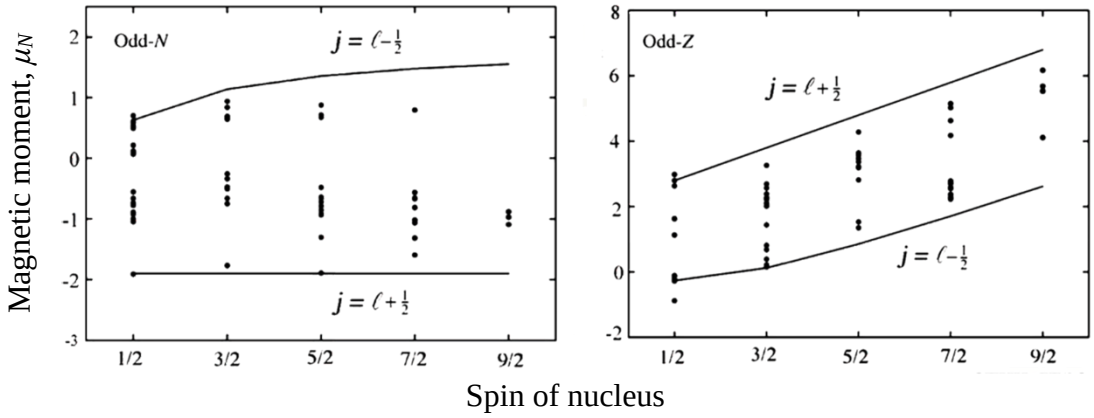

The solid lines (Schmidt lines) present magnetic dipole moments calculated under the assumption that it is formed by the single nucleon outside the core with zero magnetic dipole

moment. The difference between experimental and calculated values shows that the core is polarized by the odd nucleon.

1.6. The decay of nuclear states and level width

a) Radioactive decay of nuclei.

If at time $t = 0$ there are N_0 radioactive nuclei, then the number of radioactive nuclei at subsequent times is determined by the expression:

$$N(t) = N_0 e^{-\lambda t}.$$

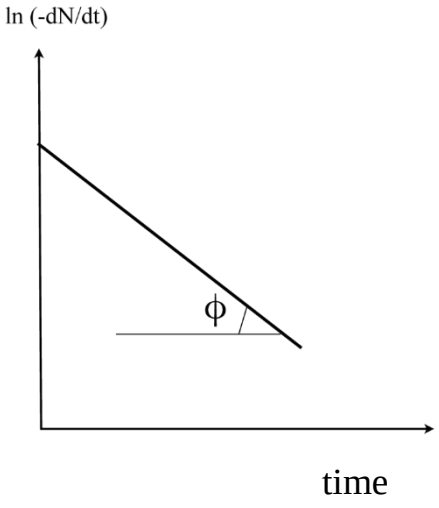

λ (decay constant) is decay probability per unit time (figure):

$$ln\left(-\frac{dN}{dt}\right) = ln(\lambda N_0) - \lambda t;$$

$$tg(\phi) = \lambda.$$

$\tau=1/\lambda$ is called the mean lifetime; $t_{1/2} = \tau \ln(2)$.

Half-life $t_{1/2}$ is the time required for a quantity to reduce to half of its initial value.

$$N\left(t_{1/2}\right) = N_0/2.$$

$$t_{1/2} = \tau \ln(2).$$

- Often the decay products of radioactive nuclei are also radioactive. This leads to decay chains. The figure shows the time dependence of the number of nuclei for the sequential decay of three nuclei: A–^{79}Sr, B–^{79}Rb, and C–^{79}Kr.

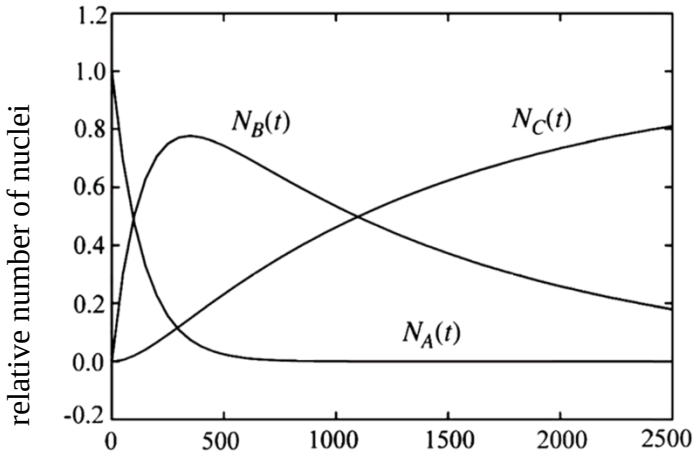

$$^{79}_{38}\mathrm{Sr} \rightarrow {}^{79}_{37}\mathrm{Rb} + e^+ + \nu_e \qquad (2.25\ \mathrm{min})$$
$$\hookrightarrow {}^{79}_{36}\mathrm{Kr} + e^+ + \nu_e \qquad (22.9\ \mathrm{min})$$
$$\hookrightarrow {}^{79}_{35}\mathrm{Br} + e^+ + \nu_e \qquad (35.04\ \mathrm{hours})$$

b) Energy Levels of Atomic Nuclei.

The spectrum of energy levels is clearly manifested in the cross sections for the scattering of electrons by nuclei. The peaks in the scattering cross sections correspond to resonant scattering by the ground and excited states of the nucleus.

$$e + {}^{12}\mathrm{C} \rightarrow e' + {}^{12}\mathrm{C}$$

The figure shows energy dependence of a number of electrons with incident momentum 495 MeV/c scattered by angle θ=65.4° (transferred momentum $q/\hbar$ =2.68 fm^{-1}) from ^{12}C target. The peaks correspond to the excited states of ^{12}C, including:

1. Ground state;
2. Individual resonances;
3. Overlapping resonances.

Excitation energies of ^{12}C for some energy levels are presented near the peaks.

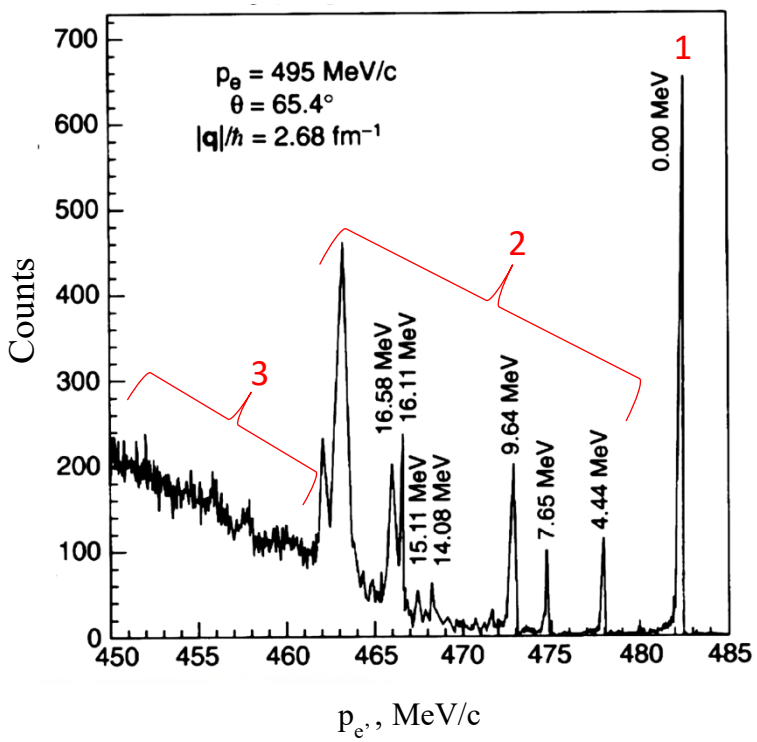

c) Energy level width.

The overlapping of resonances is associated with the small lifetime of the resonance states, which leads to a large width of the energy levels. The uncertainty of the decay time connected with the mean lifetime τ leads to the uncertainty of the level energy Γ, as follows from the relation $\Gamma \cdot \tau \sim \hbar$. The uncertainty of the energy of the excited state leads to the Lorentzian shape of the lines in the spectrum of excited states. Energy dependence of decay probability $P(E)$ is given by expression (see figure):

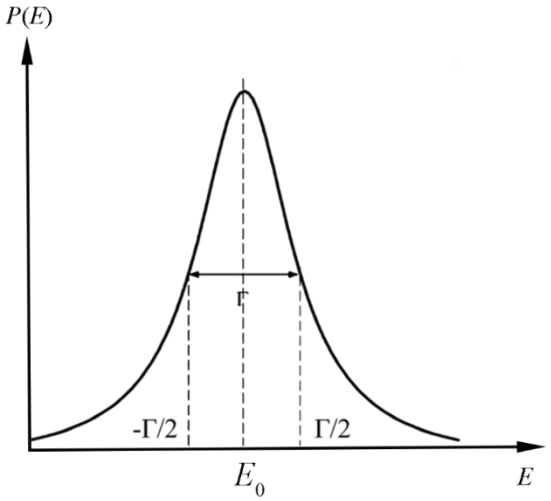

$$P(E) \sim \frac{1}{(E - E_0)^2 + (\Gamma/2)^2}$$

For example: if Γ=1 MeV then $\tau \sim 6.58 \cdot 10^{-22}$s.

d) *Energy levels scheme.*

Individual levels can be characterized by (energy levels of ^{12}C shown in the figure):

- Energy *E*,
- Spin *J*,
- Parity π,
- Width of the level Γ,
- Electric quadrupole moment,
- Magnetic dipole moment.

The arrows show possible decays of excited energy levels to the lower ones by emission of gamma quanta.

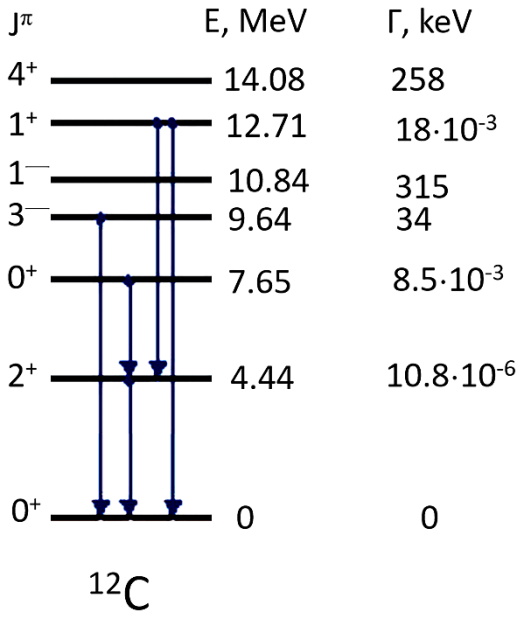

LECTURE 2

2.1. The binding energy of the nucleus and the separation energy of the nucleon

- In order to divide the nucleus into components Z protons and N neutrons, it is necessary to spend binding energy $B(Z, N)$:

$$B(Z,N) = Zm_pc^2 + Nm_nc^2 - M_{\text{nucleus}}(Z,N)c^2,$$

where m_p (m_n) is a mass of proton (neutron), and $M_{\text{nucleus}}(Z,N)$ – mass of nucleus.

- To separate one or two protons p and one or two neutrons n, it is necessary to spend separation energy S_i (i=p, n, 2p, 2n):

$$S_n = -Q_n = B(N,Z) - B(N-1,Z);$$
$$S_p = -Q_p = B(N,Z) - B(N,Z-1);$$
$$S_{2n} = -Q_{2n} = B(N,Z) - B(N-2,Z);$$
$$S_{2p} = -Q_{2p} = B(N,Z) - B(N,Z-2).$$

2.2. Semi-empirical formula for binding energies (Weizsäcker formula)

For the case of infinite nuclear matter, the binding energy of one nucleon is determined by its interaction with the nearest neighbors. In this case, the binding energy of nucleons is proportional to their number ~ A

The nucleons located on the surface of the nucleus have a smaller number of bonds than the internal ones; therefore, the total binding energy decreases by an amount proportional to the surface of the nucleus ~ $A^{2/3}$

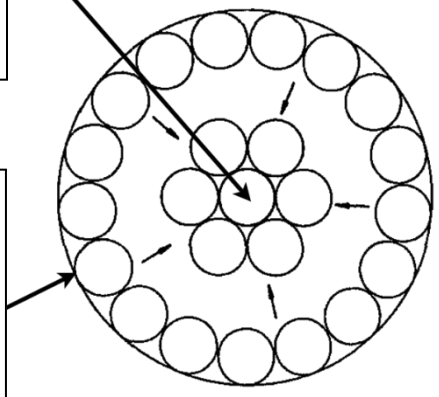

The Coulomb energy of a sphere of radius R with charge Z is proportional to Z^2 / R; therefore, the binding energy of the nucleus decreases by $\sim Z^2 / A^{1/3}$

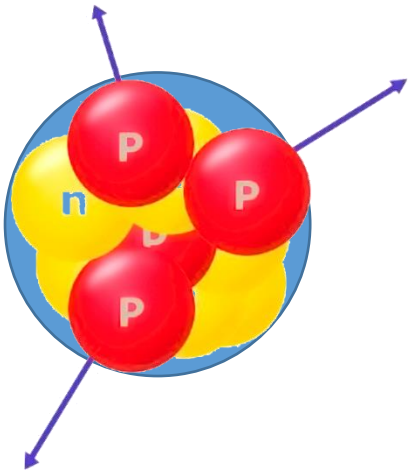

Nucleons in the nucleus obey the Pauli principle, so that a change in the number of protons or neutrons at the same mass number A leads to a decrease in the binding energy $\sim (Z\text{-}A / 2)^{2} / A$

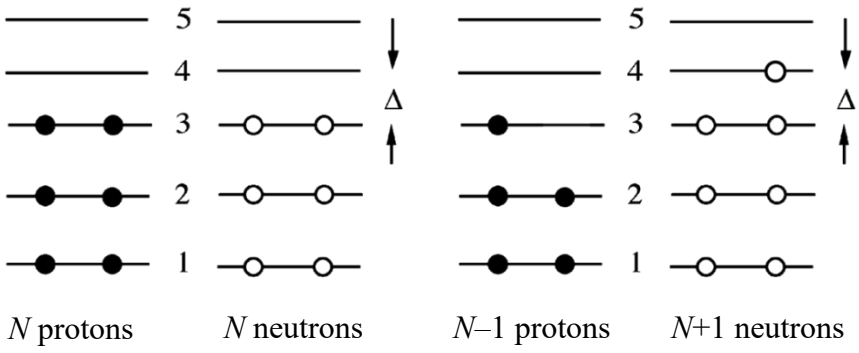

In the ground state of the nucleus, an additional bond arises between two nucleons of the same type located at the same energy level. The forces that arise are called pairing forces. This leads to a difference in the binding energies for even-even, odd-odd and odd-even nuclei.

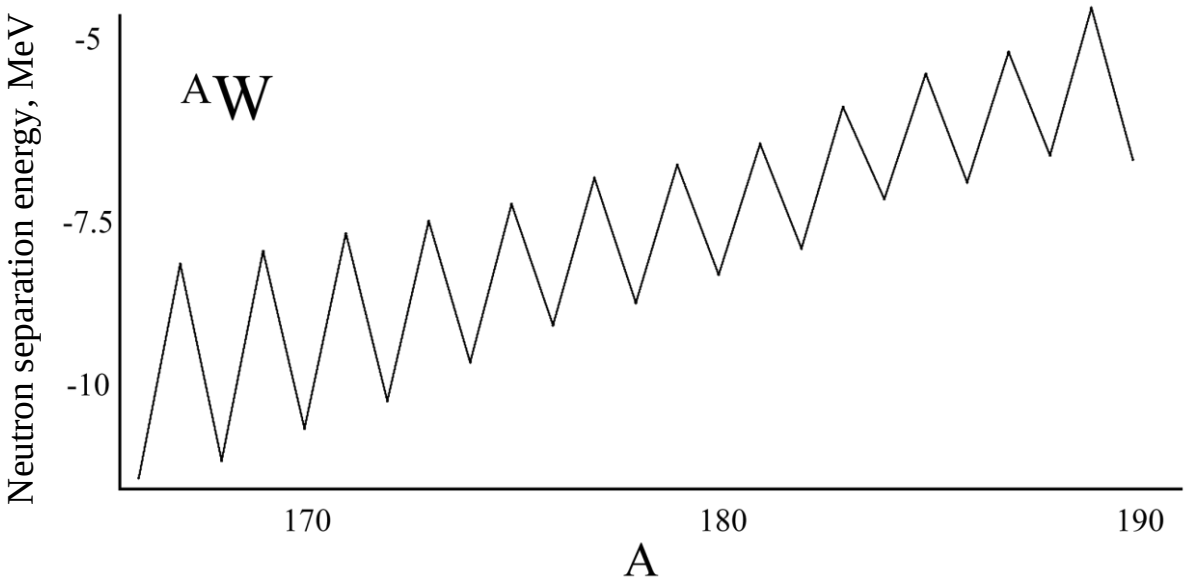

Weizsäcker formula takes into account all these effects:

$$B(Z,N) = a_v A - a_S A^{2/3} - a_{sym}(2Z - A)^2 A^{-1} - a_c Z^2 A^{-1/3} - \delta A^{-1/2}.$$

- Volume term includes a_v = 15.6 MeV;
- Surface term includes a_s = 16.8 MeV;
- Coulomb energy includes a_c = 0.72 MeV;
- Symmetry energy includes a_{sym} = 23.3 MeV;
- Pairing energy includes $\delta = \pm 12$ or 0 MeV for even, odd-odd or even-odd nuclei respectively.

The contribution of each term of Weizsäcker formula is presented in the figure below:

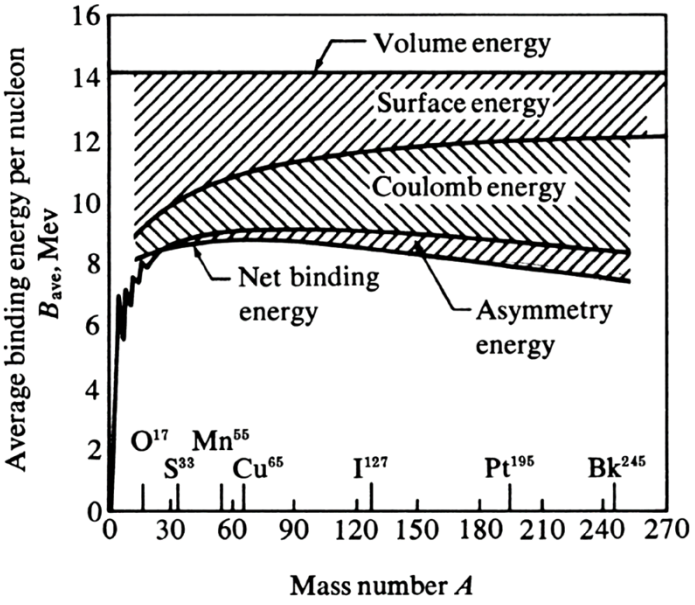

The Weizsäcker formula reproduces only the general tendency in the experimental dependence of binding energy on the number of protons and neutrons. The difference between the experimental binding energy of the nucleus and the one based on the semi-empirical formula is shown in the figure. The difference is especially large for the values of proton numbers 2, 8, 20, 28, 50, 82 and neutron numbers 2, 8, 20, 28, 50, 82,126 (*magic numbers*). In these cases values of experimental binding energies is much greater than theoretical ones. The origin of this discrepancy is explained by the *shell model*.

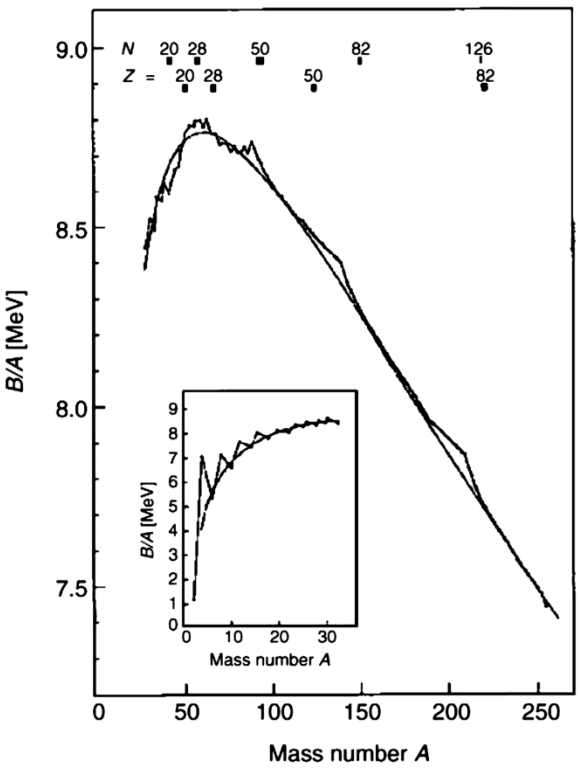

2.3. Nuclear interactions: Yukawa's theory, exchange forces

a) H. Yukawa's theory.

The interaction between nucleons occurs as a result of the exchange of spinless particles with mass M_x. To describe a free particle, one can use the Klein-Fock-Gordon equation.

$$E^2 = p^2c^2 + M_x^2c^4 \;\Rightarrow\; -\hbar^2\frac{\partial^2\phi(\boldsymbol{x},t)}{\partial t^2} = -\hbar^2c^2\nabla^2\phi(\boldsymbol{x},t) + M_x^2c^4\phi(\boldsymbol{x},t);$$

Here traditional replacement of classical number functions by the quantum operators is used. ϕ denotes the field of Yukawa's particles. We interpret the static case of $\phi(\boldsymbol{x})$ as a potential. In the static case Klein-Fock-Gordon equation takes a form:

$$\nabla^2\phi(\boldsymbol{x}) = \frac{M_x^2c^2}{\hbar^2}\phi(\boldsymbol{x}); \quad R^{-1} = \frac{M_xc}{\hbar}.$$

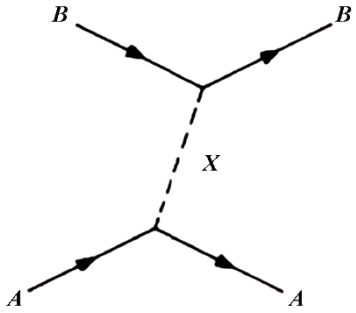

Potential $\phi(\boldsymbol{x})$ created by a point source is described by equation:

$$\nabla^2\phi(\boldsymbol{x}) - R^{-1}\phi(\boldsymbol{x}) = -g\delta(\boldsymbol{x}).$$

At M_x =0 one gets the Coulomb potential: $V(r) = -e\phi(r) = -\frac{e^2}{4\pi}\frac{1}{r}$;

For $M_x \neq 0$ one obtains the Yukawa's meson exchange potential: $V(r) = -\frac{g^2}{4\pi}\frac{e^{-r/R}}{r}$.

b) Exchange forces.

The discovery of charged pions (or pi-mesons) in 1947 and neutral pions in 1950 gave the experimental confirmation of Yukawa's concept of nucleon interaction by exchange of massive particles. The exponential decrease of Yukawa's potential in comparison with Coulomb potential explains the short-range nuclear forces.

The phenomena of saturation and short-range of nuclear forces are explained by their exchange character: the exchange of pi-meson.

If the state of two nucleons depends on the spatial $\boldsymbol{r}_1$, $\boldsymbol{r}_2$ and spin s_1, s_2 coordinates, then:

1) Nucleons can exchange by charged pi-meson with orbital angular momentum 0 — *Majorana forces* (exchange of spatial coordinates of nucleons):

$$\hat{H}_M\psi(\boldsymbol{r}_1,\boldsymbol{r}_2,s_1,s_2) = V_M(\boldsymbol{r}_2-\boldsymbol{r}_1)\psi(\boldsymbol{r}_2,\boldsymbol{r}_1,s_1,s_2).$$

2) Nucleons can exchange neutral pi-meson with orbital angular momentum 1 — *Bartlett forces* (exchange of spin coordinates of nucleons):

$$\hat{H}_B\psi(\boldsymbol{r}_1,\boldsymbol{r}_2,s_1,s_2) = V_B(\boldsymbol{r}_2-\boldsymbol{r}_1)\psi(\boldsymbol{r}_1,\boldsymbol{r}_2,s_2,s_1).$$

3) Nucleons can exchange charged pi-meson with orbital angular momentum 1 — *Heisenberg forces* (exchange of spatial and spin coordinates of nucleons):

$$\hat{H}_H \psi(\boldsymbol{r}_1, \boldsymbol{r}_2, s_1, s_2) = V_H(\boldsymbol{r}_2 - \boldsymbol{r}_1)\psi(\boldsymbol{r}_2, \boldsymbol{r}_1, s_2, s_1).$$

4) Nucleons can exchange a neutral pi-meson with an orbital angular momentum of 0 — the *Wigner force* (there is no exchange of spatial and spin coordinates of nucleons):

$$\hat{H}_W \psi(\boldsymbol{r}_1, \boldsymbol{r}_2, s_1, s_2) = V_W(\boldsymbol{r}_2 - \boldsymbol{r}_1)\psi(\boldsymbol{r}_1, \boldsymbol{r}_2, s_1, s_2).$$

2.4. Deuteron

Main properties of deuteron.

- Deuteron is a bound system of a proton and a neutron, a heavy isotope of hydrogen, denoted ^{2}H or d.
- Deuteron has only one bound state.
- Binding energy of deuteron is 2.22 MeV.
- Spin and parity of deuteron are 1^+.
- Root mean square (rms) radius of deuteron is ~4.316 fm.
- Rest energy of deuteron (mc^2) is 1876 MeV.
- Dipole magnetic moment of deuteron μ_d=0.879634 μ_N.
- Quadrupole moment of deuteron Q_d =0.282 fm^2.

a) Magnetic dipole moment of deuteron.

The deuteron spin ***J*** is the vector sum of the spins of the proton $\boldsymbol{s}_p$, the neutron $\boldsymbol{s}_n$, and their relative orbital angular momentum ***L***:

$$\boldsymbol{J}=\boldsymbol{s}_p+\boldsymbol{s}_n+\boldsymbol{L}$$

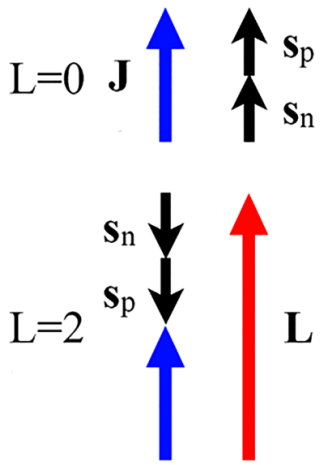

Since the internal parity of the deuteron is positive, L is an even number. There are only two possibilities (see figure):

L = 0 and L = 2.

In the case of the s-state, the magnetic moment of the deuteron is equal to the algebraic sum of the magnetic moments of the proton and neutron:

$$\mu(s)=0.879804\ \mu_N,$$

Experimental value of the magnetic moment of the deuteron μ_d=0.879634 μ_N.

$$\frac{\mu_d - \mu(s)}{\mu_d} = -0.026.$$

Consequently, the deuteron is predominantly in the s-state with a small admixture of the d-state.

$$\Psi\left({}^2\mathrm{H}\right) = \alpha\psi_s + \beta\psi_d;\ \ \alpha^2 = 0.96\ ;\ \beta^2 = 0.04.$$

The angular distribution of differential cross section of elastic scattering of protons by deuterons are given in the figure. The comparison of theoretical results with experimental ones shows that admixture of d-states in the wave function reduces the difference between theory and experiment.

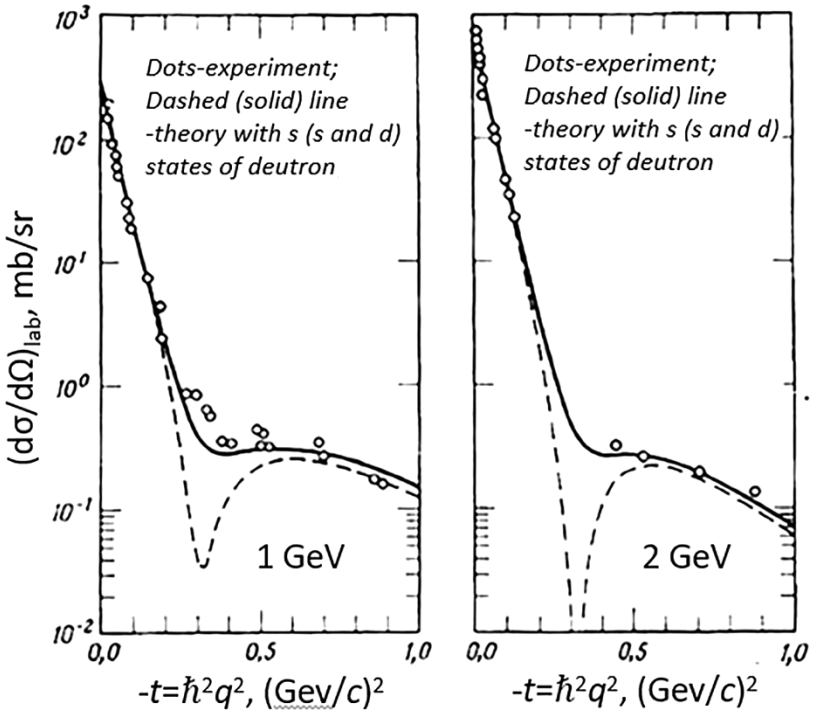

b) Electric quadrupole moment of deuteron.

Deuteron *quadrupole moment* Q=0.282 fm^2.

Q>0, it means, that deuteron has prolate deformation i.e. the deuteron wave function contains an admixture of the d-state. The nuclear forces are non-central and depend on the spin. Nuclear forces resemble *tensor forces* for interacting magnets.

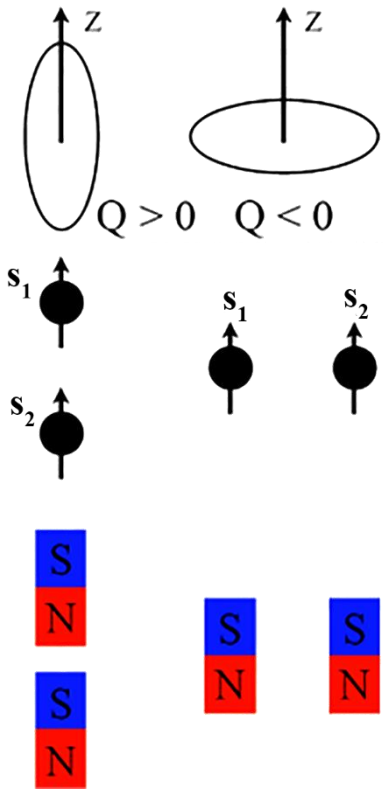

Energy of interaction of two magnets:

$$E_{12} = \left[\left(\boldsymbol{\mu}_1 \cdot \boldsymbol{\mu}_2\right) - 3\left(\boldsymbol{\mu}_1 \cdot \boldsymbol{r}\right)\left(\boldsymbol{\mu}_2 \cdot \boldsymbol{r}\right)/r^2\right]/r^3,$$

where $\boldsymbol{\mu}_1$, $\boldsymbol{\mu}_2$ — magnetic dipole moments of magnets.

By analogy, the tensor forces in the nucleon-nucleon potential are:

$$V_T = v_T(r)S_{12};\quad S_{12} = 3\left(\boldsymbol{s}_1 \cdot \boldsymbol{r}\right)\left(\boldsymbol{s}_2 \cdot \boldsymbol{r}\right)/r^2 - \left(\boldsymbol{s}_1 \cdot \boldsymbol{s}_2\right).$$

c) Binding energy and elementary theory of the deuteron.

Experimental data for the deuteron:

1) binding energy 2.225 MeV;
2) rms charge radius 2.10 ± 0.06 fm.

The binding energy of deuteron B_d is the eigenvalue of Schrödinger equation:

$$-\frac{\hbar^2}{2m}\nabla^2\Psi(\boldsymbol{r})+V(\boldsymbol{r})\Psi(\boldsymbol{r})=-B_d\Psi(\boldsymbol{r}).$$

For the case of a rectangular potential with depth V and width *b*, only the relationship between these parameters can be found from the Schrödinger equation (curve B_d). Taking into account the data on the rms charge radius from experiments on electron scattering, one can choose the depth and width of the potential.

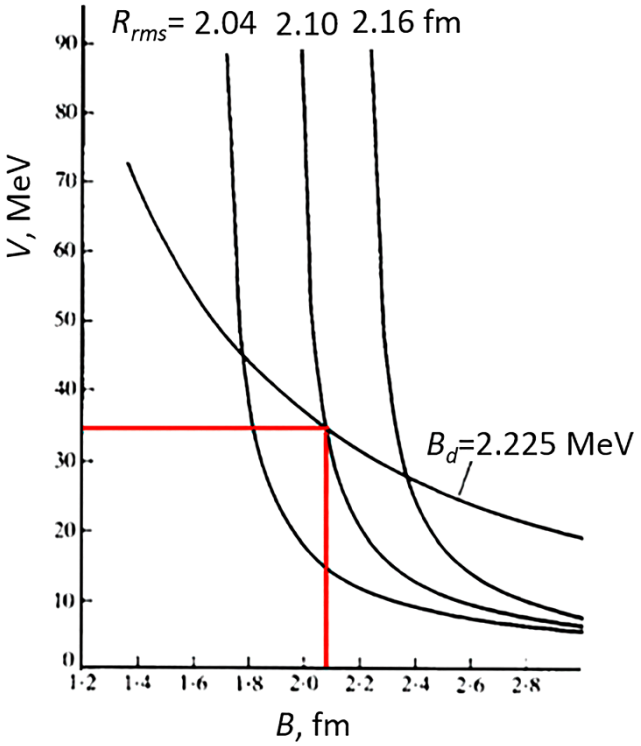

The wave function of the orbital motion of the deuteron ψ(*r*) can be found from the Schrödinger equation with a central field.

$$\psi(\boldsymbol{r})=\sum_L u_L(r)r^{-1}Y_L(\Theta,\varphi)\cdot$$

A good description (at L = 0) of the experimental data gives a potential in the form of a rectangular well, with a depth of V_0 ~ 35 MeV and a width of ~ 2 fm.

A significant radius of ~ 4 fm and a low binding energy E_b ~ 2.225 MeV indicate the "looseness" of the deuteron. It has the same radius as the nucleus with A = 40-50.

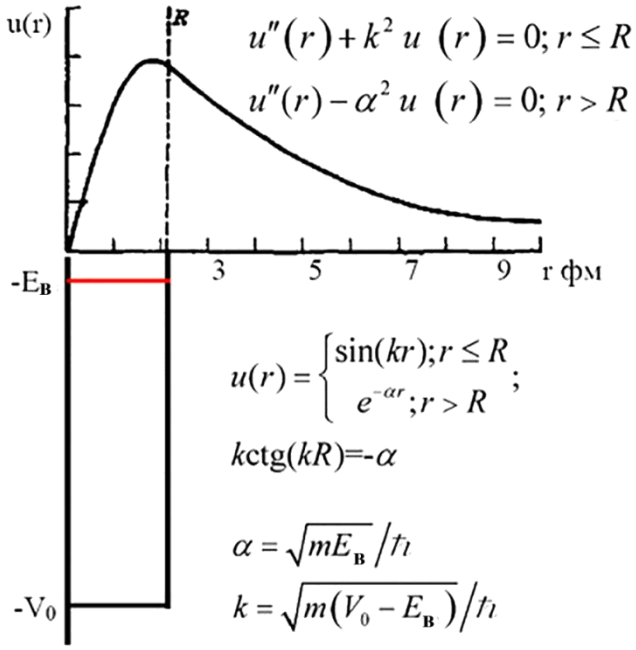

LECTURE 3

3.1. Elements of the scattering theory

The problem of scattering of a nonrelativistic particle by the potential $V(r)$ is solved using the time-independent Schrödinger equation.

$$-\frac{\hbar^2}{2m}\nabla^2\psi(\boldsymbol{r})+V(r)\psi(\boldsymbol{r})=E\psi(\boldsymbol{r}).$$

The wave function is written as $\psi(\boldsymbol{r})=e^{ikz}+\psi_{\text{pacc}}(\boldsymbol{r});\ \ \psi_{\text{pacc}}(\boldsymbol{r})=f(\theta,\varphi)\frac{e^{ikr}}{r}.$

Here f is the scattering amplitude, it describes the dependence on the angles of the outgoing spherical wave. Determination of this dependence is the main goal of the scattering experiment.

The scattering amplitude is related to the differential effective cross section by the formula:

$\frac{d\sigma}{d\Omega}=\left|f(\boldsymbol{q})\right|^2$, here $\boldsymbol{q}$ is momentum transfer.

Since the deuteron has no singlet states, to study the interaction of nucleons at $S = 0$, it is necessary to use nucleon-nucleon scattering. We use two approximations:

- the potential of nucleon-nucleon interaction is rectangular with depth V and radius R;
- we restrict ourselves to the angular momentum $L = 0$.

Angular momentum is quantized$\Rightarrow\ mvR\sim\hbar L;$ according to the de Broglie ratio $mv=\hbar/\lambda$.

Hence, the orbital angular momentum L = 0 corresponds to the values of the impact parameter R*:* $mvR<\hbar\Rightarrow R<\lambda$.

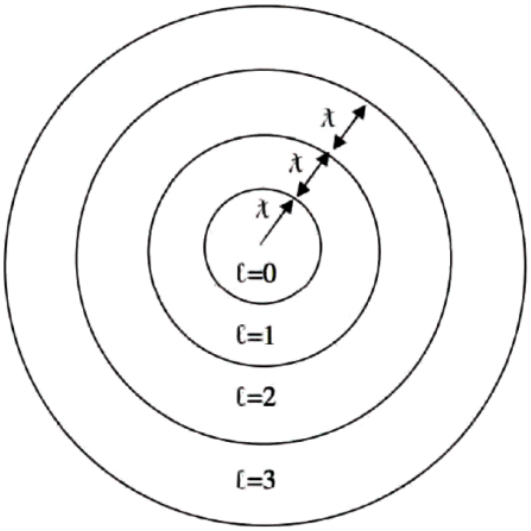

Therefore, if the reduced wavelength of the incident particle is greater than the radius of nuclear forces (≈ 1 fm), then scattering occurs only at $L = 0$, which sets the upper limit for the energy E <20 MeV.

3.2. Scattering of nucleons at low energies

Consider the solution of the Schrödinger equation for the case of a rectangular potential well. Expanding the wave function in terms of states with different angular momenta:

$$\psi(\boldsymbol{r}) = \sum_{L=0}^{\infty} \psi_L(r) Y_{LM=0}(\theta,\varphi),$$

leaving only the term with L = 0 (which corresponds to energies E <20 MeV) and passing to the functions u (r) = rψ$_0$ (r), we obtain:

$$-\frac{\hbar^2}{m}\frac{d^2u(r)}{dr^2} + V(r)u(r) = Eu(r);\ V(r) = \begin{cases} -V_0, & r \le R \\ 0, & r > R \end{cases}.$$

Solutions of this equation are:

$$r \le R \Rightarrow u(r) = A\sin(k_1 r) + B\cos(k_1 r);\quad k_1 = \left[m(E+V_0)\right]^{1/2}/\hbar;\ B=0.$$

$$r > R \Rightarrow u(r) = C\sin(k_2 r) + D\cos(k_2 r) = F\sin(k_2 r + \delta);\quad C = F\cos(\delta);\quad D = F\sin(\delta);\quad k_2 = \left[mE\right]^{1/2}/\hbar.$$

From continuity and smoothness of $u(r)$: $F\sin(k_2 R + \delta) = A\sin(k_1 R)$:

$$k_2 F\cos(k_2 R + \delta) = k_1 A\cos(k_1 R).$$

Dividing the second equation by the first, we get: $k_2\,\mathrm{ctg}(k_2 R + \delta) = k_1\,\mathrm{ctg}(k_1 R)$.

δ is called the scattering phase; δ =0 in the absence of potential (free movement); δ > 0 in the case of the attraction potential; δ < 0 in the case of a repulsive potential.

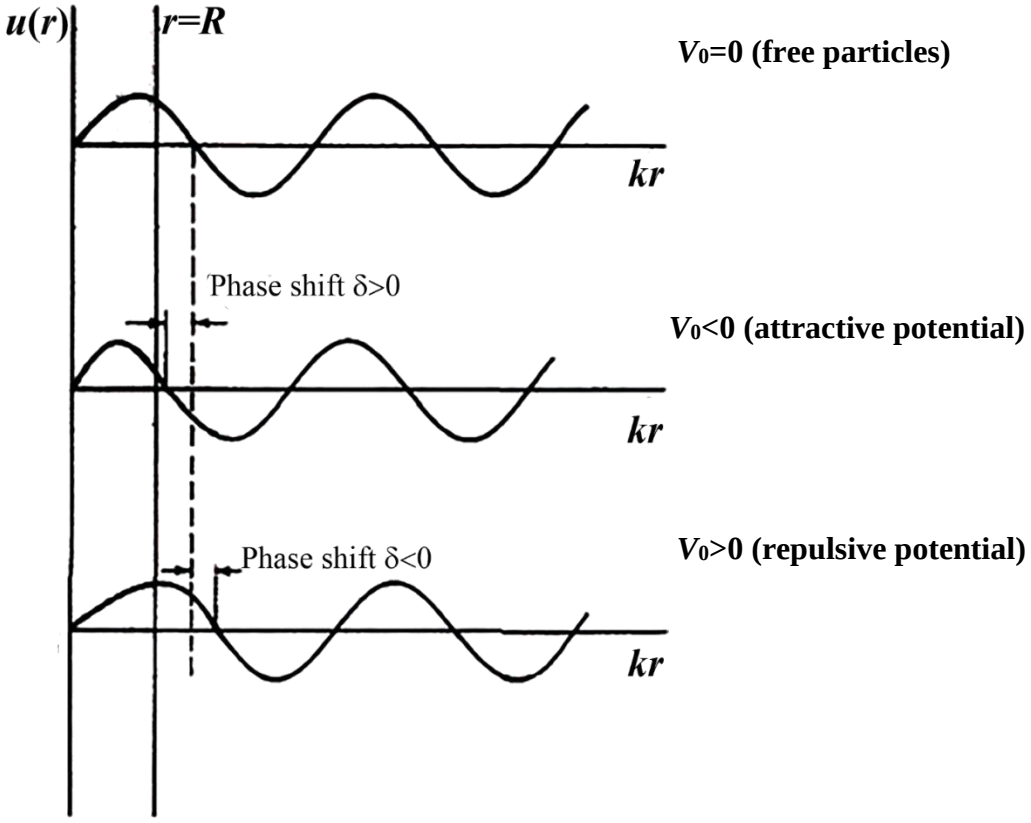

V_0=0 (free particles)

V_0<0 (attractive potential)

V_0>0 (repulsive potential)

$$\psi(r)=\frac{1}{r}\sum_{L=0}u_L(r)P_L(\cos\vartheta);\ \int_0^{\pi}P_L(\cos\vartheta)P_M(\cos\vartheta)\sin\vartheta d\vartheta=2\delta_{LM}/(2L+1);$$

$$u_L(r)=\frac{2L+1}{2}\int_0^{\pi}r\psi(r)P_L(\cos\vartheta)\sin\vartheta d\vartheta \qquad (1)$$

From (1) it follows: $\exp(ikr\cos\vartheta)=\frac{1}{2ikr}\left[\exp(ikr)-\exp(-ikr)\right]+\frac{1}{r}\sum_{L=1}\left[A_L(\vartheta)\right].$

$$\exp(ikr\cos\vartheta)+\frac{1}{r}f(\vartheta)\exp(ikr)=\frac{1}{2ikr}\left[(1+2ikf_0)\exp(ikr)-\exp(-ikr)\right]+\frac{1}{r}\sum_{L=1}\left[B_L(\vartheta)\right]. \qquad (2)$$

Equating the previously obtained wave function:

$F\sin(k_2r+\delta_0)=\frac{F}{2i}\left[\exp(ik_2r+i\delta_0)-\exp(-ik_2r-i\delta_0)\right]$ to the term for L=0 from (2), we obtain the relationship between the amplitude and phase of the scattering $1+2ik_2f_0=\exp(2i\delta_0)$. Then $f_0=\left[\exp(2i\delta_0)-1\right]/2ik_2=\exp(i\delta_0)\sin(\delta_0)/k_2.$

The scattering phase of the wave with L = 0 is related to the effective differential cross section by the formula:

$$d\sigma/d\Omega=\sin^2\delta_0/k_2^2$$

Then the total cross section is $\sigma=4\pi d\sigma/d\Omega=4\pi\sin^2\delta_0/k_2^2$.

3.3. Neutron-proton scattering at low energies

Consider the case of low energy neutron scattering (<10 keV) by proton. For such energy k_1=0.92 fm^{-1}, k_2=0.92 fm^{-1} . By analogy with the structure of the deuteron, we introduce the parameter α:

$$\alpha=-k_1\mathrm{ctg}(k_1R)$$

$$\sin^2\delta_0=\frac{\cos(k_2R)+(\alpha/k_2)\sin(k_2R)}{1+(\alpha/k_2)^2};\qquad \sigma=4\pi\frac{\cos(k_2R)+\frac{\alpha}{k_2}\sin(k_2R)}{k_2^2+\alpha^2}.$$

Assuming, by analogy with the deuteron, R=2 Fm, α=0.2 fm^{-1}, we obtain for the low-energy neutron scattering cross section: $\sigma=4\pi(1+\alpha R)/\alpha^2=4.6$ barn .

However, the experimental cross section for the scattering of low-energy neutrons by protons gives a cross section of the order of 20.4 barn (fig. below).

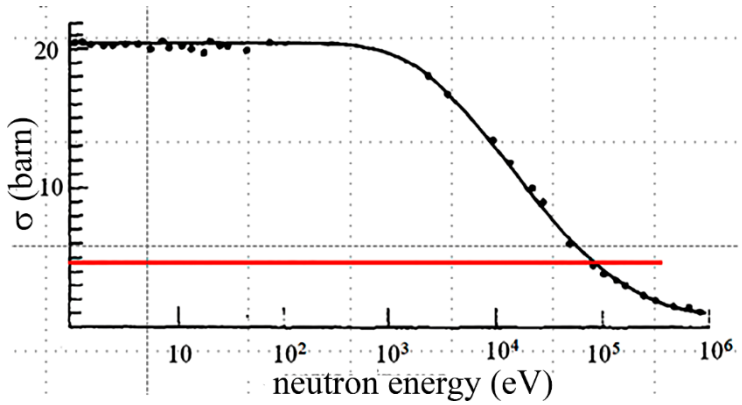

The reason is that the proton-neutron system can be in two states of total spin($S = s_p + s_n$): S=0 (singlet state); S=1 (triplet state: S_z =0, ±1).

Then the total cross section $\sigma = \left(3\sigma_{\text{tripl.}} + \sigma_{\text{singl.}}\right)/4$.

Since the cross section calculated above corresponds to the case of a deuteron, and the total cross section is 20.4 барн, $\sigma_{\text{singl.}} = 67.8\,\text{barn}$. This difference in cross sections is due to the *spin dependence of nuclear forces.*

3.4. Scattering by a hydrogen molecule

A hydrogen molecule can be in two states - orthohydrogen (proton spins are parallel) and parahydrogen (spins are antiparallel).

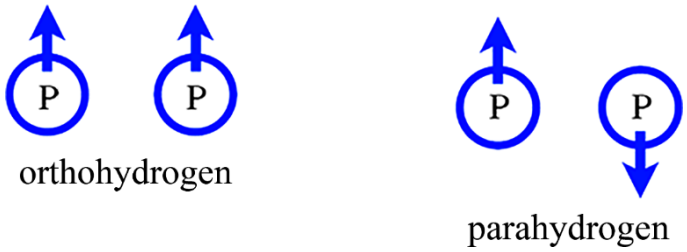

In the case of incident neutron energy $E_n < 0.01\text{MeV}$, the de Broglie wavelength is greater than 0.05 nm, which exceeds the size of a hydrogen molecule. This leads to interaction with two protons at once, so the cross section depends on $\left|\psi_1 + \psi_2\right|^2$, где ψ_i – wavefunction of i-th proton (i=1, 2).

Such low energies exclude rotational degrees of freedom. We introduce the parameter of the scattering length a:

$$\lim_{\lambda\to\infty}\sigma = 4\pi a^2$$

$$a = \lim_{\lambda\to\infty}\frac{\sin\delta_0}{k}.$$

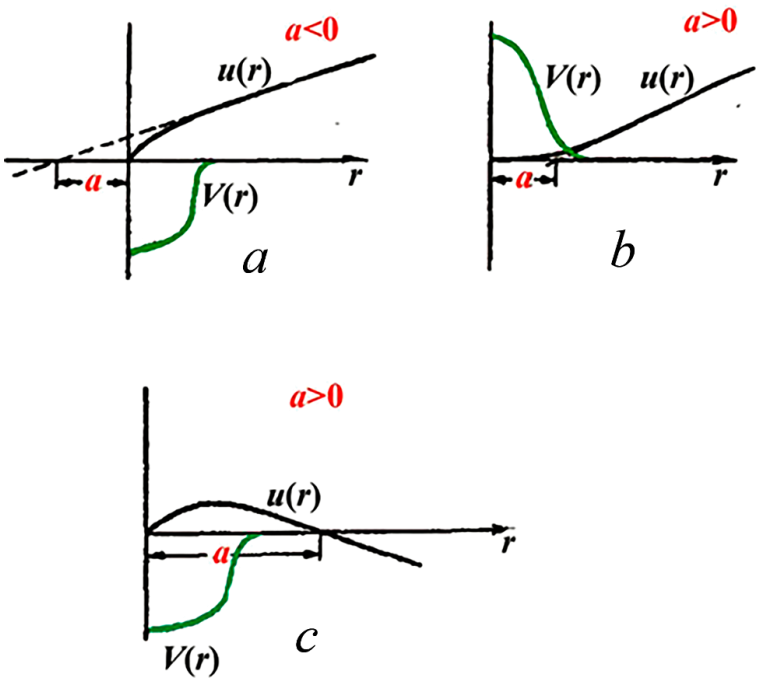

a) attractive potential with negative scattering length;

b) the repulsive potential with a positive scattering length;

c) an attractive potential with a positive scattering length, suggesting the presence of a bound state.

3.5. Differential cross-section of neutron-proton scattering and exchange forces

Consider the angular distribution of scattered nucleons:

$$d\sigma/d\Omega = \left| f\left(\boldsymbol{q}\right)\right|^2;$$

$$f\left(\boldsymbol{q}\right) = -\frac{m}{2\pi\hbar^2}\int V\left(\boldsymbol{x}\right)e^{i\boldsymbol{q}\cdot\boldsymbol{x}/\hbar}d^3x.$$

The magnitude of the momentum transmitted:

$$q = 2p\sin\left(\theta/2\right).$$

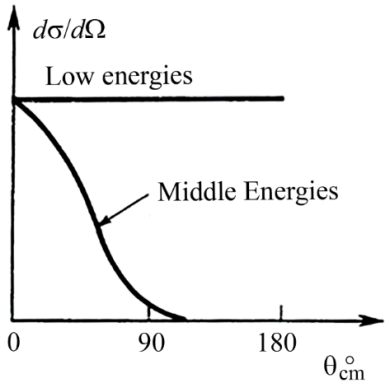

The fig. above shows theoretical prediction for the n-p scattering cross section from the first Born approximation.

The maximum transmitted momentum is $2p$. At low energies $2pR/\hbar \ll 1$, cross section is isotropic. At high energies, in the case of small-angle scattering, the transferred momentum is small — the cross section is large. In backward scattering at $2pR/\hbar \gg 1$, the exponential oscillates rapidly and the integral is small, the cross section decreases rapidly.

Experimental values of the effective differential cross section for n-p scattering in comparison with theoretical ones are shown in the figs. below.

Small energies (14 MeV)

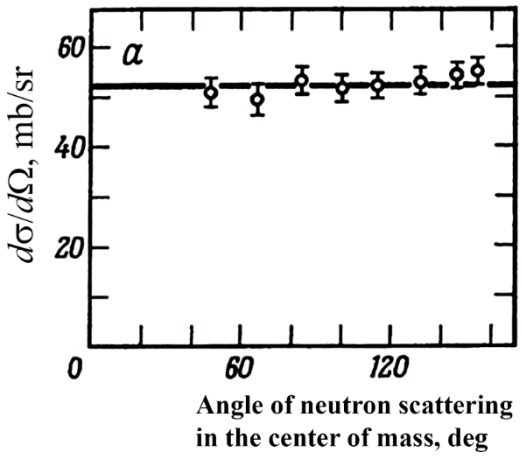

High energies

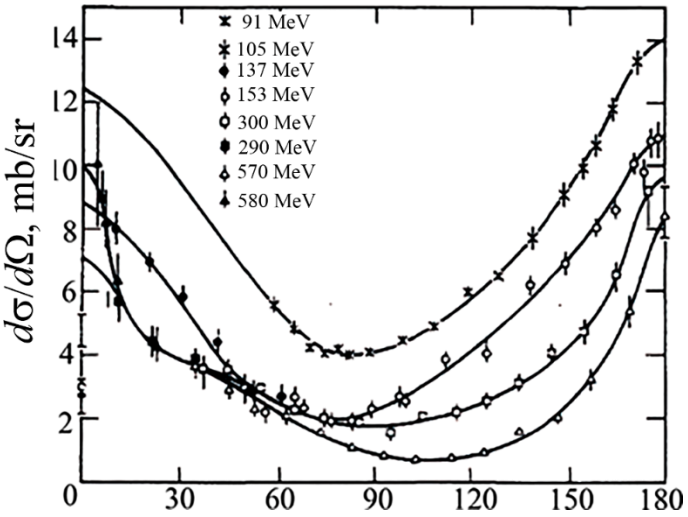

At high scattering energies, the cross section exhibits a pronounced peak in the backward direction. This behavior of the cross section indicates the existence of nucleon-nucleon exchange forces that convert a proton into a neutron and vice versa.

The neutron continuing to move forward turns out to be a proton, and the target proton is a neutron flying backward in the center of mass system.

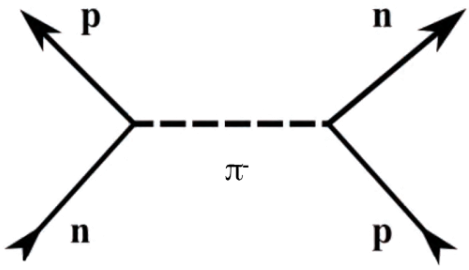

3.6. Scattering of identical nucleons and comparison with proton-neutron scattering

In quantum mechanics, to obtain the total probability of scattering of identical nucleons, it is necessary to add the scattering amplitudes $f(\Theta)$, $f(\pi-\Theta)$, taking into account the antisymmetry properties:

$$(d\sigma/d\Omega)_{\Theta} = (d\sigma/d\Omega)_{\pi-\Theta} = \left| f(\Theta) \pm f(\pi-\Theta) \right|^2$$

The plus sign refers to the singlet state (the spin function is antisymmetric), the minus sign refers to the triplet state (the spin function is symmetric).

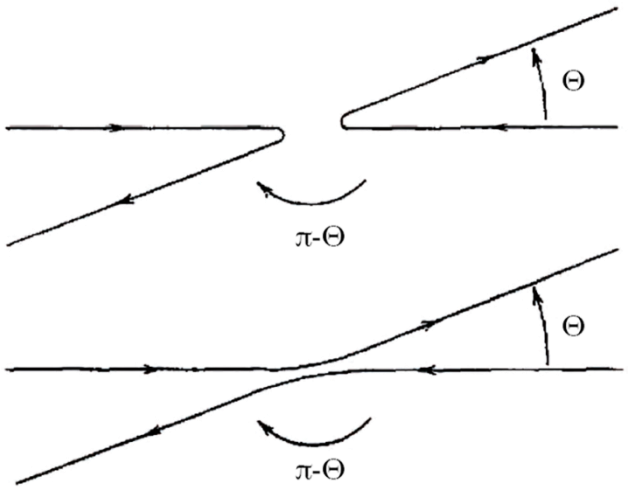

The corresponding function of spatial coordinates is symmetric in the first case and antisymmetric in the second. The scattering of two identical fermions (pp or nn) cannot occur in a triplet even (S = 1, L - even) or singlet odd (S = 0, L - odd) states, since in accordance with the definition of parity

$$f_L(\pi-\Theta) = (-1)^L f_L(\Theta).$$

Differences between the pp and np systems:

1) Coulomb repulsive force (essential for small-angle scattering at low energies)
2) Particle identity— at protons transposition

$$\Psi(\boldsymbol{r}, s_1, s_2) = -\Psi(-\boldsymbol{r}, s_2, s_1).$$

When transposing the spatial coordinates (L is the orbital angular momentum of the relative motion):

$$\Psi(-\boldsymbol{r}, s_1, s_2) = (-1)^L \Psi(\boldsymbol{r}, s_1, s_2).$$

When only the spin coordinates are transposed, the wave function is unchanged for triplet states and changes sign for singlet states. Therefore, in the pp system, only the following states are possible (S is the total spin, J is the total moment):

S=0; L=0, 2, 4,…; J=L. S=1; L=1, 3, 5,…; J=L-1, L, L+1.

3) No bound states in pp system.

The sign of nuclear forces is determined from the interference of Coulomb and nuclear scattering.

Fig. below shows cross section of pp scattering at an angle of 45º. The bump at 380 keV proves the attractive nature of nuclear forces.

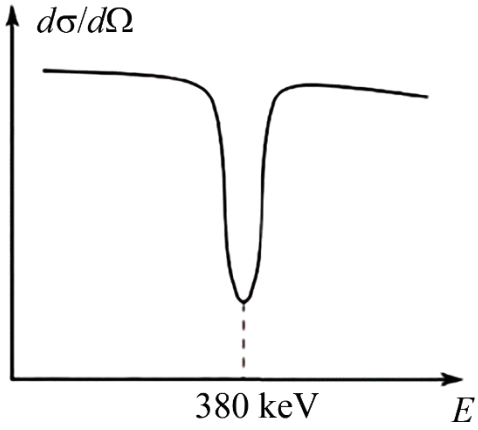

3.7. Isotopic spin. Empirical backgrounds for the introduction of isospin

- After subtracting the corrections that take into account the influence of the Coulomb repulsive forces in pp scattering, it turns out that pp and pn interactions have approximately the same magnitude and approximately the same radius.
- This result was confirmed in the study of nuclear mass defects of ^{3}H and ^{3}He.
- *The forces acting between any two nucleons in the same states are the same, if we ignore the effects of electromagnetic interaction.*
- Nuclear forces have the property of saturation, since nucleons interact only with their nearest neighbors.
- The masses of isobaric multiplets observed in light nuclei confirm with good accuracy the charge independence of nuclear forces.
- The scattering length a is the same for (pp), (np) and (nn) systems, if we first subtract the effects due to the charge and magnetic moment of the particles.
- The masses of the neutron and proton differ by 0.1% of their value, and it can be assumed that this difference in mass is of an electromagnetic nature.

3.8. Isospin formalism. Isospin nonconservation. Isospin in nuclei

The charge independence of nuclear forces makes it possible to introduce a new conserved quantum number - isospin. A neutron and a proton are two states of the same particle - a nucleon.

To describe the states of a nucleon, an isospin space with an isospin vector is introduced. Its mathematical properties are similar to those of a spin, i.e. isospin is characterized by two quantum numbers: the quantum number of the isospin I and the quantum number of the projection of the isospin I_3 ($I_3 = -I, -I + 1, \ldots, I$; the total of possible projections is $2I + 1$). Different states of one particle correspond to different values of the isospin projection. A nucleon has two states (proton and neutron), therefore $2I^{(\text{nucleon})}+1=2$, that is, $I^{(\text{nucleon})} = 1/2$.

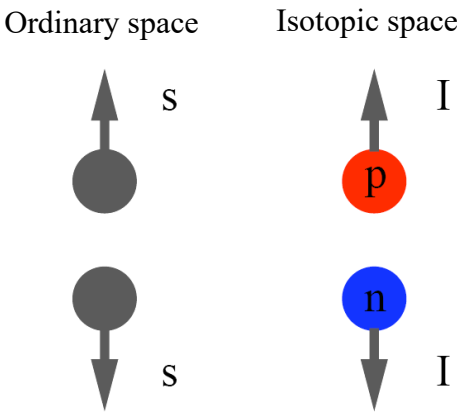

For a proton $I_3 = + 1/2$. For a neutron $I_3 = -1 / 2$. It is convenient to use the Dirac notation: $|I, I_3\rangle$: proton $|1/2, 1/2\rangle$, neutron $|1/2, -1/2\rangle$. The nucleon charge q is determined by the formula: $q = e(I_3 + 1/2)$.

- Isospin can be attributed to elementary particles.
- A particle with isospin I in the absence of an electromagnetic field will in reality be represented by $2I + 1$ subparticles. These subparticles form an isospin multiplet.
- These subparticles differ in electrical properties, but the rest of the physical properties are almost the same.

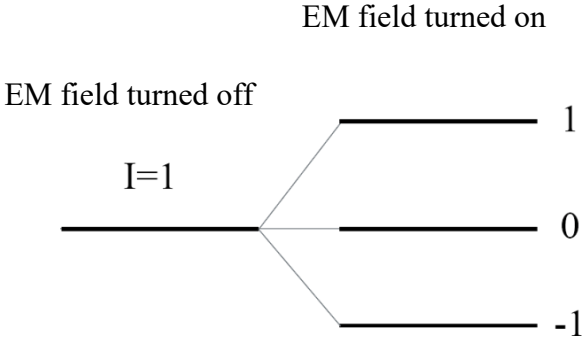

- There are three π-mesons:

  π^+, π^0, π^-.

  - $2I^{(\pi)}+1=3 \Rightarrow I^{(\pi)}=1$.
  - The charges of these particles are related to the isospin projection: $q = eI_3^{(\pi)}$.

$$I_3^{(\pi)} = \begin{cases} +1, \pi^+, m = 139.569 \text{ MeV}/c^2 \\ 0, \pi^0, m = 134.964 \text{ MeV}/c^2 \\ -1, \pi^-, m = 139.569 \text{ MeV}/c^2 \end{cases}$$

Fig. below shows interaction of nucleons by the exchange of π – meson. A neutron, emitting a π^- meson, turns into a proton. The proton, absorbing the π^- meson, turns into a neutron.

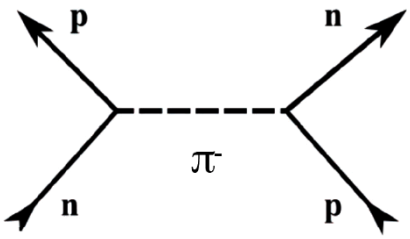

Isotopic spin (isospin) of an atomic nucleus.

The isospin of a system consisting of several particles is the result of the addition of the isospins of all particles in the system. The rules for adding isospins are similar to the rules for adding spins. Hence the third projection of the isospin of a nucleus consisting of *Z* protons and *N* neutrons:

$$I_3^{(Z,N)} = Z \times \frac{1}{2} + N \times \left(-\frac{1}{2} \right) = \frac{Z-N}{2} = Z - A/2 .$$

The total isospin of a nucleus consisting of *A* nucleons is equal to the sum of the isospins of its constituent nucleons, summed according to the addition rule of angular momenta:

$$\vec{I} = \sum_{i=1}^{A} \vec{I}^{(i)} .$$

Hence, the quantum number of the isospin *I* of the nucleus takes the values:

$$\left| Z - N \right| / 2 \le I \le A/2.$$

I and I_3 take integer (if *A* is even) or half-integer (if *A* is odd) values.

Mirror nuclei.

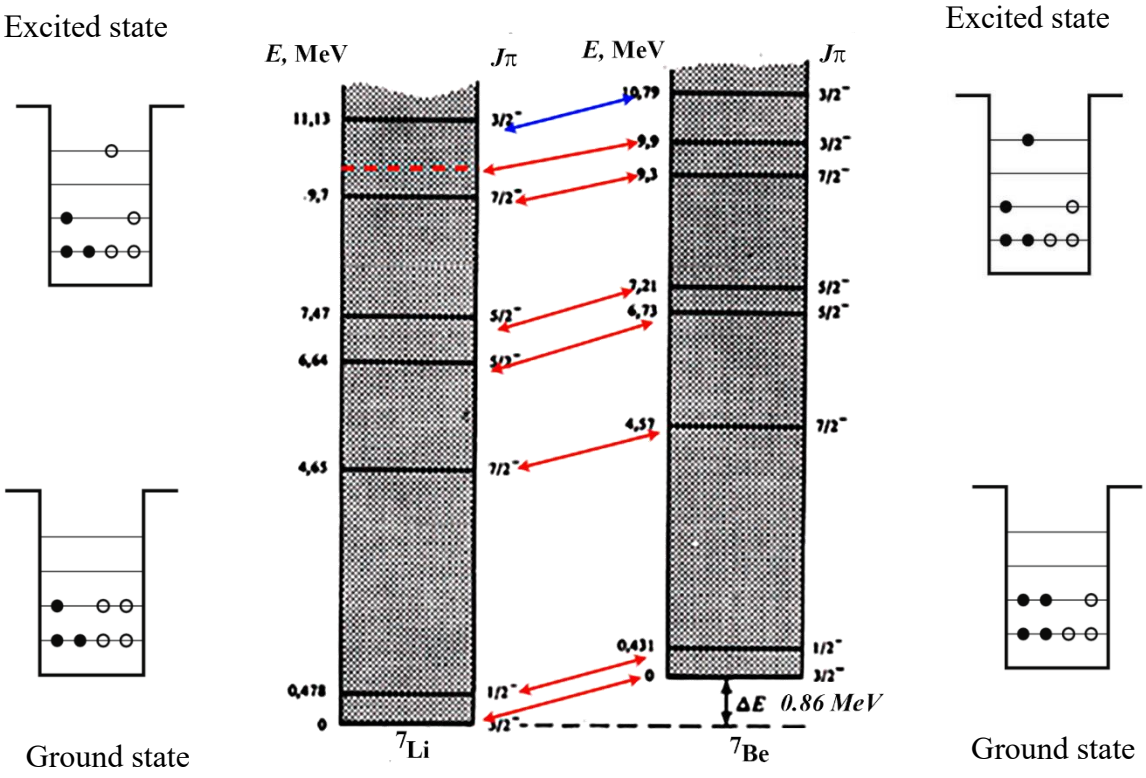

pp- and *nn*-interactions are the same.

Charge independence of nuclear forces: strong interaction in pp, nn, pn pairs in the same state is the same.

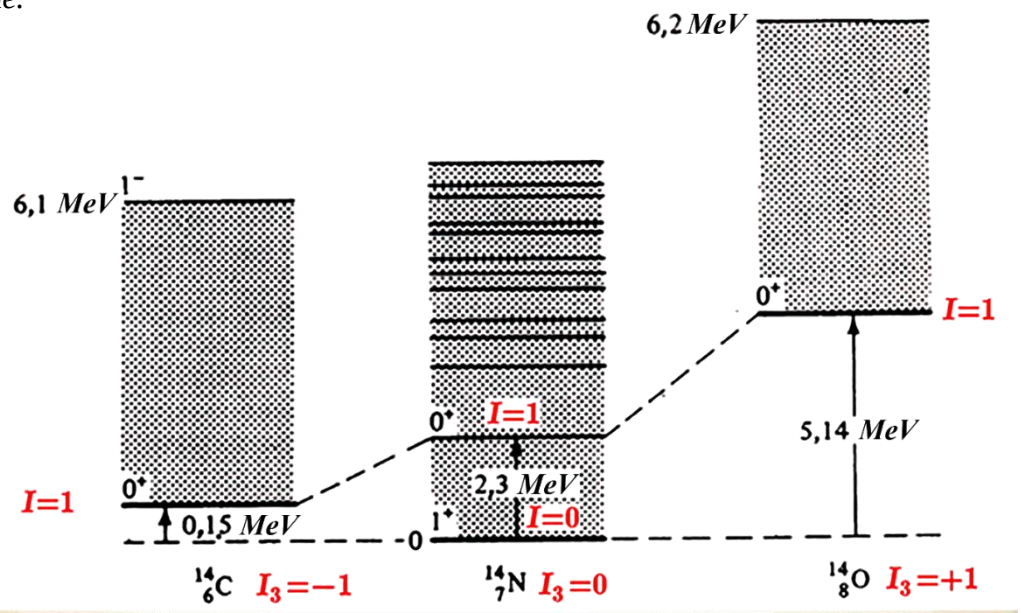

Fig. shows isotopic triplet: ground states in ^{14}C and ^{14}O, and excited 0^+ in ^{14}N. The differences in the energies of the states are associated with the influence of the Coulomb forces.

The isospin I_{gs} of the ground state of the nucleus takes the smallest possible value:

$$I_{gs} = I_{min} = |I_3| = |N - Z|/2 .$$

3.9. Generalized Pauli principle for nucleons

Pauli's principle for identical particles with half-integer spin.

Wave function of N identical particles $\psi\left(\vec{r}_1,\vec{s}_1;\ldots;\vec{r}_i,\vec{s}_i;\ldots;\vec{r}_k,\vec{s}_k;\ldots;\vec{r}_N,\vec{s}_N\right)$ must be antisymmetric with respect to the exchange of spatial $\vec{r}$ and spin $\vec{s}$ coordinates of any pair of particles.

$$\psi\left(\vec{r}_1,\vec{s}_1;\ldots;\vec{r}_i,\vec{s}_i;\ldots;\vec{r}_k,\vec{s}_k;\ldots;\vec{r}_N,\vec{s}_N\right)=-\psi\left(\vec{r}_1,\vec{s}_1;\ldots;\vec{r}_k,\vec{s}_k;\ldots;\vec{r}_i,\vec{s}_i;\ldots;\vec{r}_N,\vec{s}_N\right).$$

GENERALIZED Pauli's principle for identical particles with half-integer spin.

Wave function of N nucleons $\psi\left(\vec{r}_1,\vec{s}_1,\vec{\tau}_1;\ldots;\vec{r}_i,\vec{s}_i,\vec{\tau}_i;\ldots;\vec{r}_k,\vec{s}_k,\vec{\tau}_k;\ldots;\vec{r}_N,\vec{s}_N,\vec{\tau}_N\right)$ must be antisymmetric with respect to the exchange of spatial $\vec{r}$, spin $\vec{s}$ and isospin $\vec{\tau}$ coordinates of any pair of particles.

$$\psi\left(\vec{r}_1,\vec{s}_1,\vec{\tau}_1;\ldots;\vec{r}_i,\vec{s}_i,\vec{\tau}_i;\ldots;\vec{r}_k,\vec{s}_k,\vec{\tau}_k;\ldots;\vec{r}_N,\vec{s}_N,\vec{\tau}_N\right)=-\psi\left(\vec{r}_1,\vec{s}_1,\vec{\tau}_1;\ldots;\vec{r}_k,\vec{s}_k,\vec{\tau}_k;\ldots;\vec{r}_i,\vec{s}_i,\vec{\tau}_i;\ldots;\vec{r}_N,\vec{s}_N,\vec{\tau}_N\right)$$

.

Corollary: the wave function of the deuteron is even with respect to the permutation of the spatial (L = 0, 2) and spin (S = 1) variables⇒odd with respect to the permutation of isospin variables (⇒I_{deutron}=0)⇒ $\exists$ bound pairs *pp и nn* with the same angular momentum and spin (I_3(*pp*)=+1, I_3(*nn*)=—1).

- The Hamiltonian of nuclear forces depends on the value of I.
- For a given value of I, nuclear interactions are independent of I_3.
- Consequently, the Hamiltonian of the nuclear interaction must be invariant with respect to rotations in the isospin space (the law of conservation of isospin in the nuclear interaction).
- Neglecting electromagnetic effects, isospin is a good quantum number.

LECTURE 4

GAMMA PROCESSES

4.1. Gamma radiation: sources, interaction of gamma rays with matter

The nucleus can spontaneously transit into a state lower in energy (in this case, a γ – quantum is emitted) or decays into various final products. A necessary condition for such a transformation:

$$M \geq \sum_i m_i .$$

Here M is the mass of the initial nucleus, and m_i are the masses of the final products.

Decay types:

α–decay (emission of ^{4}He nuclei);

- β–decay ($e^{\pm}$, ν_e, $\tilde{\nu}_e$);
- γ–decay;
- spontaneous fission;
- nucleons emission;
- clusters emission (nuclei from ^{14}C to ^{32}S)

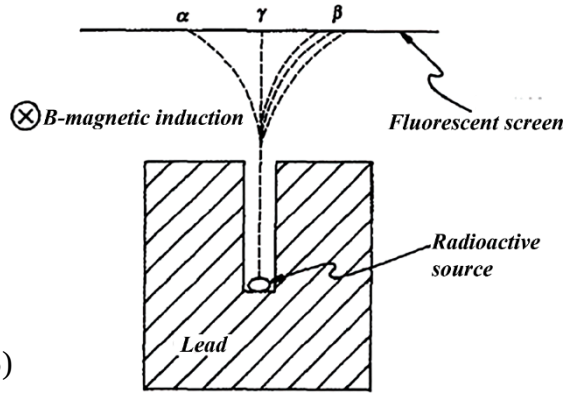

In the case when the decay of a nucleus with the emission of a nucleon is energetically impossible, the excited state is discharged due to the emission of γ – quanta — electromagnetic radiation with an energy of more than 100 keV.

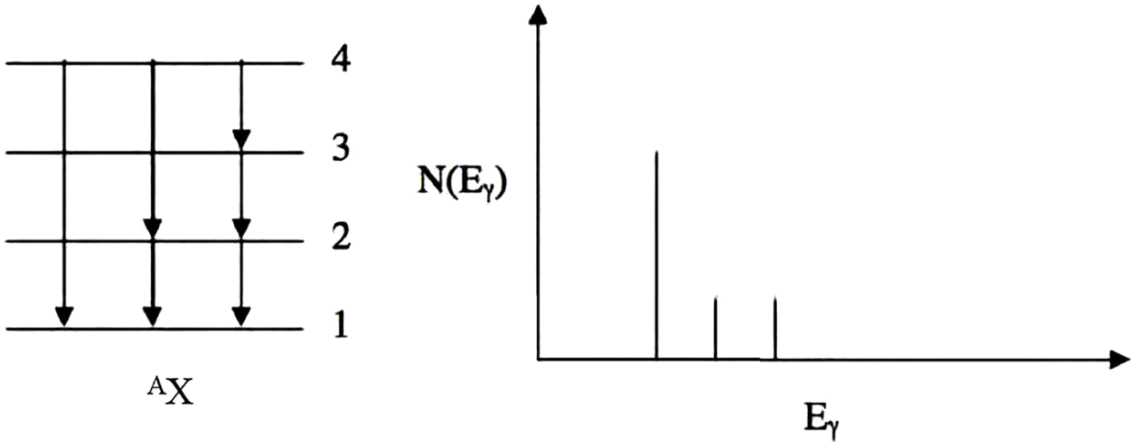

γ – radiation of nuclei is due to the interaction of individual nucleons of the nucleus with the electromagnetic field. An isolated free nucleon cannot emit (absorb) a γ – quantum (laws of conservation of energy and momentum). Inside the nucleus, a nucleon can emit a quantum, transferring part of the momentum to other nucleons. γ – radiation is not an intra-nucleon phenomenon, but an intranuclear one.

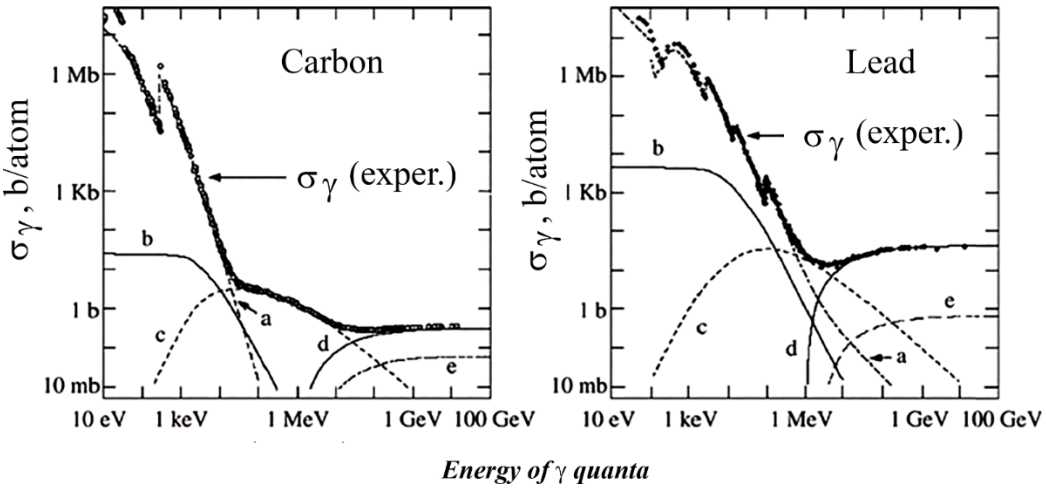

Experimental values of the cross section of γ – quanta scattering on carbon and lead: a – photo effect; b– coherent scattering; c– Compton scattering; d– pairs production in the field of nucleus; e– pairs production in the field of atomic electrons.

a) Photo effect.

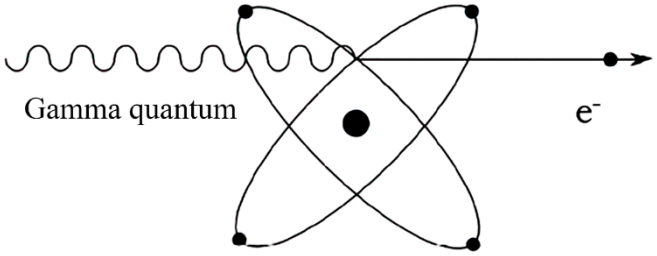

- In the case of bound electrons (with the binding energy E_b), the process of complete absorption of the incident γ – quantum (with frequency ν) and the emission of an electron with energy $E_e = h\nu - E_b$ are possible.
- The absorption cross section of the γ – quantum is especially large on the *K* shell (≈80%)
- The probability τ of the photo effect of a γ – quantum with energy E_γ on an atom with a charge *Z*:

$$\tau \cong \text{const} \times Z^n \Big/ E_\gamma^{3.5},$$

where $4 \le n \le 5$ for energies 0.1 MeV < E_γ <5 MeV.

For the case of low energies, the cross section for the photoelectric effect on the *K* – shell is:

$$\sigma_{\text{Ph}}^{K} = \left(\frac{32}{\varepsilon^7}\right)^{1/2} \alpha^4 Z^5 \sigma_{\text{T}},$$

where $\varepsilon = E_\gamma / \left(m_e c^2\right)$ – reduced energy of photon;

$\sigma_T = 8\pi r_e^2 / 3 = 0.665$ b – Thomson cross section of elastic photon scattering by electrons;

$r_e = e^2 / \left(m_e c^2\right) = 2.818$ fm – classical electron radius.

At high energies $\varepsilon \gg 1$ cross section is:

$$\sigma_{\text{Ph}}^K = 4\pi r_e^2 Z^5 \alpha^4 / \varepsilon .$$

b) Compton effect.

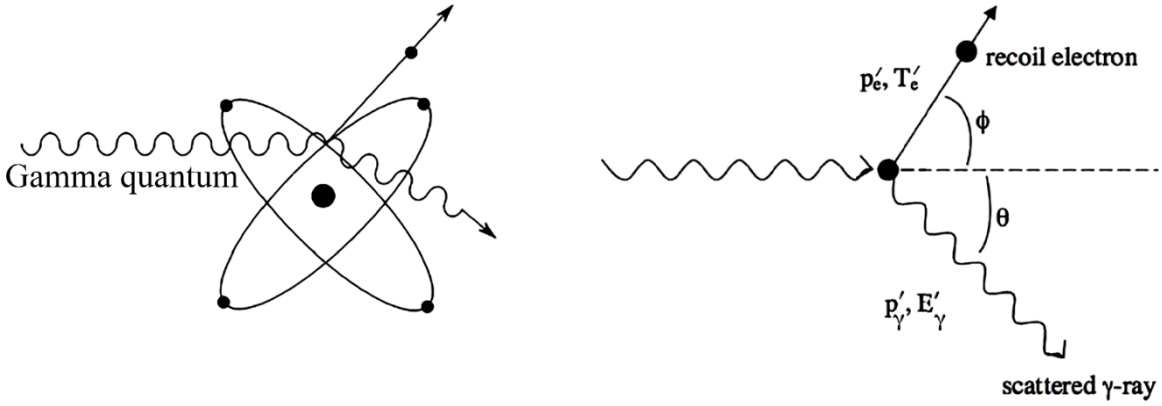

Initially, the energy-momenta of an electron at rest and a γ-quantum:

$$\boldsymbol{P}_e = \left(m_e c^2, 0\right); \quad \boldsymbol{P}_\gamma = \left(0, \vec{P}_\gamma\right).$$

After scattering: $\boldsymbol{P}_e + \boldsymbol{P}_\gamma = \boldsymbol{P}_e' + \boldsymbol{P}_\gamma'$.

From this it is possible to determine the energy of a γ-quantum scattered through an angle θ:

$$E_\gamma' = E_\gamma / \left[1 + \varepsilon\left(1 - \cos\theta\right)\right]; \quad \varepsilon \equiv E_\gamma / \left(m_e c^2\right).$$

The difference between the energies of the γ-quantum before and after the collision is transferred to the electron:

$$T_e' = E_\gamma \varepsilon \left(1 - \cos\theta\right) / \left[1 + \varepsilon\left(1 - \cos\theta\right)\right].$$

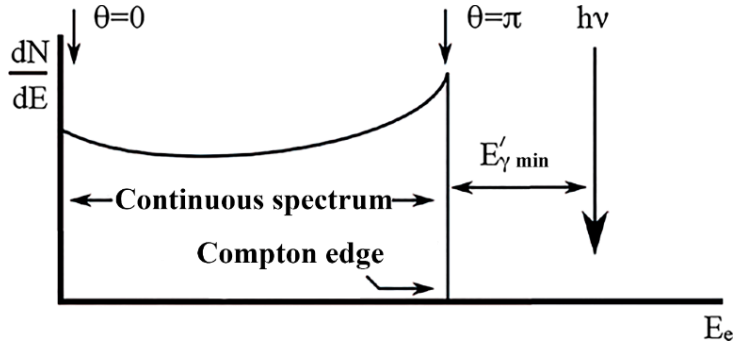

Consider two limiting cases.

1) Scattering of γ – quanta at small angles θ ~ 0:

$$E'_\gamma = E_\gamma; \quad T'_e = 0.$$

2) Backscattering of γ – quanta θ~π:

$$E'_{\gamma,\min} = E_\gamma \big/ (1+2\varepsilon) \underset{E_\gamma \gg m_e c^2}{\rightarrow} m_e c^2 \big/ 2 = 0.256 \text{ MeV}; \quad \varepsilon \equiv E_\gamma \big/ \left(m_e c^2\right);$$

and the maximum electron energy (Compton edge):

$$T'_{e,\max} = E_\gamma \, 2\varepsilon \big/ (1+2\varepsilon) \underset{E_\gamma \gg m_e c^2}{\rightarrow} E_\gamma \left(1 - 1/2\varepsilon\right).$$

After the γ – quantum is scattered through the angle θ, its wavelength increases by the value:

$$\Delta\lambda = \lambda' - \lambda = \Lambda(1-\cos\theta); \quad \Lambda = \hbar \big/ \left(m_e c\right) \approx 385 \text{ fm} \quad \textit{—Compton electron wavelength}.$$

The total cross section for the Compton scattering of a γ – quantum by an electron is given by the Klein-Nishina-Tamm formula:

$$\sigma = 2\pi r_e^2 \left\{ \frac{1+\varepsilon}{\varepsilon^2} \left[\frac{2(1+\varepsilon)}{1+2\varepsilon} - \frac{\ln(1+2\varepsilon)}{\varepsilon} \right] + \frac{\ln(1+2\varepsilon)}{2\varepsilon} - \frac{1+3\varepsilon}{(1+2\varepsilon)^2} \right\}; \quad \varepsilon \equiv E_\gamma \big/ \left(m_e c^2\right).$$

c) *Pairs production in the field of charged body*.

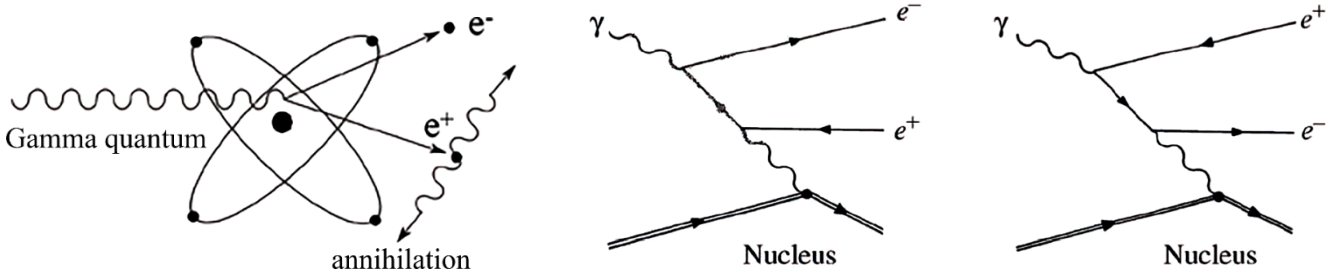

- The formation of e⁻— e⁺ pairs occur in the field of a charged body.
- The threshold energy of the γ – quantum for the formation of a pair in the field of the nucleus ($M_{ядр} \gg m_e$): $E_\gamma > 2m_e c^2$.
- The threshold energy of the γ – quantum for the formation of a pair in the electron field is $E\gamma > 4m_e c^2$. The probability of this process is much lower than the probability of birth in the field of a nucleus.
- The cross section of the process is determined by the energy ε and the charge of the nucleus - the absence of screening and complete screening.

$$1 \ll \varepsilon < \alpha^{-1} Z^{-1/3}: \; \sigma_{\text{pair}} = 4\alpha \, r_e^2 \, Z^2 \left[7\ln(2\varepsilon)/9 - 109/54 \right].$$

$$\varepsilon \gg \alpha^{-1} Z^{-1/3}: \; \sigma_{\text{pair}} = 4\alpha \, r_e^2 \, Z^2 \left[7\ln\left(183 Z^{-1/3}\right)/9 - 1/54 \right].$$

d) Relative contributions of three main processes of interaction of γ – quanta with matter.

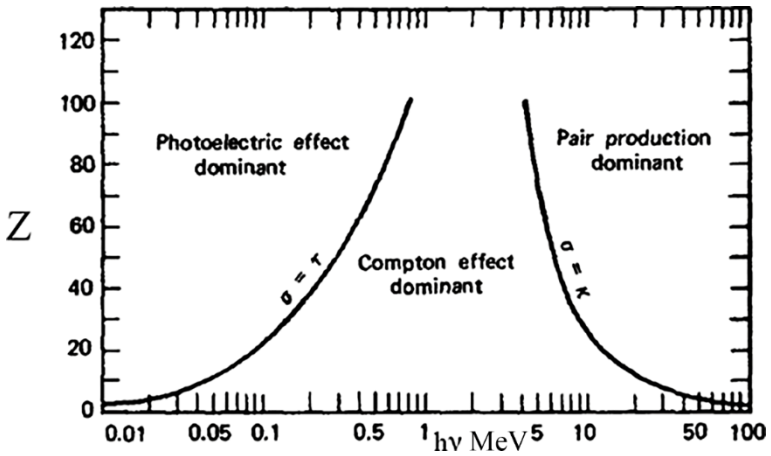

The curves show the energies at which (for a given charge *Z*) the photoelectric effect and Compton scattering have the same probability (left curve), and also pair production and Compton scattering have the same probability (right curve).

Full effective section:

$$\sigma_{tot} = \sigma_{Ph} + \sigma_{Compton} + \sigma_{pair}$$

Attenuation of the beam I_0 at a distance x at a particle density n: $I = I_0 \exp\left(-\sigma_{tot} \cdot n \cdot x\right)$

4.2. Registration methods and spectra of gamma rays

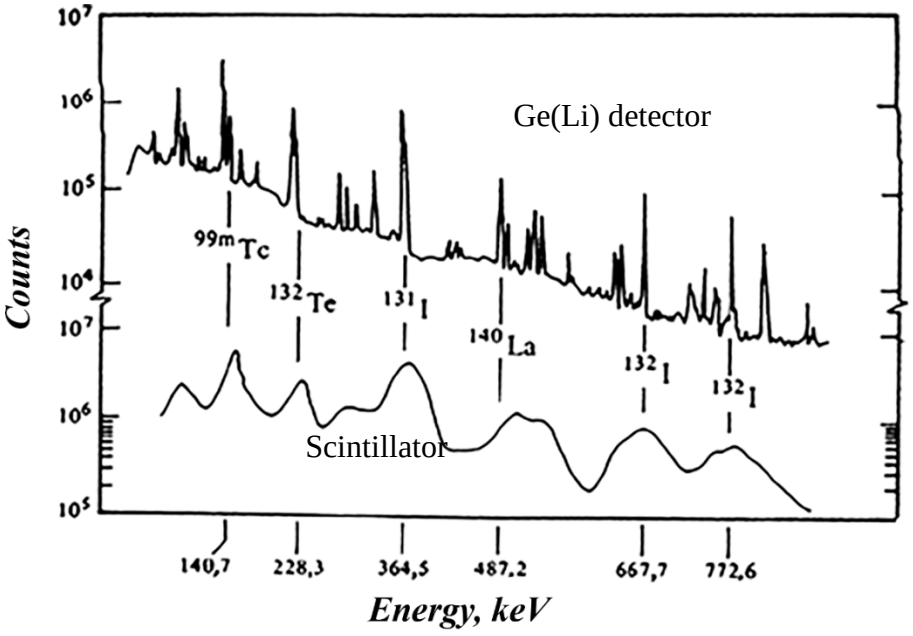

- Scintillation gamma spectroscopy – crystals NaI(Tl);
- Semiconductor detectors— Ge(Li);
- Combined methods (spark chamber + scintillators) - at high energies.

4.3. Multipolarity of gamma radiation

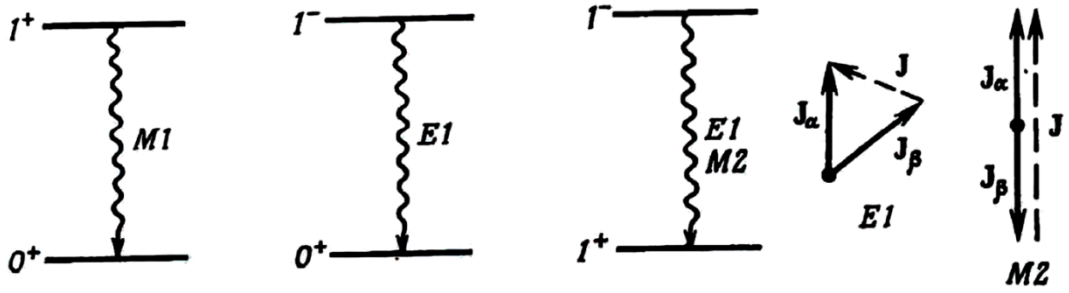

The emitted electromagnetic radiation is characterized by spatial parity π and angular momentum J – a positive integer.

- For electric radiation EJ: $\pi=(-1)^J$
- For magnetic radiation MJ: $\pi=(-1)^{J+1}$

Transitions between states α and β are limited by the laws of conservation of angular momentum and spatial parity:

$$J_\alpha = J_\beta + J,$$
$$\pi_\alpha = \pi_\beta \cdot \pi.$$

The probability $\lambda^{(J)}$ of electric and magnetic transitions of multipolarity J between two single-particle levels with total angular momenta $J_\alpha=J+1/2 \rightarrow J_\beta=1/2$ was obtained by V. Weisskopf (1908–2002):

$$\lambda^{(J)}_{\text{electric}}\left(\text{s}^{-1}\right)=10^{21}\frac{4.4\left(J+1\right)}{J\left[\left(2J+1\right)!!\right]^2}\left(\frac{3}{J+3}\right)^2\left[\frac{E_\gamma\left(\text{MeV}\right)}{197}\right]^{2J+1}\left[R\left(\text{fm}\right)\right]^{2J};$$

$$\lambda^{(J)}_{\text{magnetic}}\left(\text{s}^{-1}\right)=10^{21}\frac{1.9\left(J+1\right)}{J\left[\left(2J+1\right)!!\right]^2}\left(\frac{3}{J+3}\right)^2\left[\frac{E_\gamma\left(\text{MeV}\right)}{197}\right]^{2J+1}\left[R\left(\text{fm}\right)\right]^{2J-2}.$$

Here J is the angular momentum carried away by the gamma quantum, R is the radius of the nucleus. Since R is greater than 1 fm, then for the same multipolarity of radiation J, the probability of electric radiation is greater than magnetic. The probability of gamma decay increases with increasing radiation energy. E_γ <197 MeV, therefore the high angular momentum makes it difficult for the gamma – decay of the nucleus.

Multipole radiation

The use of a single-particle model allowed V. Weisskopf to estimate the speed of electromagnetic radiation of various multipolarity. In the one-particle model, it is assumed that radiation occurs when only one nucleon passes from one level of the atomic nucleus to another.

The figure shows the transition rates with the participation of one proton in a nucleus with a mass number A = 100. It can be seen from the figure that the probability of EJ radiation is higher than the probability of MJ radiation, and the probability of radiation sharply decreases with an increase in its multipolarity J.

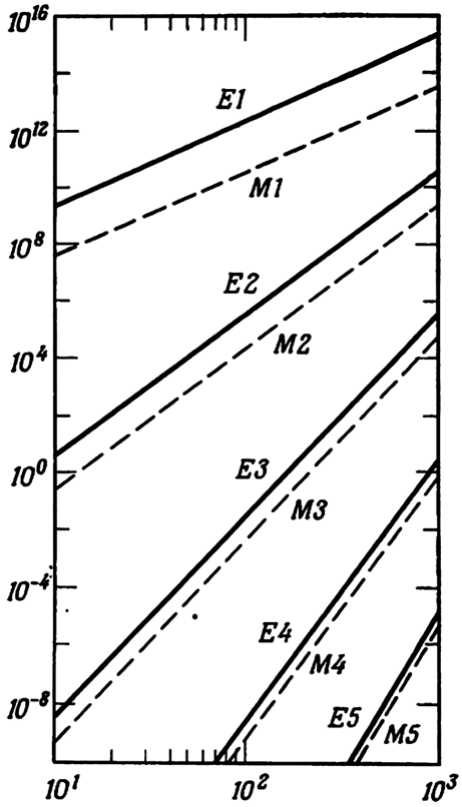

4.4. Gamma decay of isomers

Isomers are long-lived excited states of nuclei (metastable states).

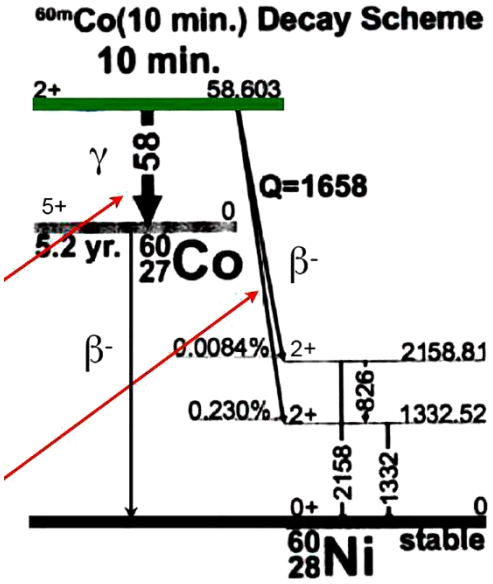

Deexcitation of the metastable state $^{60m}Co(2^+)$ occurs due to two unlikely processes:

a. Emission of γ – quanta with an energy of 58 keV: *M*3, *E*4, *M*5, *E*6, *M*7. Large multipolarities and low energy make γ – radiation unlikely. After γ – decay, ^{60}Co (5^+), emitting an electron, decays into the ground state ^{60}Ni (0^+).

b. β^- decay of $^{60m}Co(2^+)$ into excited states of ^{60}Ni (2^+) with subsequent transition of ^{60}Ni (2^+) to the ground state 0^+ due to the emission of gamma quanta. The figure shows the radiation energy in keV.

4.5. Conversion

The phenomenon of internal conversion consists in the fact that an atomic nucleus, which is in an excited state with energy E_i, can go to a state with a lower energy E_f, transferring the energy $W_{if} = E_i - E_f$ to one of the electrons of the atomic shell. As a result of internal conversion, an electron with energy $T_e = W_{if} - E_{K,L,M,\ldots}$ is emitted, where $E_{K,\,L,\,M,\ldots}$ is electron binding energy on *K*–, *L*–, *M*–,… shells. Internal conversion competes with γ – radiation. In the case of 0→0 transitions, internal conversion is the only way to remove the excitation of the nucleus. The peaks corresponding to the emission of electrons from different shells are observed against the background of a continuous spectrum of β^- - decay.

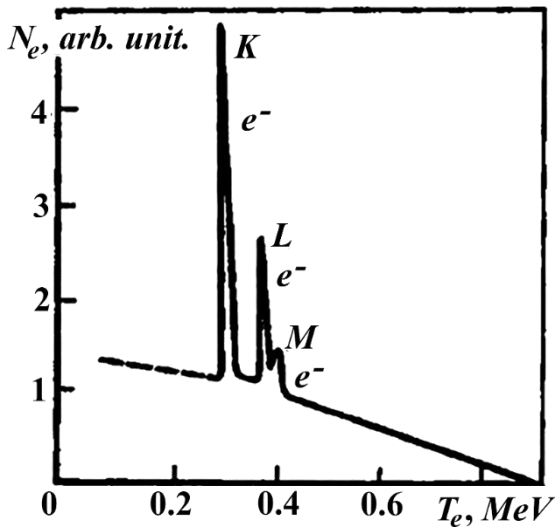

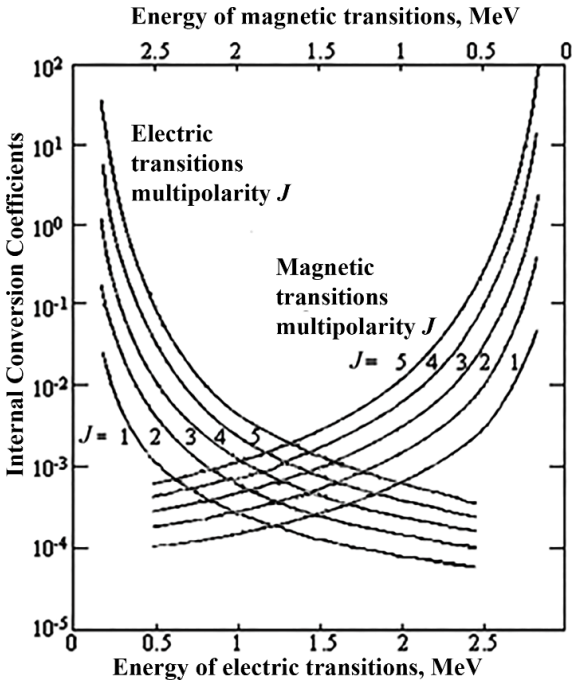

The competition between γ – radiation and internal conversion is characterized by the internal conversion coefficient (ICC), which is equal to the ratio of the probability of emission of a conversion electron N_e to the probability of emission of a γ – quantum N_γ:

$$\alpha = N_e / N_\gamma = \alpha_K + \alpha_L + \alpha_M + \ldots,$$

where α_K, α_L, α_M,… —partial ICC for electrons from *K*–, *L*–, *M*–, … shells. The ICC value strongly increases with an increase in the multipolarity of the transition and a decrease in its energy, and increases with an increase in the nuclear charge ($\alpha \sim Z^3$). The process of internal conversion is accompanied by *X*-ray radiation arising from the transition of electrons from the outer shells of the atom to the states of the *K*–, *L*–, *M*–,… shells released as a result of the conversion.

ALPHA DECAY

4.6. Alpha decay: basic experimental data, alpha-decay region, decay chains

a) Basic experimental data.

- α– decay is the emission from the nucleus of α–particle (^{4}He nucleus):

$$^{A}Z \rightarrow {}^{(A-4)}(Z-2) + {}^{4}\text{He}.$$

- Energetically, such a decay is possible if the condition for the binding energy is satisfied: $B(2,4) > B(Z,A) - B(Z-2,A-4)$.

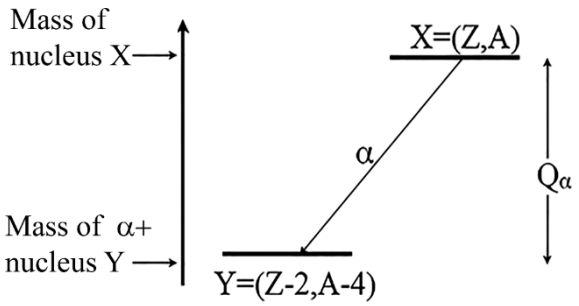

The *Q* value of the reaction $Q_\alpha = B(Z-2,A-4) + B(2,4) - B(Z,A)$.

The energy of the emitted α– particle $E_\alpha = Q_\alpha M_d / (M_d + M_\alpha)$, where M_d and M_α are masses of daughter nucleus and alpha particle.

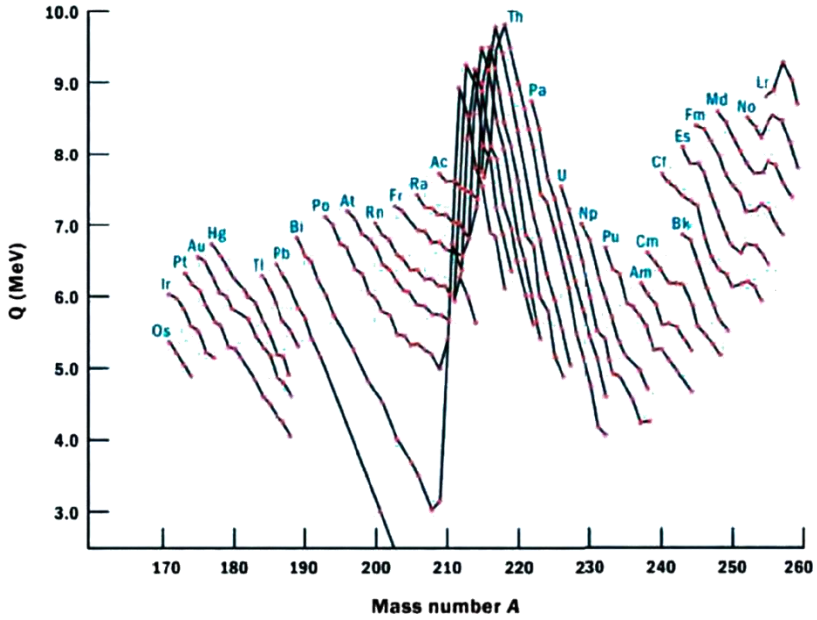

- When comparing the alpha decay energies of different isotopes of the same element, a regular decrease in energy is observed with an increase in the mass number.
- This rule is valid for nuclei with $A<209$ and $A>215$ and is violated for intermediate elements.
- This allows alpha particle energies to be predicted for unknown isotopes.

Decay with the emission of a α – particle can occur with the formation of a residual nucleus in an excited state. This leads to the appearance of a fine structure α – particle spectra.

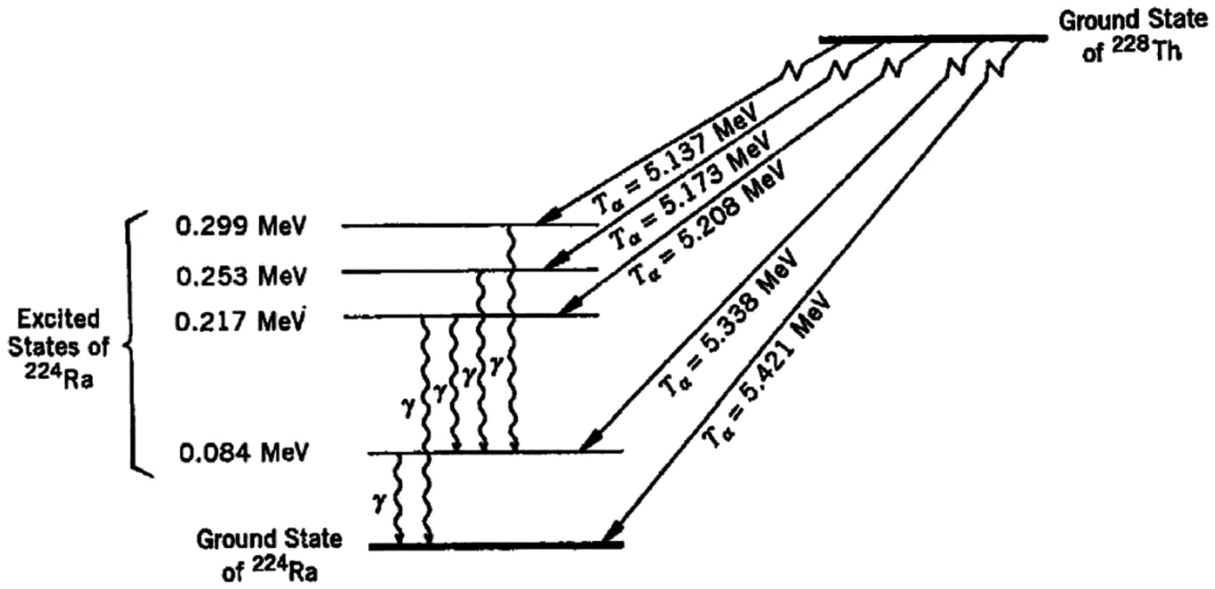

b) Alpha decay region.

There is a region of nuclei that allow spontaneous alpha decay.

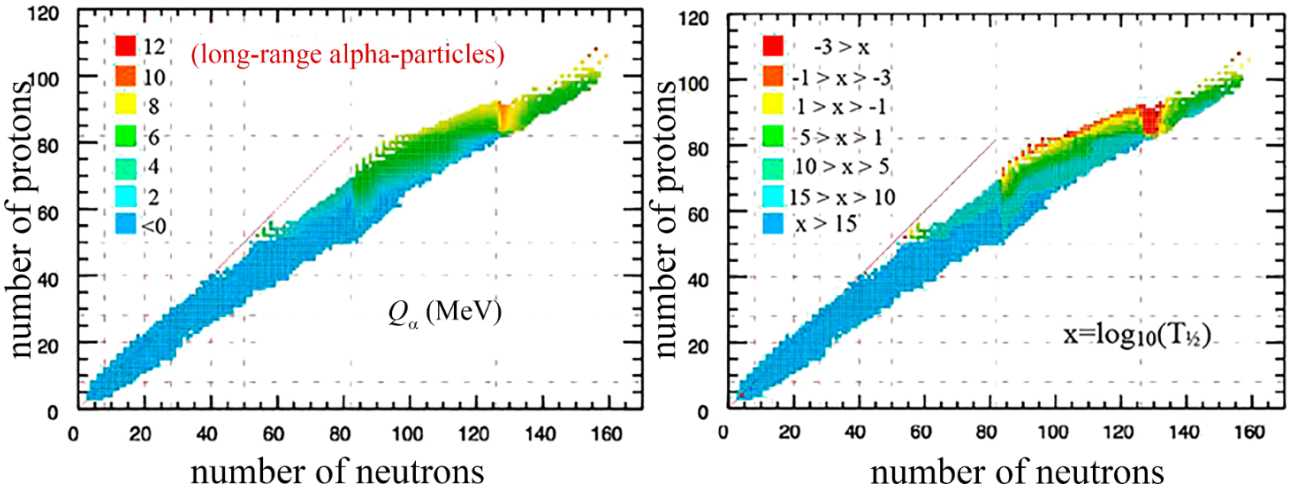

Unstable nuclei with respect to alpha decay.

c) Decay chains.

All natural radioactive nuclides with *A*> 209 can be arranged in three successive chains called decay chains or radioactive cascade.

Each decay chain begins with a α – radioactive nuclide called the parent isotope, and each subsequent radioactive element of the chain is a decay product of the previous one.

Three main decay chains (or families) are observed in nature, commonly called the thorium series (parent isotope thorium-232), the uranium series (parent isotope uranium-238) and actinium series (parent isotope uranium-235).

The fourth chain, the neptunium series (parent isotope neptunium-237, $T_{1/2}$= 2.14 million years) is already extinct in nature.

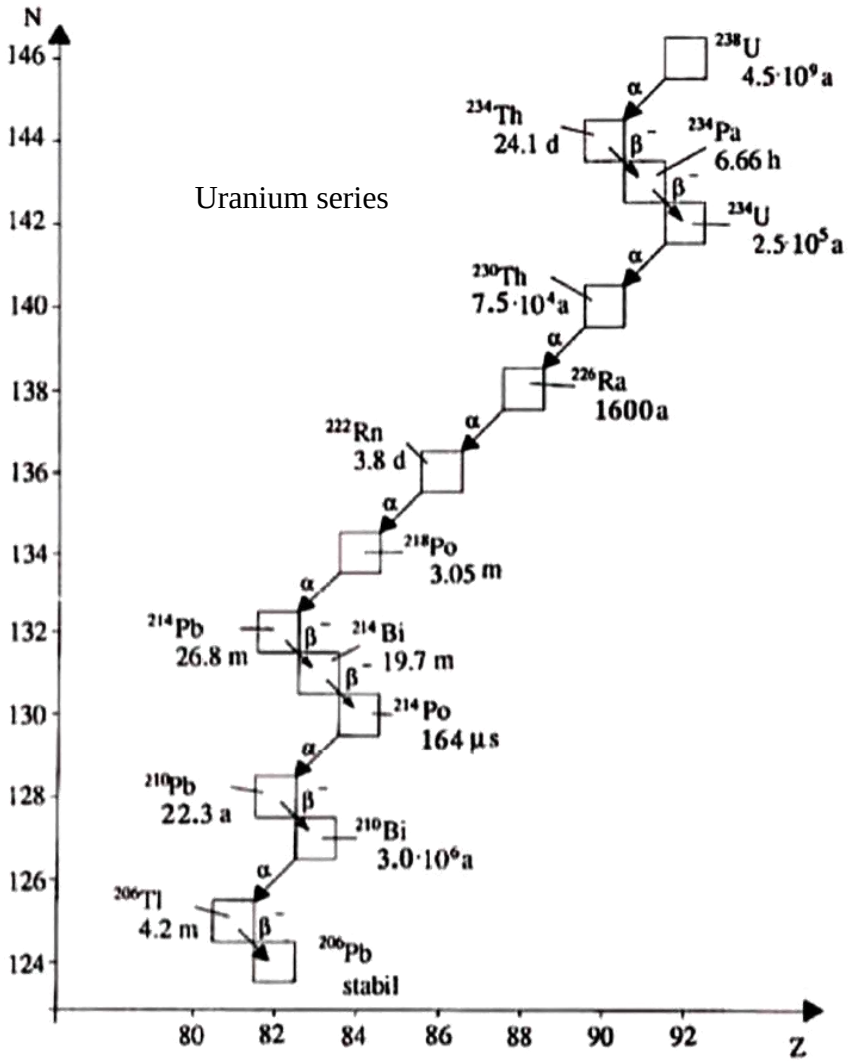

4.7. Energy ratios in alpha decay. Geiger-Nuttall's law

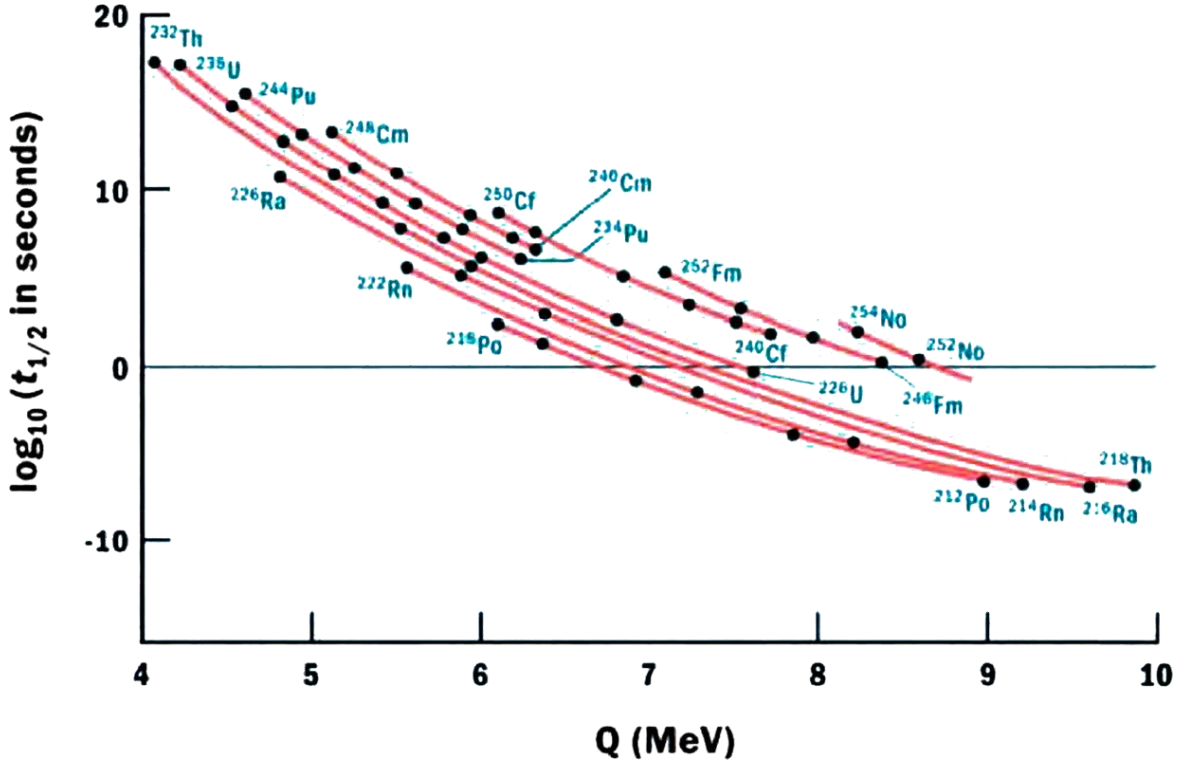

Geiger and Nuttall found that for all three decay chains, the decay constant λ and the α-particle range in the substance R_α are related by the relation:

$$\lg(\lambda) = A \cdot \lg(R_\alpha) + B,$$

with the same constant A for all three radioactive families. Since the range is related to the α-particle energy by a power function a similar relation should be fulfilled for the values of α-particle energies and the quantities Q of the reaction.

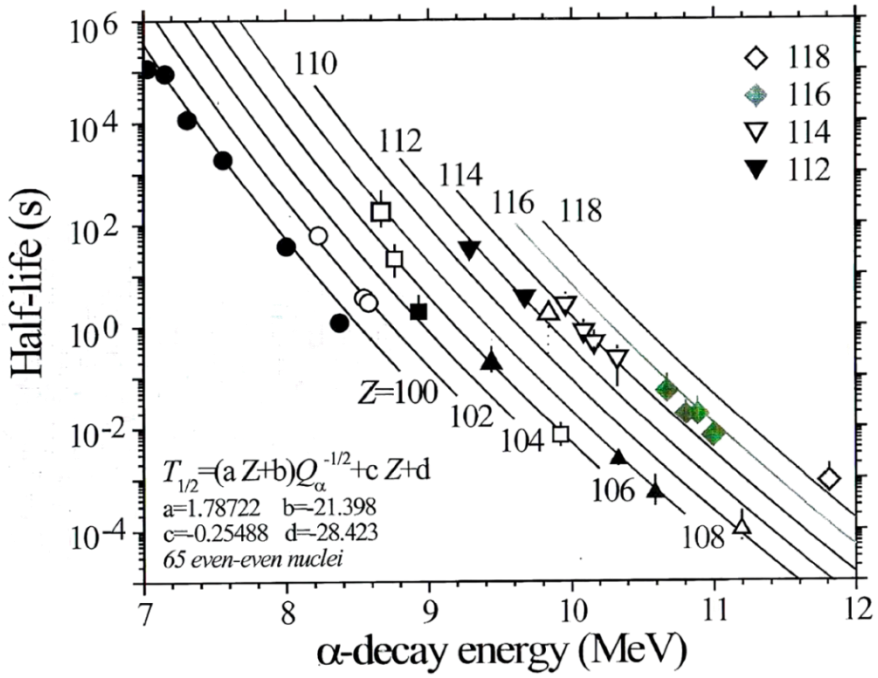

4.8. Theoretical interpretation of alpha decay

The transmittance is described as:

$$T = \mathrm{e}^{-G},$$

where G is the Gamow factor:

$$G = \frac{2}{\hbar}\int_{R}^{r_C}\left[2m\left|V_C(r) - E_\alpha\right|\right]^{1/2} dr .$$

On the figure $R=a$, $r_C = b$.

The probability of a α-particle emission is proportional to its velocity (the number of "approaches" to the barrier):

$$w = \frac{v_\alpha}{2R}T .$$

$$G = 4Z\alpha\left(\frac{2mc^2}{E_\alpha}\right)^{1/2}\left[\cos^{-1}\sqrt{\frac{R}{r_C}} - \sqrt{\frac{R}{r_C}\left(1-\frac{R}{r_C}\right)}\right]$$

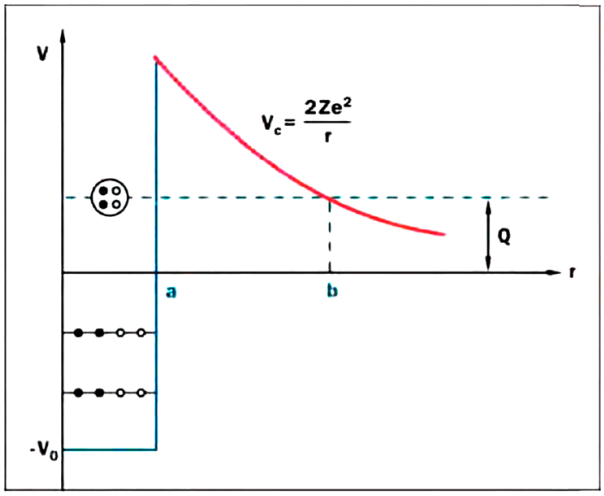

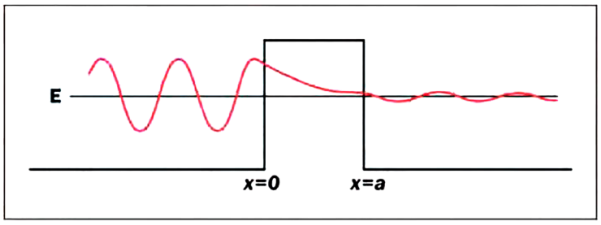

Thus for α–particle with the energy of 5 MeV and for barrier equal to 40 MeV:

$$G \sim 4\pi\alpha Z/\beta, \text{ where } \beta = v_\alpha / c.$$

$$G \sim \frac{Z}{\beta} \sim \frac{Z}{\sqrt{E_\alpha}};$$

$$\log_{10} t_{1/2} = a + b\,Z\,E_\alpha^{-1/2},$$

which allows to explain the Geiger – Nuttall's law.

LECTURE 5

BETA PROCESSES

5.1. Types of beta-decay

- β-decay - the process of spontaneous transformation of an unstable nucleus into an isobar nucleus with a charge different from the initial one by $\Delta Z = 1$, due to the emission of an electron (positron) or the capture of an electron from the atomic shell;
- β-decay is due to weak interaction, the intensity of which is 10^{14} times less than the nuclear one;
- β-decay processes take place whenever they are energetically possible;
- the spectrum of emitted β-decay particles is continuous.

a) Electron emission.

$${}^{A}Z \rightarrow {}^{A}\left(Z+1\right)+e^{-}+\tilde{\nu}_{e}$$

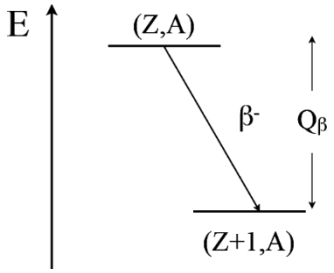

β- decay occurs with the emission of an electron and an electron antineutrino from the nucleus.

$$Q_{\beta}=\left[M\left(A,Z\right)-M\left(A,Z+1\right)-m_{e}\right]c^{2}$$

An example of β-decay - neutron decay: $n \rightarrow p + e^{-} + \tilde{\nu}_{e} + 0.782$ MeV.

The neutron mean lifetime is 879.4±0.6 s.

b) Positron emission.

$${}^{A}Z \rightarrow {}^{A}\left(Z-1\right)+e^{+}+\nu_{e}.$$

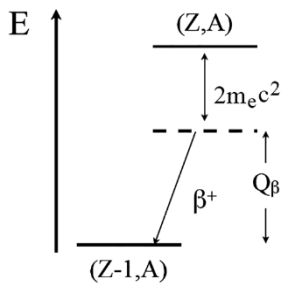

- β^+ decay occurs with the emission of a positron and an electron neutrino from the nucleus.

$$Q_{\beta^+} = \left[M(A,Z) - M(A,Z-1) - m_e \right] c^2 ;$$

- β^+ decay is possible only in the case when:

$$M_Z c^2 > M_{(Z-1)} c^2 + 2 m_e c^2 ,$$

where M_Z and M_{Z-1} are the masses of atoms with a nuclear charge Z and (Z-1).

- β^+ decay of a free proton is impossible!

c) Electron capture.

$$e^- + {}^A Z \rightarrow {}^A (Z-1) + \nu_e .$$

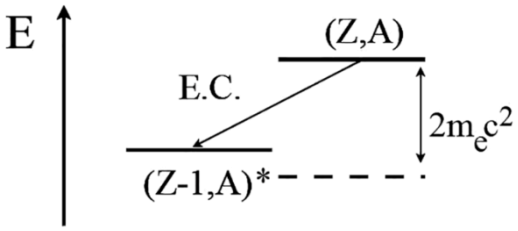

- The nucleus can capture an electron from the atomic shells. Typically, a *K*-electron is captured.
- A new atom is formed in an excited state (*) with a hole in the *K* shell. Its transition to the ground state is accompanied by the emission of characteristic *X*-rays.

$$Q_{EC} = \left[M(A,Z) - M(A,Z-1) + m_e \right] c^2 .$$

d) Competing beta decays.

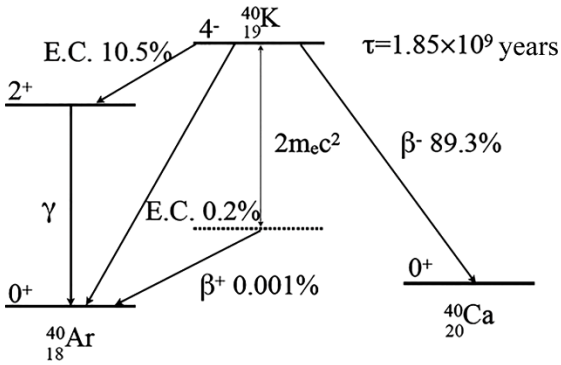

15 mg of ^{40}K in the human body results in an annual radiation dose of 0.5 mSv.

e) Values of *Q* Reaction.

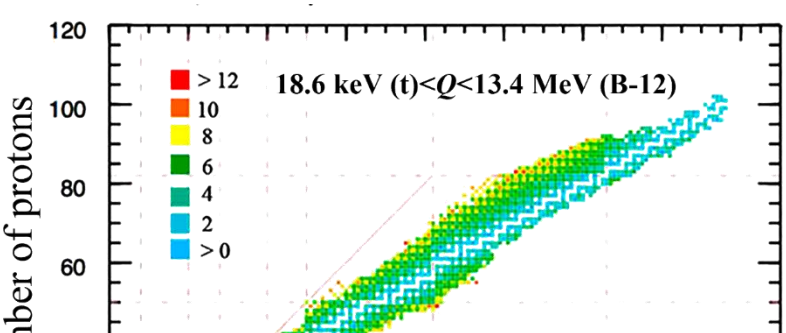

5.2. Shape of the beta spectrum. Experimental proof of the existence of neutrinos

a) Shape of beta spectrum.

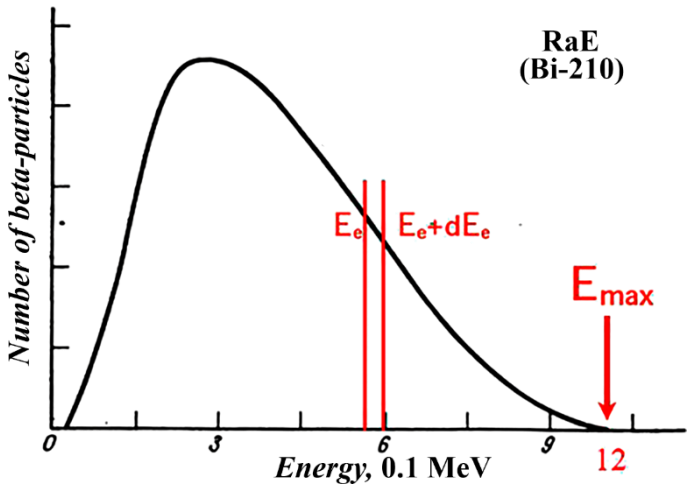

The beta decay of RaE element was considered ($^{210}_{83}\mathrm{Bi}$):

Questions:

- Why is the spectrum continuous?
- Where do electrons come from in the nucleus?

Wolfgang Pauli (1900-1958) hypothesis: there is a new uncharged particle (*antineutrino* $\tilde{\nu}_e$), weakly interacting with matter:

$n \rightarrow p + e^{-} + \tilde{\nu}_e + 0.782$ MeV.

$dw \sim d\vec{p}_e \cdot d\vec{k}$ —the probability of e^{-} emission with a momentum in the interval $d\vec{p}_e$ and $\tilde{\nu}_e$ with a momentum in the interval $d\vec{k}$.

We put $m_\nu = 0$, Q is β – decay energy, E – kinetic energy of an electron:

$$E = c\sqrt{p^2 + m^2c^2} - mc^2 . \qquad (*)$$

The β-decay energy is distributed between e^- and $\tilde{\nu}_e$:

$$Q = E + ck ;$$

$$dw = D\delta\left(Q - E - ck\right) d\vec{p}_e \cdot d\vec{k} = \frac{1}{c^3} D\delta\left(Q - E - ck\right) p^2 dp \left(ck\right)^2 d\left(ck\right) d\Omega_e d\Omega_k ; \qquad (**)$$

N_0– total number of decays. Then $d\omega$ – number of decays with momentum e from p up to $p+dp$ is obtained by integrating (**) over (ck) and angles:

$$d\omega = \frac{\left(4\pi\right)^2}{c^3} N_0 D p^2 \left(Q - E\right)^2 dp .$$

Using (*), we pass from the distribution over the momentum e^- to the distribution over its energy:

$$d\omega = \frac{\left(4\pi\right)^2}{c^3} N_0 D p^2 \left(Q - E\right)^2 dp ; \; \omega\left(E\right) \equiv \frac{d\omega}{dE} = N_0 B \sqrt{E\left(E + 2mc^2\right)} \left(E + mc^2\right) \left(Q - E\right)^2 ,$$

$$B = \left(4\pi / c^3\right)^2 D, \quad D \sim \left|\left\langle \beta \right| H_W \left| \alpha \right\rangle\right|^2 = g^2 \left|M\right|^2 , \; g = 0.89 \cdot 10^{-4} \text{ MeV} \cdot \text{fm}^3 \text{— Fermi constant.}$$

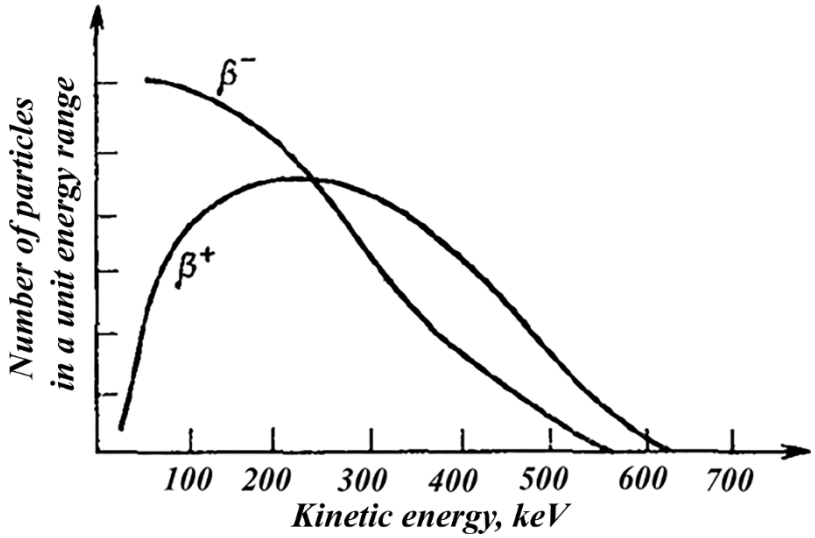

- The experimental beta-decay spectrum is distorted by the Coulomb potential of the nucleus.
- Positrons are more often observed with high energies and electrons with low energies.
- Spectral distortions are taken into account by the Fermi function $F(\pm 1, Z, E)$, where the sign corresponds to the sign of the charge of the emitted particle.
- Then the formula for the distribution of emitted beta particles can be written as:

$$d\omega/dp = \text{const} \cdot F\left(\pm 1, Z, E\right) p^2 \left(Q - E_e\right)^2 .$$

b) Experimental proof of the existence of antineutrino.

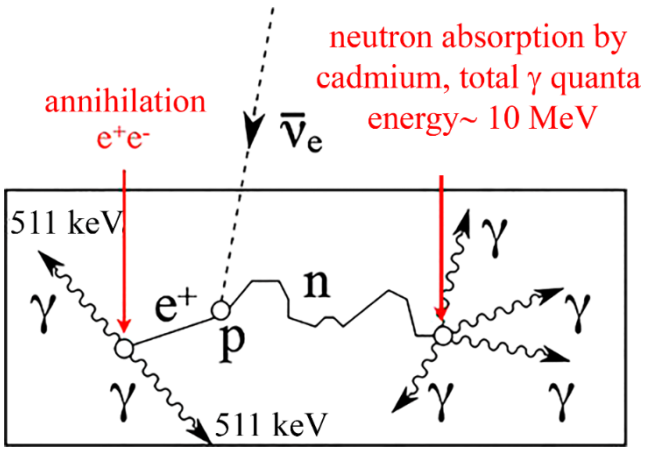

The neutrino has a cross section for interaction with nuclei of the order 10^{-44}cm^2.

Cowan and Reines experiment (1953) on the direct registration of antineutrinos. Based on the inverse beta decay,

$p + \tilde{\nu}_e \rightarrow n + e^+$.

Antineutrino flux from a nuclear reactor 10^{13} см$^{-2}$ с$^{-1}$ is headed for the target H_2O+$CdCl_2$, the number of protons is $3 \cdot 10^{28}$ см$^{-3}$. To exclude the background, the installation is located underground and surrounded by a lead and paraffin shielding. Two annihilation gamma quanta were recorded and, 5 μs later, gamma quanta from the capture of a Cd neutron. 3 events/hour were registered (Nobel Prize 1995).

c) Neutrino vs antineutrino.

Davis experiment (1955, B. Pontecorvo's chlorine-argon method).

If ν_e and $\tilde{\nu}_e$ are different particles, then cross sections of $\nu_e + n \rightarrow p + e^-$ and $\tilde{\nu}_e + n \rightarrow p + e^-$ should differ. The cross section of $\nu_e + n \rightarrow p + e^-$ has the same order of magnitude as $p + \tilde{\nu}_e \rightarrow n + e^+$ (10^{-43} cm^2).

Instead of free neutrons $^{37}_{17}\mathrm{Cl}$ with 20 neutrons was used. The target: 4000 l CCl_4. $\tilde{\nu}_e$ were taken from nuclear reactor.

Reaction: $\tilde{\nu}_e + {}^{37}_{17}\mathrm{Cl} \rightarrow e^- + {}^{37}_{18}\mathrm{Ar}$. Argon is released from CCl_4.

$T_{1/2}$ (^{37}Ar) = 35 days (electronic capture): $e^- + {}^{37}_{18}\mathrm{Ar} \rightarrow \tilde{\nu}_e + {}^{37}_{17}\mathrm{Cl}$. Electronic capture is 80% accompanied by the Auger effect with low electron energy. Registration of Auger electrons (with a Geiger counter) would indicate the formation of Ar.

Received: $\sigma_{\tilde{\nu}n} \leq 0.25\times10^{-45}$ см$^2 \ll \sigma_{\nu n}$.

Conclusion: $\nu_e \neq \tilde{\nu}_e$.

5.3. Parity nonconservation in beta-decay

The Wu experiment used the reaction $^{60}\text{Co}\rightarrow{}^{60}\text{Ni}+e^{-}+\tilde{\nu}_e$. The spins of all nuclei are oriented along the *Z* axis. In the case of conservation of parity, the number of electrons fixed in detector 1 should be equal to the number of electrons recorded in detector 2. It turned out that electrons are emitted mainly against the direction of the spin. This dependence of the electrons on the direction is a consequence of the fact that left-handed electrons participate in the weak interaction.

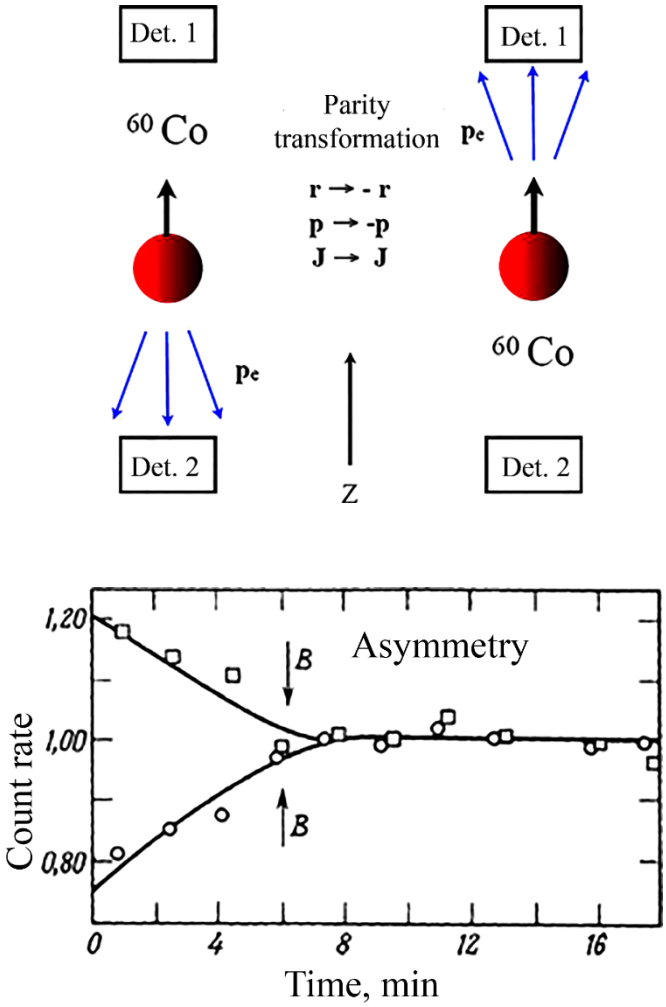

Shown is the normalized count rate for two cases of the direction of the magnetic field. When the sample was warmed up, the polarization of the nuclei was destroyed, and the effect disappeared.

5.4. Neutrino spirality

- If the probability of different directions of the spin *J* is the same, one speaks of zero polarization.
- If the spins are directed in one direction — one hundred percent polarization.
- Transverse polarization — the spin is directed perpendicular to the momentum *p*.

- Longitudinal polarization — spin is parallel to the momentum *p*.
- Right-handed particle — spin is directed along the momentum *p*.

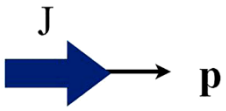

- Left-handed particle — spin is directed against the momentum *p*.

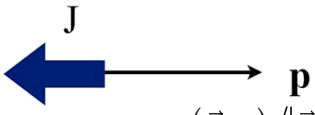

- The helicity *h* is determined by: $h = \left(\vec{J},\vec{p}\right)\Big/\left|\vec{J}\right|\left|\vec{p}\right|$. The right-handed particle has positive helicity ($h = +1$), left-handed — negative ($h = -1$).

The spirality of neutrinos can be measured experimentally (Goldhaber, 1958). The reaction was investigated:

$^{152}\mathrm{Eu}(0^{-})+e^{-} \rightarrow {}^{152}\mathrm{Sm}(1^{-})+\nu_e$ (959 keV).

The allowed transition is of the Gamow-Teller type. The spins of the excited daughter nucleus and the neutrino are antiparallel, since they scatter in different directions, their helicity will be the same. The excited nucleus emits an *E*1 gamma-ray.

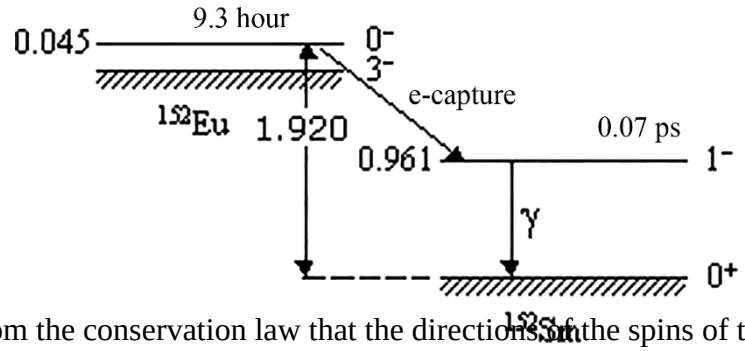

It follows from the conservation law that the directions of the spins of the photon and samarium coincided. Thus, the photon has the same helicity as the nucleus, and, accordingly, the same helicity as the neutrino. The selection of the required photons is performed using resonant scattering on a samarium target.

The experimental setup is shown in the figure:

1– samarium source;

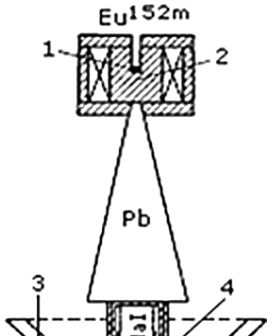

2 – analyzing magnet;

3 – diffuser Sm_2O_3;

4–photomultiplier tube (PMT) protection.

The experiments have shown that the spirality of neutrinos is always negative (h = -1). Neutrino always has left-handed helicity, and antineutrino always right-handed.

5.5. Types of beta decay transitions

a) Fermi theory of beta decay.

Consider beta decay $^{17}\mathrm{F} \rightarrow {}^{17}\mathrm{O} + e^+ + \nu_e$.

Initial state takes the form: $\Psi_0 = \psi_p\left(\vec{r}_p\right)$ (single proton state).

Final state (neutron, positron and neutrino):

$$\Psi_f = \psi_n\left(\vec{r}_n\right)\psi_e\left(\vec{r}_e\right)\psi_\nu\left(\vec{r}_\nu\right).$$

$$\text{Transition probability} = \frac{2\pi}{\hbar}\left|H_{f0}\right|^2 \rho_f\left(E_0\right),$$

where H_{f0} — matrix element of transition from initial to final state:

$$H_{f0} = \int \Psi_f^* \hat{H} \Psi_0 d^3\vec{r}_n d^3\vec{r}_p d^3\vec{r}_e d^3\vec{r}_\nu ;$$

$\rho_f(E_0)$ — the density of final states at the decay energy E_0. Fermi suggested that at the moment of interaction, all 4 particles are at the same point in space

$H_{f0} = G_w \int \psi_n^*\left(\vec{r}\right)\psi_e^*\left(\vec{r}\right)\psi_\nu^*\left(\vec{r}\right)\psi_p\left(\vec{r}\right)d^3\vec{r}$, G_w determines the energy of interaction.

For the electron and neutrino, we use the plane wave approximation (normalized to the volume *V*):

$$\psi_\nu\left(\vec{r}\right) = e^{i\left(\vec{k}_\nu,\vec{r}_\nu\right)}\Big/\sqrt{V}; \quad \psi_e\left(\vec{r}\right) = e^{i\left(\vec{k}_e,\vec{r}_e\right)}\Big/\sqrt{V}; \Rightarrow \quad H_{f0} = \frac{G_w}{V}\int \psi_n^*\left(\vec{r}\right)\psi_p\left(\vec{r}\right)e^{-i\left(\vec{k}_e+\vec{k}_\nu,\vec{r}\right)}\, d^3\vec{r}.$$

Using the smallness of the exponent:

$$H_{f0} = \frac{G_w}{V}\int \psi_n^*\left(\vec{r}\right)\psi_p\left(\vec{r}\right)d^3\vec{r} - \frac{iG_w}{V}\left(\vec{k}_e+\vec{k}_\nu, \int \psi_n^*\left(\vec{r}\right)\vec{r}\,\psi_p\left(\vec{r}\right)d^3\vec{r}\right).$$

If $\int \psi_n^*\left(\vec{r}\right)\psi_p\left(\vec{r}\right)d^3\vec{r} \neq 0$, then the transition is called allowed, if $M = 0$ - forbidden.

For the considered case of decay ^{17}F: $\int \psi_n^*(\vec{r})\psi_p(\vec{r})\,d^3\vec{r} \approx 1 \Rightarrow \quad H_{f0} \approx \frac{G_w}{V} M$.

b) Transition types.

Allowed transitions are:

1) *Fermi transitions*: the total spin of leptons is zero (singlet state). Do not change: orbital angular momentum of the nucleus *L*, parity *P*, isospin *I*.

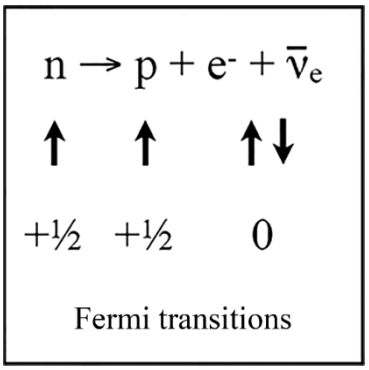

$\Delta L=0$, $\Delta P=0$, $\Delta I=0$, $\Delta I_3=\pm 1$, $\Delta J=0$.

2) *Gamow-Teller transitions:* the total spin of leptons is equal to unity (triplet state). Transitions $0 \rightarrow 0$ are prohibited.

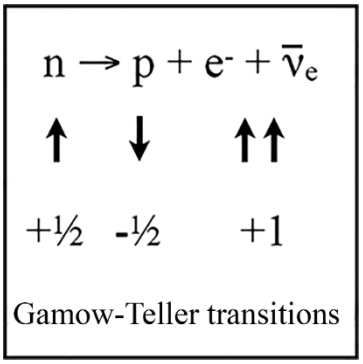

$\Delta L= 0$, $\Delta P=0$, $\Delta I=0, \pm 1$, $\Delta I_3=\pm 1$, $\Delta J=0, \pm 1$.

Forbidden decays are those which are substantially more improbable than Fermi and Gamow-Teller transitions, due to parity π violation, and as a result have long decay times.

In this case the angular momentum (*L*) of the lepton system can be non-zero (in the center-of-mass frame of the system).

5.6. Generations of leptons. Electron, muon, and tau neutrino

1-st generation	2-nd generation	3-d generation
e^- 0.511 MeV	μ^- 105.7 MeV	τ^- 1784 MeV
ν_e <1.1 eV	ν_μ <190 keV	ν_τ <18.2 MeV

5.7. Decays of pions and muons

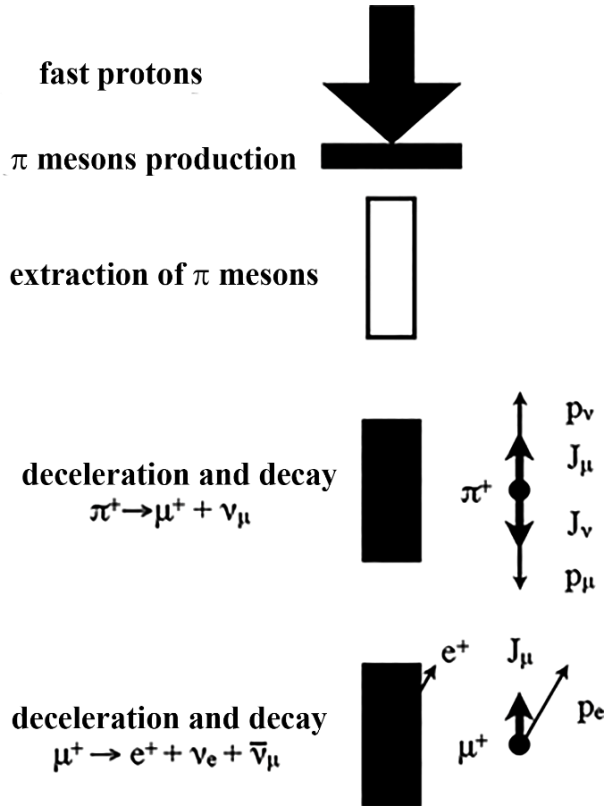

Muon.

- Spin ½.
- Mass 105.66 МэВ/c^2.
- Mean life $2.2 \cdot 10^{-6}$c.
- Decay channels:

$$\mu^- \to e^- + \tilde{\nu}_e + \nu_\mu$$
$$\mu^+ \to e^+ + \nu_e + \tilde{\nu}_\mu.$$

- Muons can be obtained from decays of π-mesons and in electron-positron collisions.

Muon decay is a purely lepton process.

Time dilation proof and decay of muon.

When cosmic radiation interacts with air molecules, pi-mesons are formed, producing muons at an altitude of about 20 km. To reach the earth's surface, muons need more than 66 μs with a lifetime of 2.2 μs. Conclusion: Einstein's SRT is valid.

$$t' = \frac{t - \beta x/c}{\sqrt{1-\beta^2}}; \beta = V/c.$$

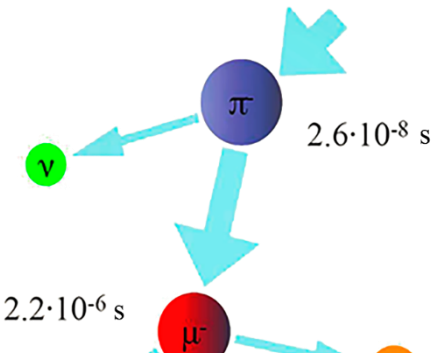

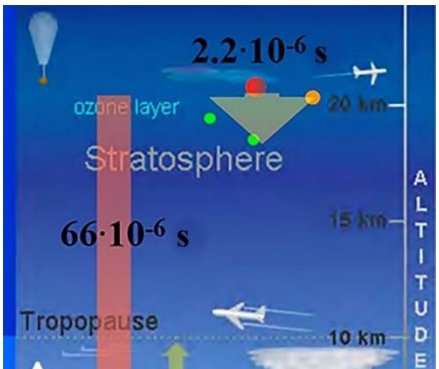

5.8. Neutrino mass. Solar neutrino

a) Curie plot and neutrino mass.

If we write the distribution formula in the form:

$$\left[\frac{d\omega/dp}{F(\pm 1,Z,E)}\frac{1}{p^2}\right]^{1/2} = \left[N(p)/p^2\right]^{1/2} = \text{const}\cdot(Q-E_e),$$

The experimental dependence of left side expression on E_e is called a ***Curie*** plot. ***Curie*** plot is a straight line if neutrino mass is equal to zero.

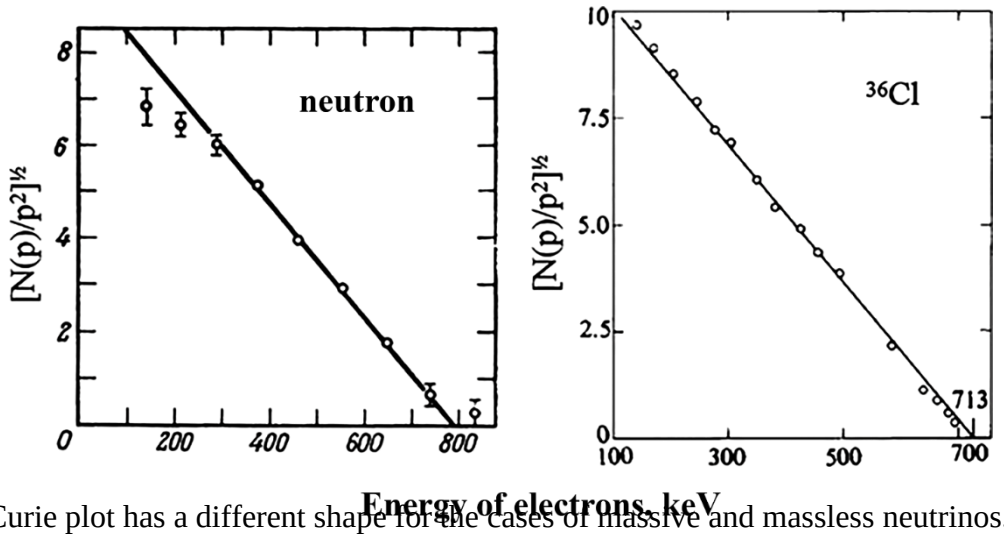

The Curie plot has a different shape for the cases of massive and massless neutrinos. In the given example, the decay of tritium is considered.

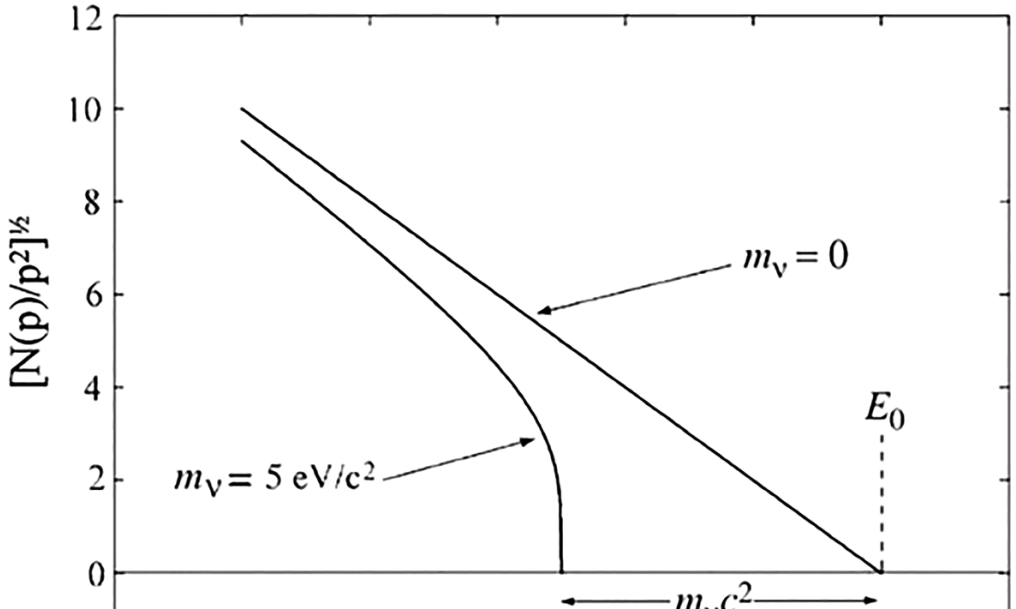

b) Solar neutrinos.

Only about 1/3 of electron neutrinos from the Sun are detected in comparison with theoretical predictions. How can this be explained?

Suppose the existence of 3 types of neutrinos with definite masses: ν_1, ν_2, ν_3.

Neutrinos emitted in decays are the linear combinations of these neutrinos.

For simplicity, we will restrict ourselves to two types of neutrinos (a good approximation to experiment). Neutrinos emitted in beta processes are a mixture of ν_1 and ν_2 neutrinos.

$$\nu_e = \cos\theta_{12}\,\nu_1 + \sin\theta_{12}\,\nu_2, \quad \theta_{12} - \text{mixing angle}$$
$$\nu_\mu = -\sin\theta_{12}\,\nu_1 + \cos\theta_{12}\,\nu_2$$

Then the time evolution of an electron neutrino born on the Sun can be written in the form:

$$\left|\nu_e(t)\right\rangle = e^{-iE_1 t/\hbar}\cos\theta_{12}\left|\nu_1\right\rangle + e^{-iE_2 t/\hbar}\sin\theta_{12}\left|\nu_2\right\rangle.$$

Probability of detecting a muonic neutrino at time *t*:

$$P_{\nu_\mu}(t) = \left|\left\langle\nu_\mu\left|\nu_e(t)\right\rangle\right|^2 = \sin^2(2\theta_{12})\sin^2\left[\frac{1}{2}\frac{(E_1 - E_2)t}{\hbar}\right]$$

Since the masses of neutrinos are small $m_\nu c^2 \ll pc$, the approximation can be written: $E_i \approx pc + \frac{1}{2}m_i c^2\frac{m_i c}{p}$.

If electron neutrinos are formed on the Sun as a result of beta decay, then, having flown to the Earth a distance *L* with a speed of about *c* in a time $t = \frac{L}{c}$, they partially turned into muonic ones with a probability:

$$P_{\nu_\mu}(t) = \sin^2(2\theta_{12})\sin^2\left[\frac{1}{4}\left(m_1^2 - m_2^2\right)\frac{c^3 L}{pc\hbar}\right].$$

Thus, the neutrino changes its type while moving towards the Earth (neutrino oscillations).

LECTURE 6

NUCLEAR STRUCTURE

6.1. Magic numbers

Experimental data show that at definite values of N and Z atomic nuclei have special properties.

The figure below shows the relative abundance in nature of various nuclei depending on the nuclear charge Z. Nuclei with the number of neutrons N = 50, 82, 126 correspond to three very clear peaks on the curve.

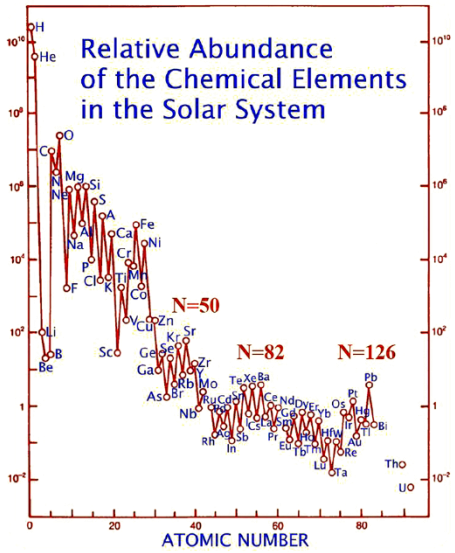

The experimental values of the binding energies of nuclei containing Z = 2, 8, 20, 28, 50, 82 protons or N = 2, 8, 20, 28, 50, 82, 126 neutrons are higher than the predictions of the semiempirical formula, which corresponds to a higher binding energy. These values are called magic numbers.

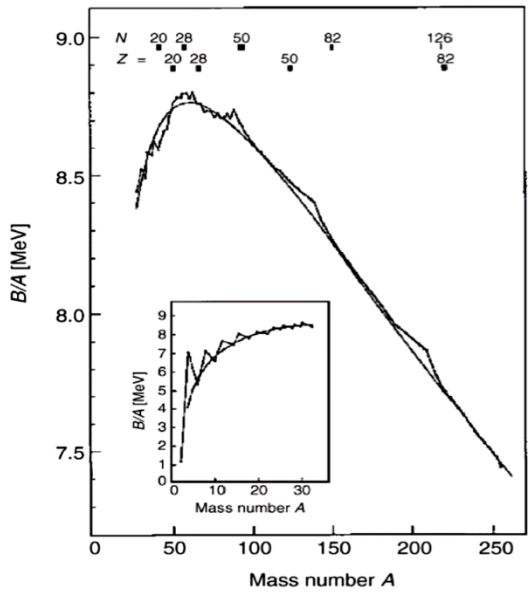

The cross section for the (n, γ) reaction (figure below) is almost two orders of magnitude lower for nuclei containing N = 28, 50, 82, and 126 neutrons. This indicates a reduced probability of the addition of an additional neutron for such nuclei.

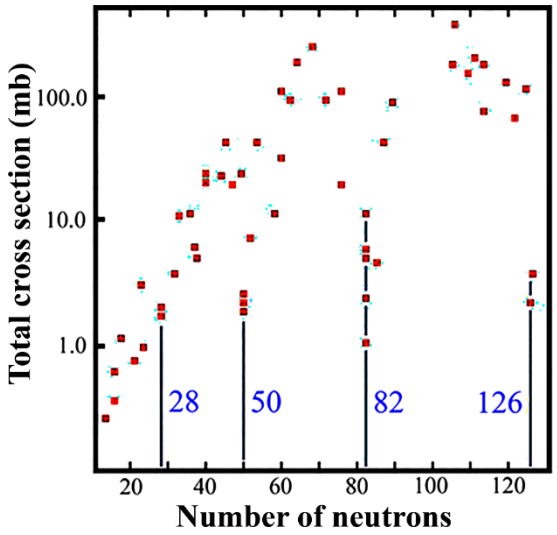

In atoms the peaks on the ionization potential curve correspond to filled electron shells. When the electron is the last to complete the main shell, it turns out to be especially tightly bound.

In nuclei the neutron separation curve demonstrates two effects:

- when N is even, the neutron is more strongly bound to the nucleus (similarly for protons);
- a nucleon is bound more strongly if N = 2, 8, 20, 28, 50, 82, 126 for neutrons or Z = 2, 8, 20, 28, 50, 82 for protons (the figure shows the result for a calcium nucleus with an increased binding energy for N = 20 and 28).

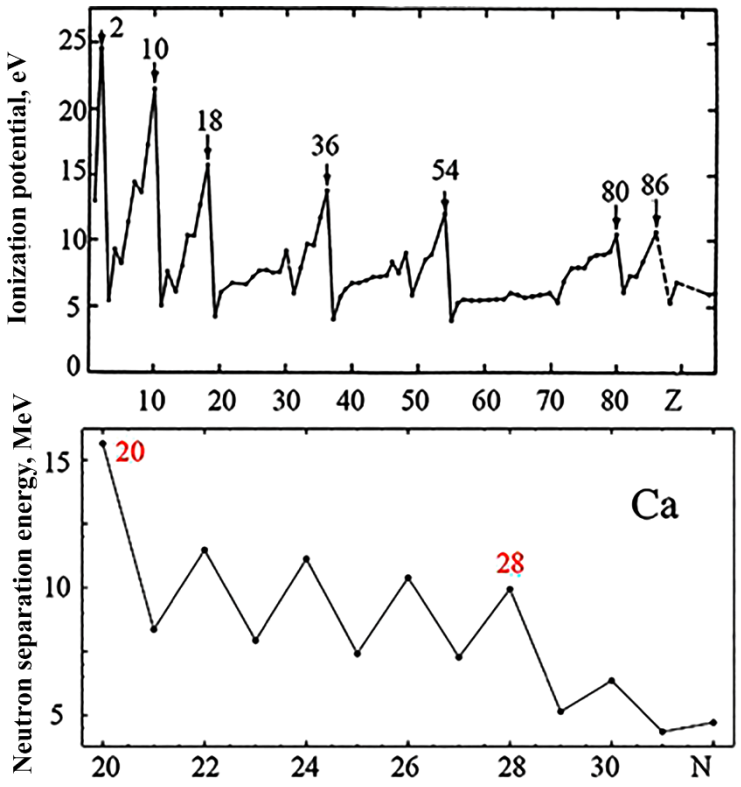

It is more difficult to excite a stable shell; therefore, its first excited state is high in energy. The figure shows the first excited states of lead isotopes. The energy of the excited state $Z = 82$, $N = 126$ is almost 2 MeV higher than in the case of open shells. In addition, the value of the spin of the excited state of the closed shell changes.

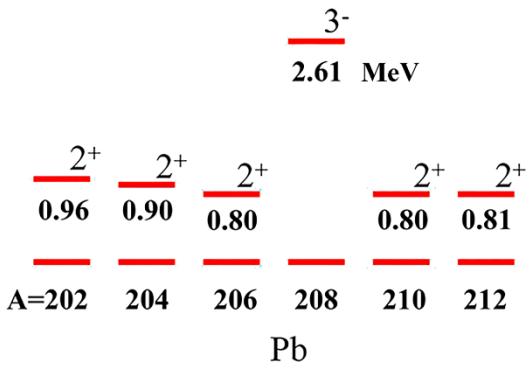

6.2. Shell model and spin-orbit interaction

- The simplest potential wells used to build a shell model are a rectangular well and an oscillator.
- The group of energy-degenerate levels corresponding to a certain value of N is called the "oscillatory shell".
- The degeneracy multiplicity of each level is $(N + 1)(N + 2)$
- Only the first three magic numbers can be described using the harmonic oscillator model.

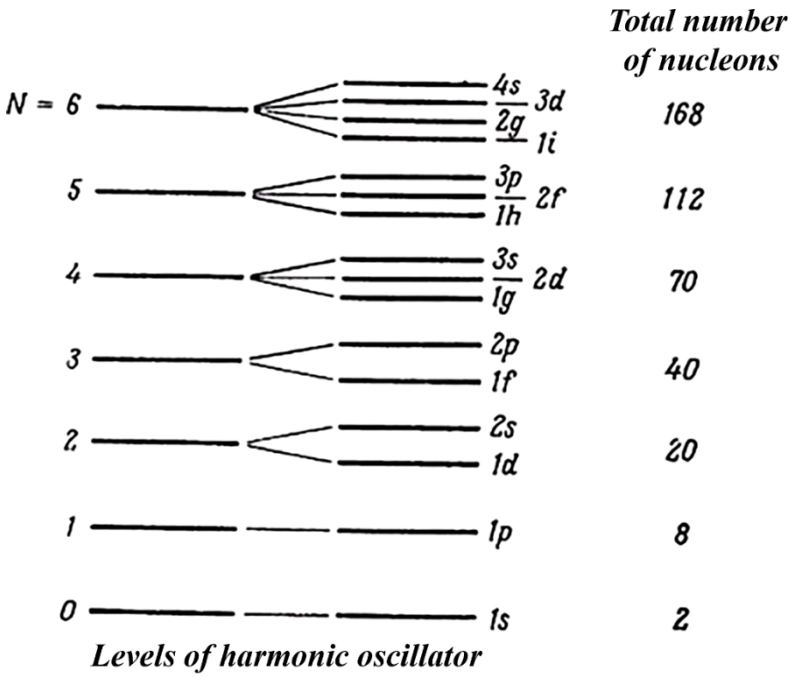

Since the nuclear interaction is short-range, the realistic potential should repeat in shape the distribution of matter in the nucleus. For intermediate and heavy nuclei, the Woods-Saxon potential is used.

$$V_{\text{central}}(r) = -\frac{V_0}{1+e^{(r-R)/a}}.$$

Here R is the radius of the nucleus, and a is diffuseness. However, this potential also cannot describe the entire set of magic numbers. By analogy with atomic physics, a realistic potential should contain a part describing the spin-orbit interaction.

$$V_{\text{total}}(r) = V_{\text{central}}(r) + V_{\text{ls}}(r)\left(\vec{L},\vec{S}\right),$$

where $\vec{L}$ - orbital angular momentum, $\vec{S}$ - spin.

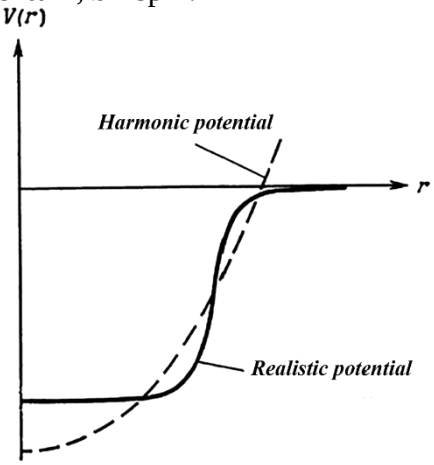

Let us define the vector $\vec{J}$ as the sum of the orbital and spin moments:

$$\vec{J}^2 = \vec{L}^2 + \vec{S}^2 + 2\vec{L}\cdot\vec{S},$$
$$\vec{L}\cdot\vec{S} = \left(\vec{J}^2 - \vec{L}^2 - \vec{S}^2\right)/2.$$

Then, for the eigenvalue of the product LS, we can write:

$$\left\langle \vec{L}\cdot\vec{S} \right\rangle = \hbar^2\left[\, j(j+1) - l(l+1) - s(s+1)\right]/2 = \hbar^2 \begin{cases} l/2 & \text{for } j = l+1/2 \\ -(l+1)/2 & \text{for } j = l-1/2 \end{cases}.$$

This leads to the splitting of the energy levels by the value:

$$\Delta E_{ls} = \frac{(2l+1)}{2}\hbar^2 \langle V_{ls} \rangle.$$

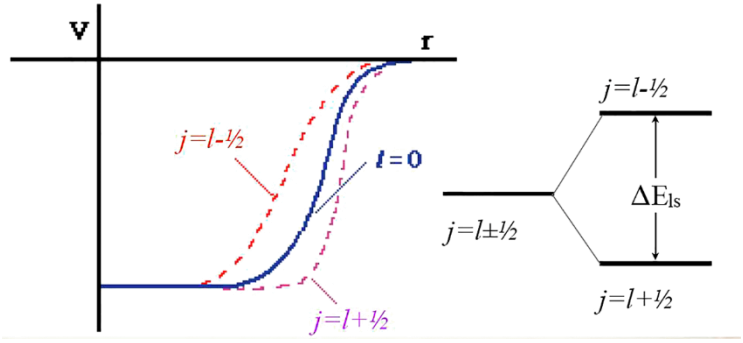

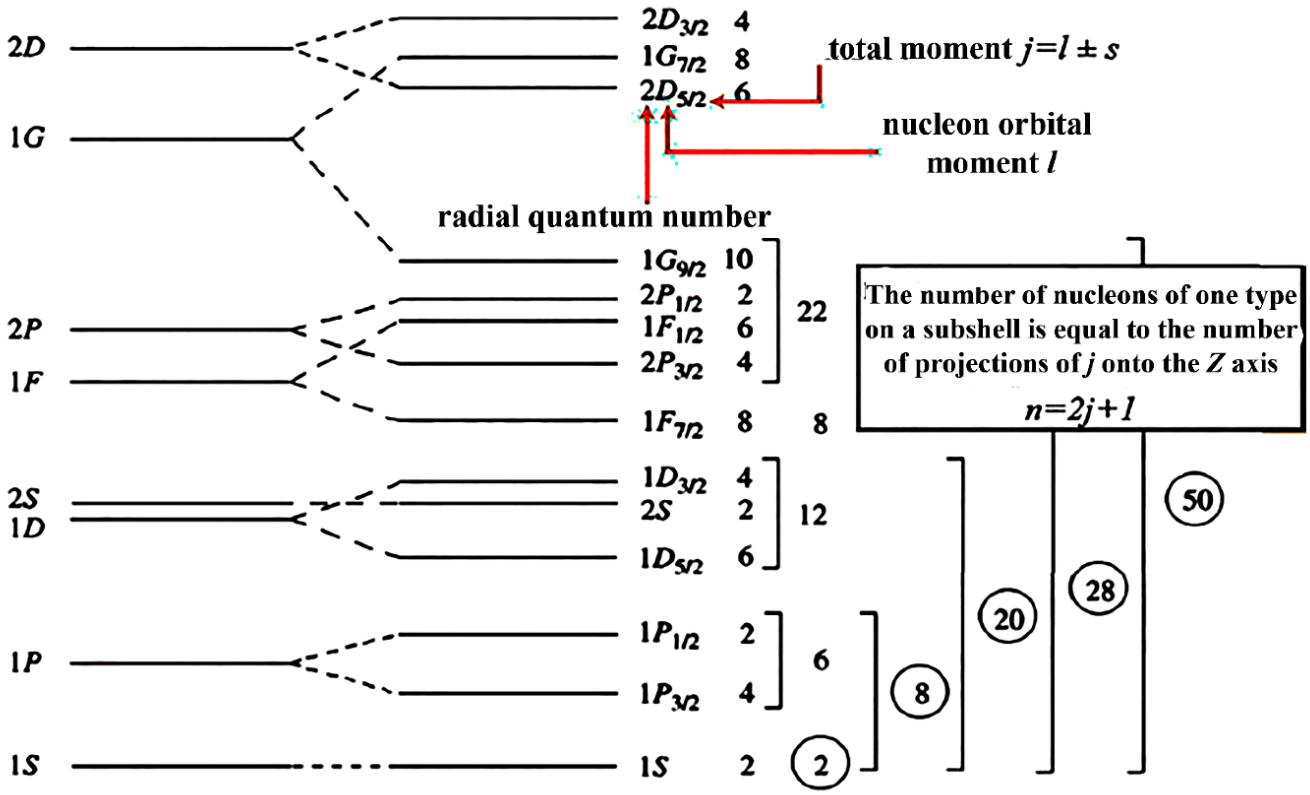

The figure shows single-particle levels in the Woods-Saxon potential well with spin-orbit interaction. Introduction of spin-orbit interaction leads to correct magic numbers.

6.3. Magnetic moments of nuclei

The magnetic moment of one particle with angular momentum $\vec{L}$ and spin $\vec{S}$ are:

$$\vec{\mu}_i = g_l \vec{L}_i + g_s \vec{S}_i .$$

For protons: $g_l = \mu_0$, $g_s = 5.5845\,\mu_0$; for neutrons: $g_l = 0$, $g_s = -3.8263\,\mu_0$.

$\mu_0 \equiv e\hbar/2m_p c$ – nuclear magneton.

For full angular moment j:

if $j = l + s \Rightarrow \mu = l g_l + g_s/2$. If $j = l - s \Rightarrow \mu = \frac{j}{j+1}[(l+1)g_l - g_s/2]$.

Combining into one formulas for $j = l \pm s = l \pm 1/2$, we get:

$$\mu = j\left[g_l \pm \frac{g_s - g_l}{2l+1} \right]$$ — Schmidt's formula.

For odd *Z*, even *N*.

Solid lines in the figure below are plotted under the assumption that the magnetic dipole moment of the nucleus is formed by the last odd proton according to the Schmidt formula.

$$g_l = \mu_0, \quad g_s = 5.5845\,\mu_0$$

Points in the figure below are experimental values.

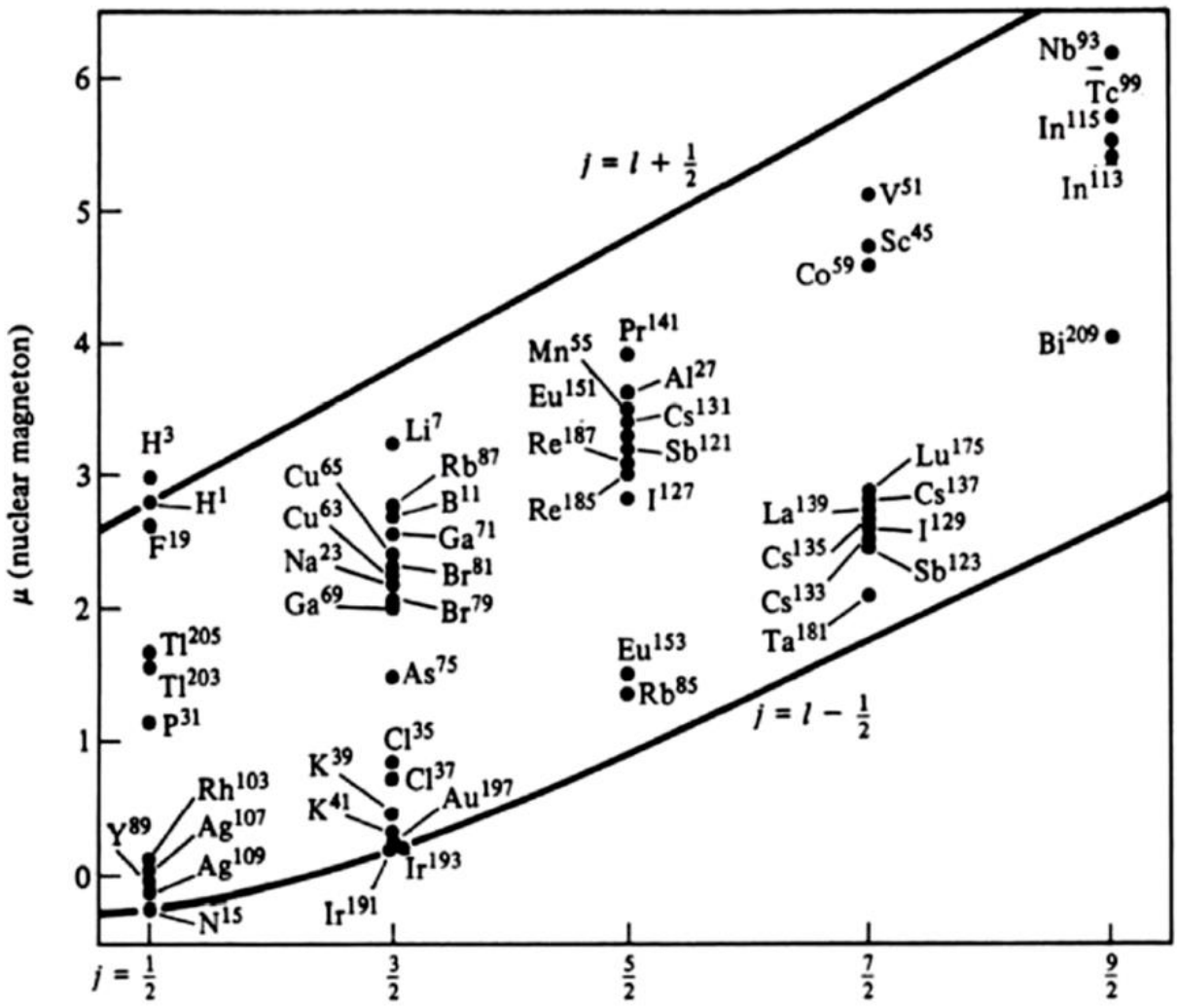

For even *Z*, odd *N*.

Solid lines in the figure below are drawn under the assumption that the magnetic dipole moment of the nucleus is formed by the last odd neutron according to the Schmidt formula.

$$g_l = 0, \quad g_s = -3.8263\,\mu_0.$$

Points are experimental values. The discrepancy between theory and experiment is due to the orientation of the magnetic moments of the core in the magnetic field of an odd nucleon.

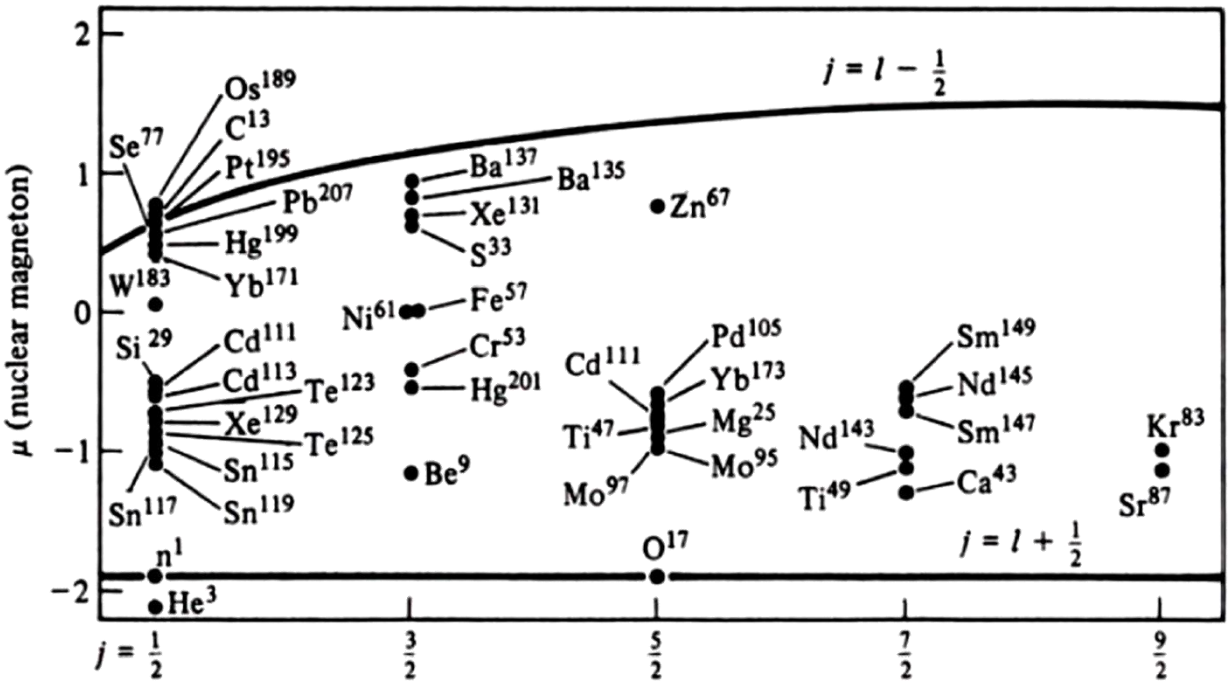

6.4. Nuclear rotation

The rigid rotor model with odd valence particle is presented in the figure below:

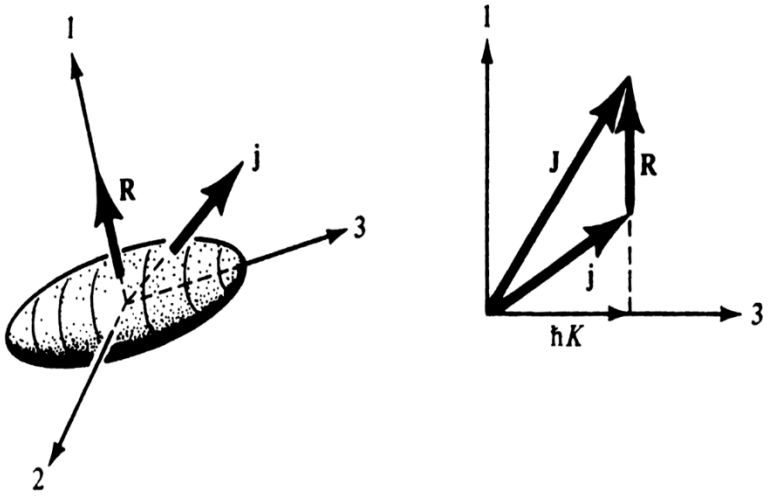

Here $\vec{R}$ — angular momentum of the elliptical core of the nucleus, directed perpendicular to the axis of symmetry, so that $R_3 = 0$. The angular momentum of a valence nucleon is j. Total angular momentum: $\vec{J} = \vec{R} + \vec{j}$

In this case, the spin is no longer a “good” quantum number, but only its projection $\hbar K$.

The total angular momentum J and its component J_3 along the axis of symmetry of the nucleus satisfy the following eigenvalue equations:

$$\vec{J}^2_{\text{оп}}\psi = \hbar^2 J\left(J+1\right)\psi;$$
$$J_{3,\text{оп}}\psi = \hbar K\psi.$$

The total energy of rotational motion for $J \geq K$ is:

$$E_{J,K} = \frac{\hbar^2}{2T}[J(J+1) - K^2] + E_{sp}.$$

Here E_{sp} is the energy of one-particle excitation, T is the moment of inertia. The sequence of levels belonging to a given K value is called a rotational band. The level with the lowest spin is the head level of the band. In the case $K = 0$, the level spins are even numbers. For $K > 0$, the spins are determined by the formula:

$$J = K, K+1, K+2, \ldots$$

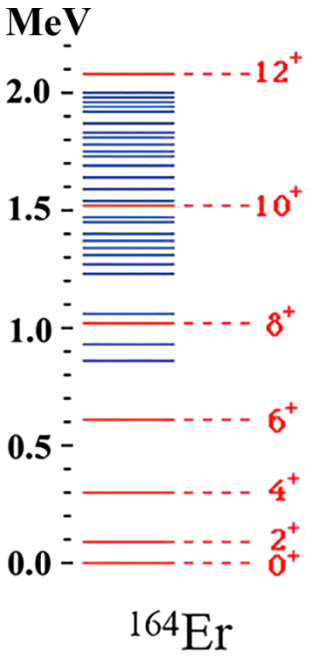

6.5. Nuclear vibrations

- Mathematically, the surface function of a geometric figure can be expanded in a series of spherical harmonics.

$$R = R_0\left[1 + \sum_{l=0}^{\infty}\sum_{m=-l}^{+l}\alpha_{lm}Y_l^m(\theta,\varphi)\right].$$

- If the expansion coefficients do not depend on time, the deformation is constant.
- If the expansion coefficients depend on time, the form fluctuates.
- l - multipolarity

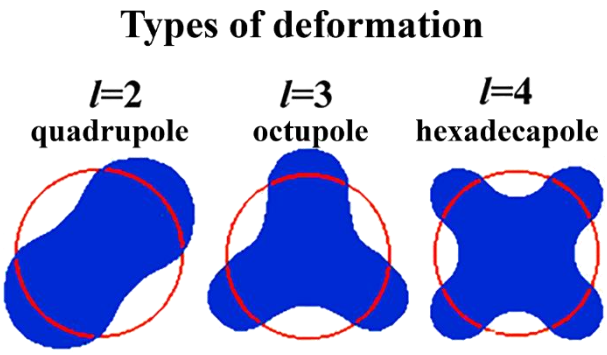

For phonons of a certain multipolarity, the spectrum is equidistant - 1 phonon, 2 phonons, etc. Excitation with $J^P = 2^+$ corresponds to one quadrupole phonon of an even-even nucleus. States with a large number of phonons correspond to the moment obtained as a result of the vector addition of the moments of individual phonons. In this case, the states with J = 1 and 3 are forbidden for two phonons (Bose-Einstein statistics). Therefore, for n = 2 phonons in an even-even nucleus, only excitations with $J^P = 0^+, 2^+$, and 4^+ are formed (figure below).

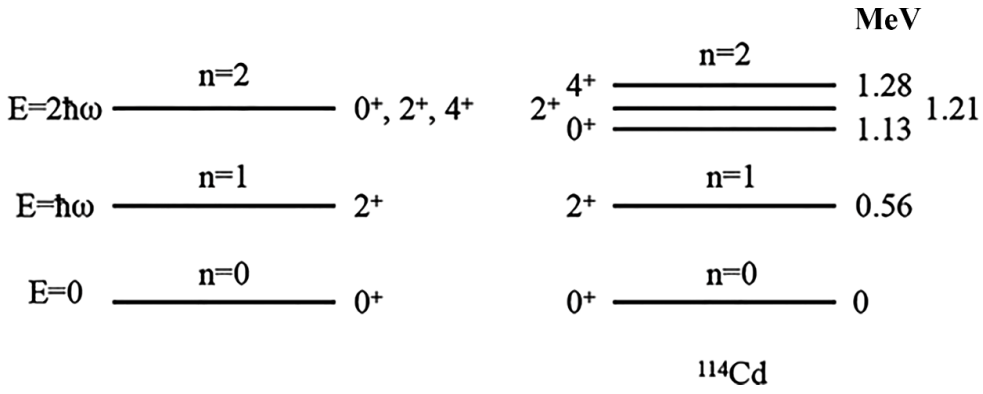

NUCLEAR FISSION

6.6. Nuclear fission: main experimental data, mechanisms of fission

Fission of atomic nuclei is called their decay into two fragments of comparable mass. Fission can be spontaneous or induced (caused by interaction with an incident particle).

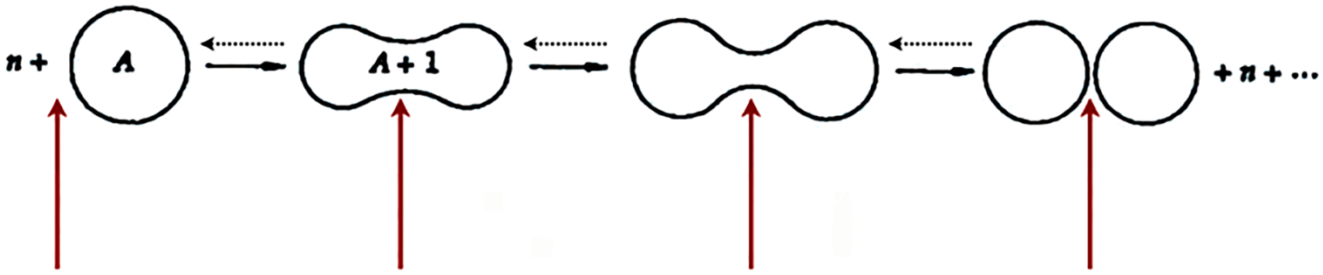

Nucleus absorption of a neutron

Transition to a deformed excited state

The Coulomb energy decreases, the surface energy increases. The nucleus passes through the "saddle point"

Neck rupture, nucleus divided into two fragments. The fragments transforms into a spherical state, the excess excitation energy is removed due to the emission of neutrons.

Spontaneous fission of an atomic nucleus is energetically possible if the sum of the masses of the nuclei-fragments is less than the mass of the parent nucleus (that is, the total binding energy of nuclei-fragments must be greater than the binding energy of the parent nucleus:

$$W(A_1, Z_1) + W(A_2, Z_2) \geq W(A, Z);\ A = A_1 + A_2,\ Z = Z_1 + Z_2).$$

Suppose that a nucleus with charge Z and mass number A is divided into two identical fragments $(A_1 = A_2 = A/2\,; Z_1 = Z_2 = Z/2)$. Neglecting the even-odd term in the Weizsacker formula, we obtain:

$$—0.26\alpha_2 A^{2/3} + 0.37\alpha_3 \frac{Z^2}{A^{1/3}} \geq 0$$

$$\alpha_2 = 17.8 \text{ MeV},\ \alpha_3 = 0.711 \text{ MeV}.$$

From this we find the necessary condition for spontaneous nuclear fission:

$$\frac{Z^2}{A} \geq 17$$

Quadrupole deformation of the nucleus can be described as:

$$R(\vartheta) = R_0[1 + \alpha_2 P_2(cos\vartheta)].$$

Surface and Coulomb energies for spherical nucleus:

$$E_s^0 = 4\pi R_0^2 S A^{2/3} = a_s A^{2/3};\ E_C^0 = \frac{3}{5}\frac{Z^2 e^2}{R_0 A^{1/3}} = a_C \frac{Z^2}{A^{1/3}}$$

Surface and Coulomb energies for deformed nucleus:

$$E_s = E_s^0\left(1 + \frac{2}{5}\alpha_2^2\right);\ E_C = E_C^0\left(1 - \frac{1}{5}\alpha_2^2\right),$$

Here s – surface tension, α_2 – quadrupole deformation parameter.

When the changes in the Coulomb and surface energies $(\Delta E_C = E_C^0 - E_C,\ \Delta E_s = E_s - E_s^0)$ are equal, the nucleus becomes unstable to fission. At this point, the condition is fulfilled:

$$\frac{E_C^0}{2E_s^0} = 1.$$

$$x = \frac{E_C^0}{2E_s^0} = \frac{1}{2}\left(\frac{\text{Coulomb energy of a charged sphere}}{\text{Surface energy of a spherical nucleus}}\right).$$

Fission parameter

$$x = \left(\frac{a_C}{2a_s}\right)\left(\frac{Z^2}{A}\right) = \left(\frac{Z^2}{A}\right)/\left(\frac{Z^2}{A}\right)_{\text{critical}};\ \left(\frac{Z^2}{A}\right)_{\text{critical}} = 50.883\left[1 - 1.7826\left(\frac{N-Z}{A}\right)^2\right].$$

Fission barrier.

Dependence of the shape, height of the potential barrier H and fission energy E on the fission parameter.

If the energy of separation of a neutron B (n) from a nucleus (A + 1) is greater than the fission barrier, fission is possible at any energy. If the separation energy is less than the fission barrier, there is a threshold: the kinetic energy of neutrons E_n must be greater than the value (H-B (n)).

^{238}U is divided by neutrons with energies $E_n > 1$ MeV, ^{235}U is divided by neutrons of any energies.

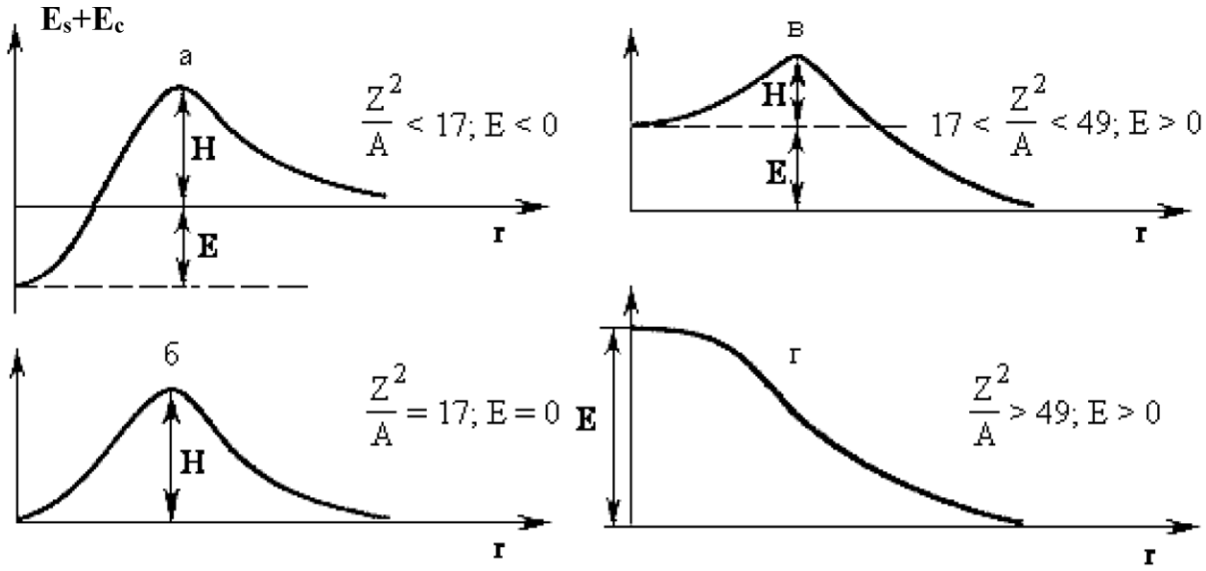

Energy distributions.

In the fission of ^{235}U by thermal neutrons, an energy of about 200 MeV is released.

- The kinetic energy of the fragments is -167 MeV.
- Fission neutron energy -5 MeV.
- Energy of prompt gamma quanta -7 MeV.
- Energy of beta particles of fission products -8 MeV.
- Energy of gamma quanta of fission products -7 MeV.
- Energy of antineutrino fission products -10 MeV.

Total: 200 MeV.

6.7. Spontaneous fission. Fission isomers

Isomeric fission of ^{242}Am (Dubna, 1961) from shape isomer (state II - 2-nd minimum of potential energy) is shown in the figure below.

$T_{1/2}$ (ε_{II})=0.014 s. $T_{1/2}$ (ε_{I})=10^{14} years.

Sub-barrier fission is a fission from excited state lower than the height of a barrier.

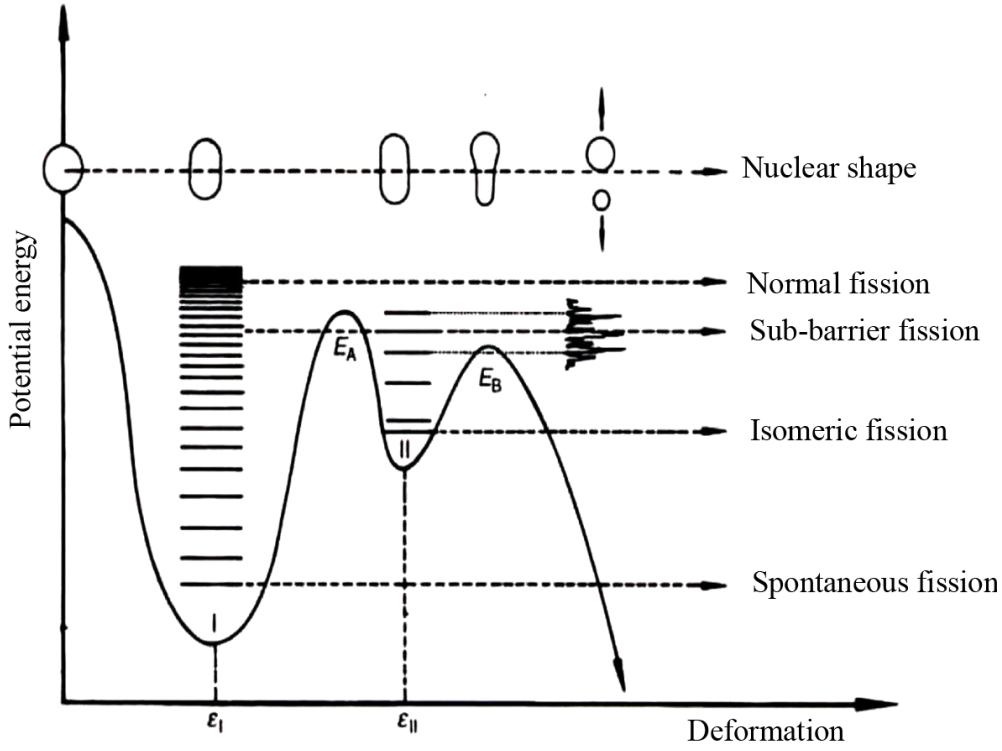

The periods of spontaneous fission of nuclei change very strongly during the transition from nucleus to nucleus due to the exponential nature of the probability of barrier penetration. For ^{232}Th nuclei, the period is more than 10^{21} years.

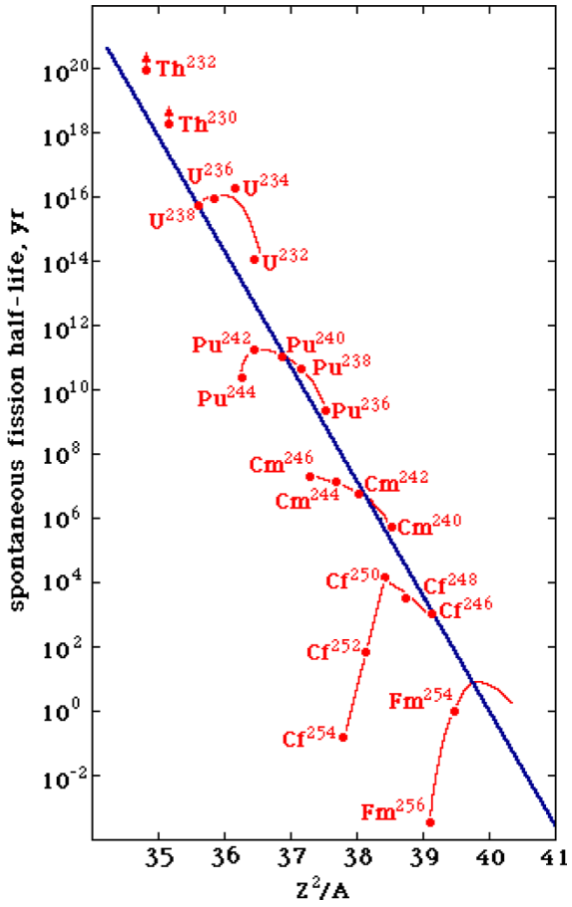

6.8. Energy relations for fission

- In the fission of a heavy nucleus, a large energy *Q* should be released, since the binding energy of a nucleon in heavy nuclei is approximately 0.8 MeV less than for medium nuclei.
- The overwhelming part of the fission energy is released in the form of the kinetic energy of fission fragments, since the nuclei-fragments scatter under the action of the Coulomb repulsive forces.
- The fragments formed during fission must be beta-radioactive and can emit neutrons. The average number of neutrons emitted in one fission act depends on the mass number and increases with increasing *Z*.

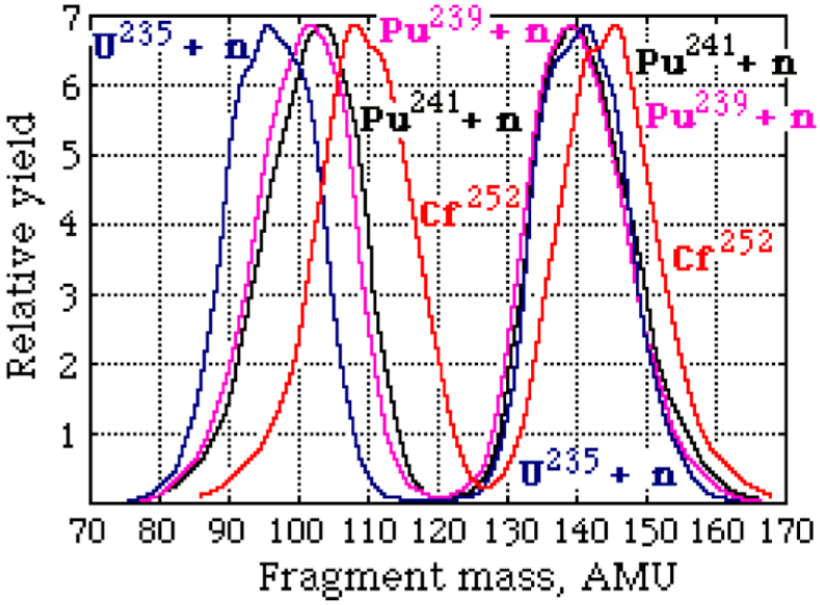

A characteristic feature of fission is that the fission fragments, as a rule, have significantly different masses. In the case of the most probable fission of ^{235}U, the fragment mass ratio is 1.46. At the same time, a heavy fragment has a mass number of 139, a light one - 95.

In fission by thermal neutrons, the probability of symmetric fission is about three orders of magnitude less than in the case of the most probable fission into fragments with A = 139 and 95.

The liquid drop model does not exclude the possibility of asymmetric fission, however, it does not even qualitatively explain the basic laws of such fission. Asymmetric fission can be explained by the influence of the shell structure of the nucleus. The nucleus tends to split in such a way that the main part of the fragment nucleons forms a stable magic core.

With an increase in the excitation energy of the nucleus, the influence of shell effects decreases and the distribution of the masses of the fragments tends to a symmetric form (figure below).

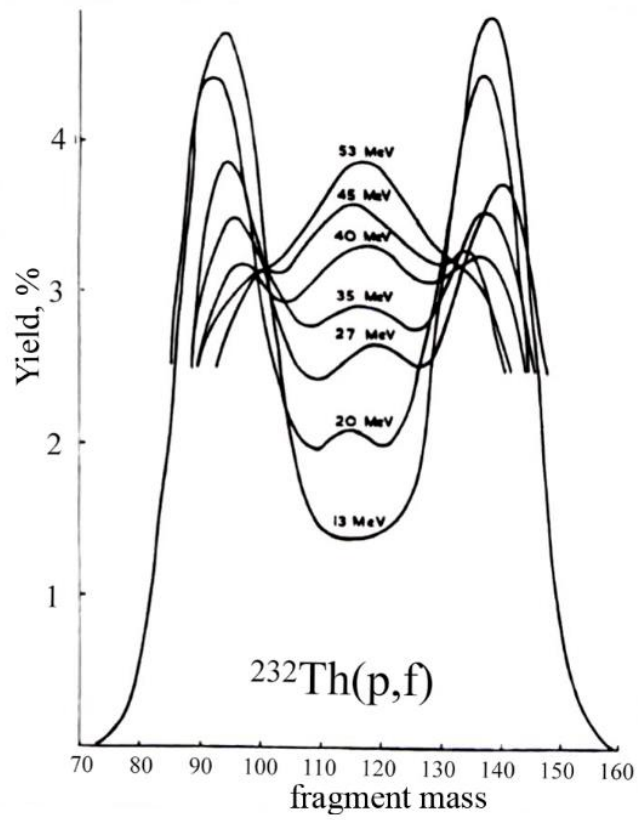

6.9. Physics of nuclear reactors

As further studies showed, the reaction of induced fission by neutrons can occur not only on U-235 nuclei. In 1941, a group of American scientists led by G. Seaborg (1912-1999, Nobel Prize in Chemistry 1951 "for discoveries in the field of chemistry of transuranic elements") irradiated a U-238 target with a flux of neutrons obtained at a cyclotron. At the same time, they observed a chain of reactions: U-239 is unstable and with a half-life of $T_{1/2}$ = 23.5 min undergoes transformation into neptunium Np-239: moreover, Np-239 is also unstable and with a half-life of 2.35 days turns into a new unknown Element Y: The newly discovered chemical element is named plutonium (Pu) after the last planet in the solar system. It turned out that Pu-239, like U-235, can fission under the influence of thermal neutrons

$$n + {}^{238}_{92}U \rightarrow {}^{239}_{92}U + \gamma; {}^{239}_{92}U \rightarrow {}^{239}_{93}Np + e^- + \tilde{\nu}_e, {}^{239}_{93}Np \rightarrow {}^{239}_{94}Y + e^- + \tilde{\nu}_e.^4,$$

and the fission occurs at a rate approximately twice the rate of fission of U-235 nuclei of the same mass. Each fission act is accompanied by the release of energy of about 200 MeV and about 3

[4] Thermal neutrons are free neutrons with kinetic energy corresponding to the average kinetic energy of gases at room temperature (0.025 eV).

neutrons. The resulting neutrons in a Pu-239 medium can cause subsequent fission reactions in plutonium nuclei, which produce more neutrons and release more energy. An avalanche-like chain reaction is formed, and the process of the appearance of new generations of neutrons and the release of energy will unfold very quickly, since the neutrons obtained as a result of fission (they are called prompt) are emitted within about 10^{-14} s. This leads to an explosion, called nuclear, while at the epicenter of the explosion the temperature of the ionized gas rises to 10^6 K, which causes a very bright glow. The process of capture of neutrons by U-235 nuclei also leads to an explosive release of energy. In this case, a sufficient mass of U-235 or Pu-239 (critical mass) is required.

The first steps in the practical application of nuclear energy fell on the years of World War II, and therefore the main attention in the countries dealing with this issue (USA, USSR, Germany) was paid to the creation of a nuclear bomb.

.However, along this path, a nuclear reactor was created, which subsequently found peaceful use. The fact is that to obtain weapons-grade Pu-239, it is necessary to irradiate U-238 nuclei with a neutron flux. As it turned out, the accelerators used at first did not allow the critical mass of Pu-239 (about 10 kg) to be reached. Then, in 1942, under the leadership of E. Fermi (1901-1954, Nobel Prize in Physics 1938, "for the proof of the existence of new radioactive elements obtained by irradiation with neutrons, and the related discovery of nuclear reactions caused by slow neutrons") during the period of work on the American project to create a nuclear bomb ("Manhattan Project"), a thermal neutron reactor was created using the induced fission process of ^{235}U nuclei in a natural mixture of U isotopes (99.3% ^{23}8U and 0.7% ^{235}U) (see figure)

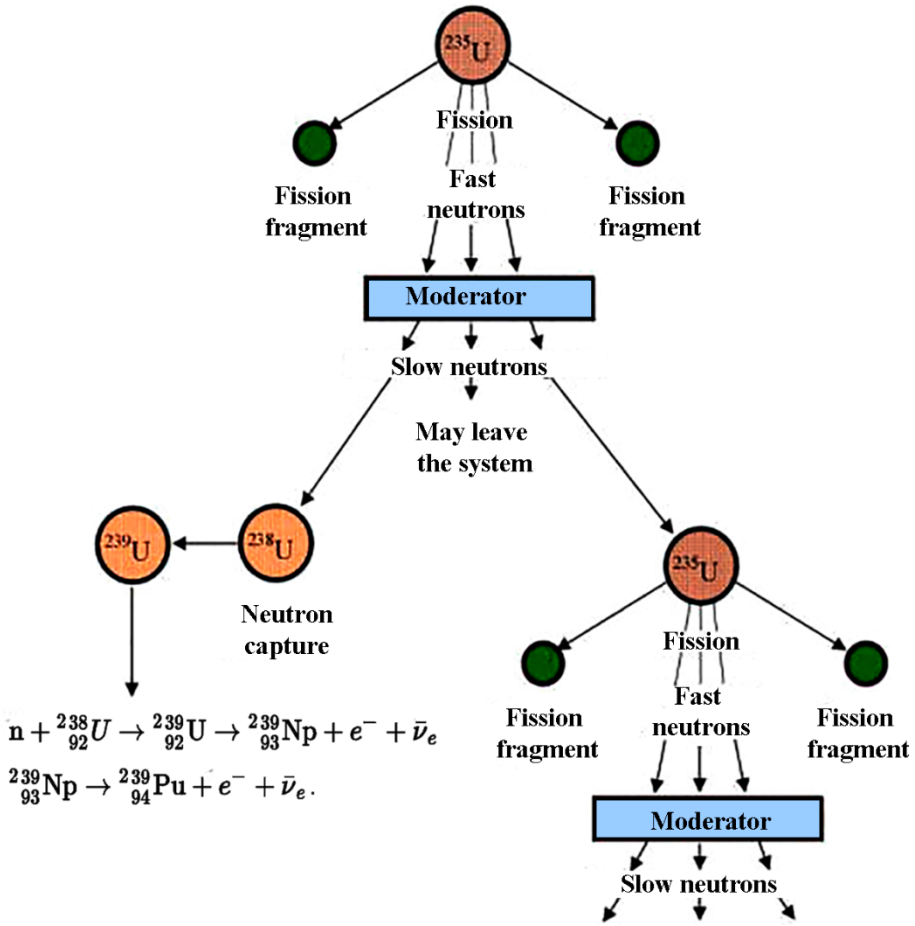

As a result of the induced fission of ^{235}U, fast neutrons are produced. But the probability of fission of uranium-235 increases with decreasing neutron energy. Therefore, a moderator is placed in the path of neutrons. Deceleration using water, which contains protons, turns out to be most effective. The equality of the masses of neutrons and protons makes it possible for neutrons to stop after the first collision (in practice, slowing down to thermal energies occurs on average after 18 collisions). However, when using water, the process of fusion of a neutron with proton with the transformation of water into heavy water is very likely. Such a process removes free neutrons from the system and thereby can extinguish the chain reaction. Therefore, in practice, when creating reactors, heavy water (Germany) or graphite (USSR, USA) was used. To slow down fast neutrons with graphite, about 110 collisions are required, which is quite acceptable. A nuclear reactor with a controlled fission reaction in a stationary mode must have a neutron multiplication factor[5] $k = 1$. To change the value of k, rods made of a substance that absorbs neutrons well are inserted into the reactor core. The immersion of the rods into the depth of the core decreases the value of k, while the removal of the rods decreases the value of k.

Some of the thermal neutrons formed after slowing down are captured by U-238, followed by the synthesis of Pu-239. This reactor was used to manufacture weapons grade ^{239}Pu for the "Fat Man" nuclear bomb dropped on August 9, 1945 on the Japanese city of Nagasaki. Three days earlier, a nuclear bomb with the affectionate nickname "Little Boy" was dropped on the Japanese city of Hiroshima, containing ^{235}U enriched to 80%. Both bombs also used a nuclear chain reaction process, with a high neutron multiplication factor, which led to an explosive release of energy. Barbaric bombing of peaceful Japanese cities, as a result of which about 20% of the population died immediately at the time of the explosions and another 20% during the first year as a result of radiation damage, had no military sense. They did not destroy the military-industrial potential of Japan and did not damage the Japanese army.

The development and use of nuclear weapons had a tremendous impact both on the organization of nuclear physics research and on the attitude of scientists towards the results of the application of their research. For the first time, such a large-scale complex scientific research was carried out, which became an integral part of a single technological chain. Nuclear physics has become in the focus of government interests. In the process of the development of nuclear weapons, the methodology for the implementation of projects of the Megascience class was worked out. About 100,000 people took part in the US program to develop a nuclear bomb. Improvement of the reactor, originally created for the production of weapons-grade plutonium, led to the creation in the

[5]The neutron multiplication factor k is the ratio of the number of neutrons causing fission reactions in the next generation to the same value in the previous generation. With the development of an uncontrolled chain reaction, $k > 1$.

USSR of the world's first nuclear power plant (1954). The typical scheme of modern nuclear reactor is shown in the figure below.

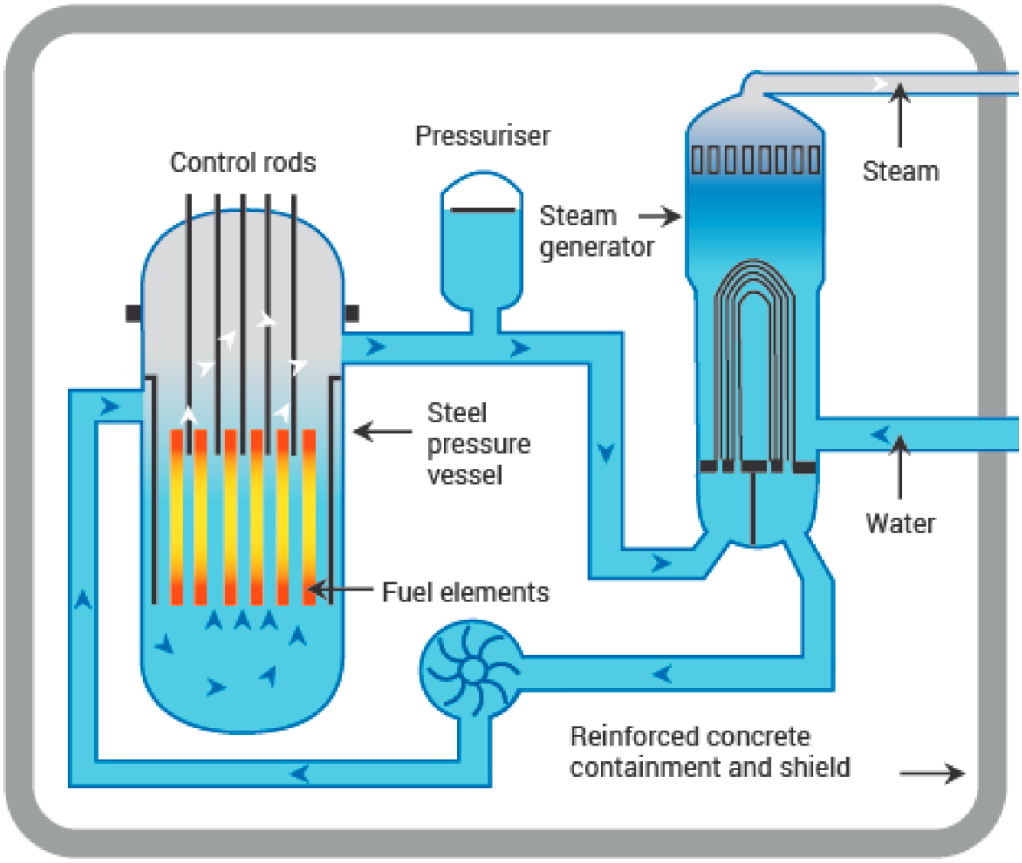

And at the same time, scientists for the first time clearly realized their personal responsibility for the results of research. Two of the three scientists who initiated the work on nuclear weapons in the United States (A. Einstein and L. Szilard) actively advocated the prohibition of the use of nuclear energy for military purposes. The discoverer of the induced fission of atomic nuclei O. Gan considered himself personally responsible for the deaths of the inhabitants of Hiroshima and Nagasaki and became the author of several memoranda against the use of nuclear weapons. The creator of modern non-classical physics, Niels Bohr, in 1944 (even before the nuclear bombings of Japanese cities) appealed to the British Prime Minister and the US President to ban the use of nuclear weapons. One of the leaders of the German nuclear program W. Heisenberg opposed the acquisition of nuclear weapons by post-war Germany and was nuclear tests. In his book “Physics and Philosophy. Part and whole” he wrote: "The invention of atomic weapons posed completely new problems for both science and scientists. The influence of science on politics is much greater than it was before the world war; and this circumstance imposes a double responsibility on scientists, especially atomic physicists". There are many such examples. The movement of scientists for peace, for the preservation of our planet and life on it, which originated among nuclear scientists, has become in our time an integral part of social life.

6.10. Nuclear medicine

However, nuclear physics also serves humanistic purposes. Among the applied problems that nuclear scientists solve, first of all, it is necessary to single out nuclear medicine. Nuclear medicine is a branch of medicine that uses nuclear physics methods to diagnose and treat diseases. Medicine is the largest area of applied nuclear physics. To understand this, just look at the fields of application of radioactive isotopes[6] and accelerators[7]

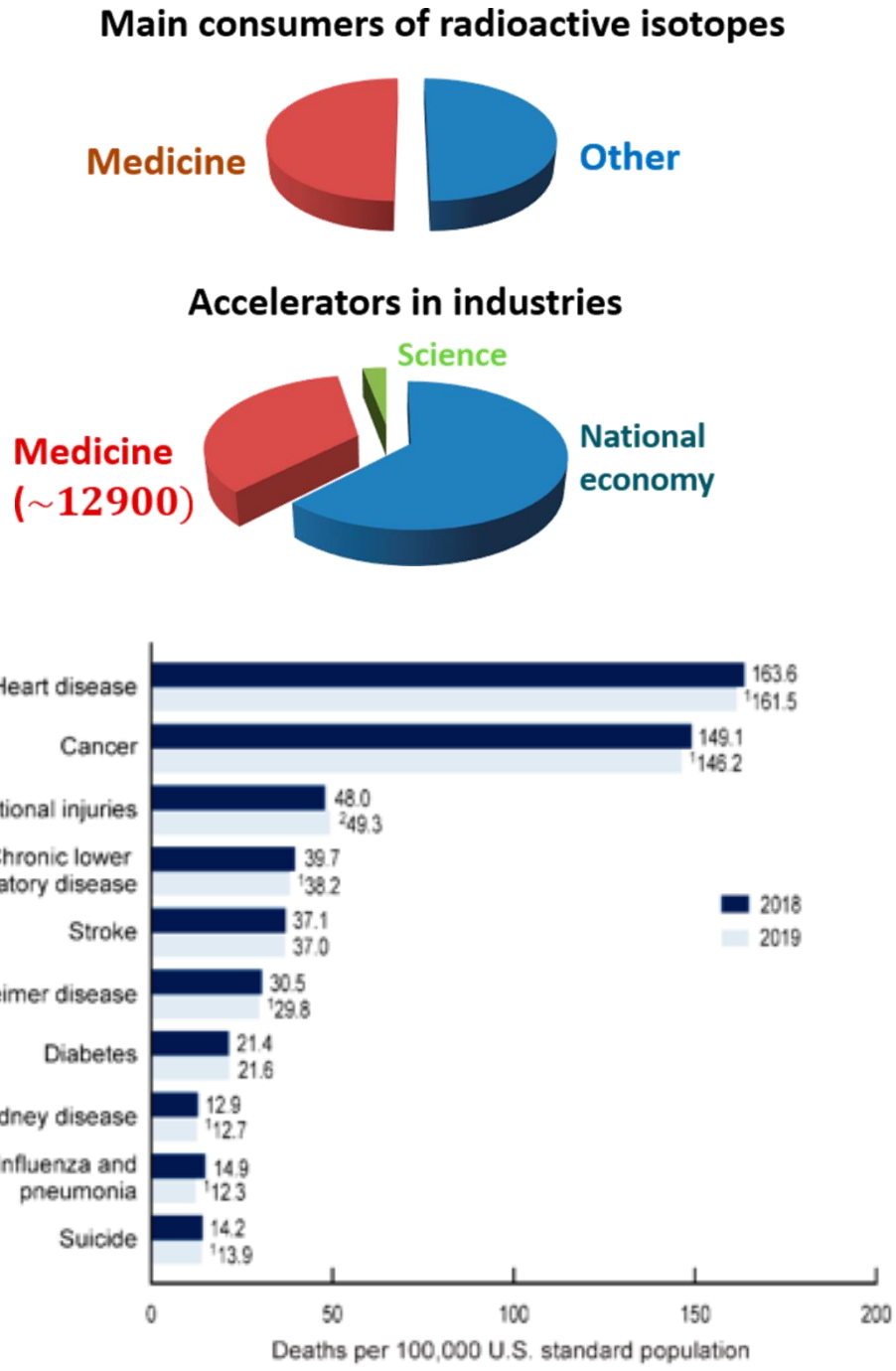

[6]Isotopes are a group of nuclei that have the same number of protons but different numbers of neutrons. Among the isotopes of one chemical element, there are both radioactive and stable ones.

[7] Charged particle accelerators are devices that accelerate charged elementary particles and ions to subluminal velocities for collisions with each other (accelerators on colliding beams) and with stationary targets.

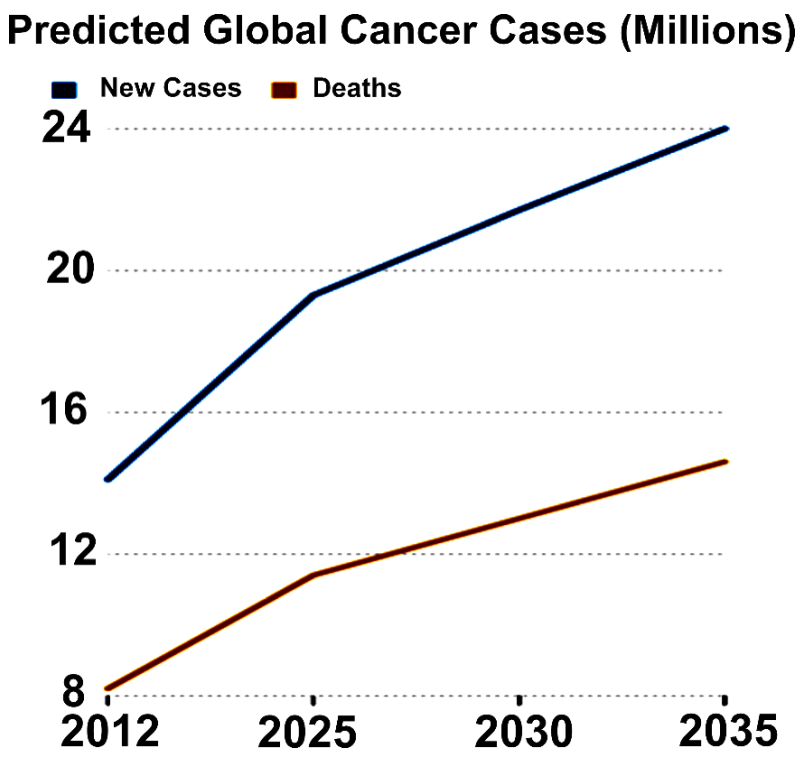

Two figure above show the leading causes of death in the Unites States and global cancer cases. Nuclear medicine turns out to be effective for the diagnosis of all the diseases presented, and in the case of oncological ones it turns out to be one of the most effective methods of treatment.

One of the origins of nuclear medicine is the method of radioactive tracers, developed by the Hungarian scientist J. De Hevesy (1885-1966). J. De Hevesy proposed to replace stable isotopes in organic tissues with radioactive ones and track the movement of chemical elements in the body. In his first studies (1935) J. De Hevesy focused on metabolism[8] of phosphorus. The human body contains about 1 g of stable phosphorus-31. It is included in cell membranes, nucleotides, mitochondria (where phosphorus-containing acid ATP is synthesized - "the fuel of life"). De Hevesy decided to replace stable phosphorus with radioactive one.

To produce radioactive phosphorus J. De Hevesy used the method developed by E. Fermi. He irradiated stable P nuclei with neutrons. Due to the electrical neutrality of neutrons, they can come close to positively charged atomic nuclei and combine with them to form a new isotope of the same chemical element. The advantage of the electrical neutrality of neutrons is especially pronounced when nuclei with a large charge enter the reaction.

[8]Metabolism is the body's metabolism. Changes in the intensity of metabolic processes in tissues depend on the degree of functional and organic disorders.

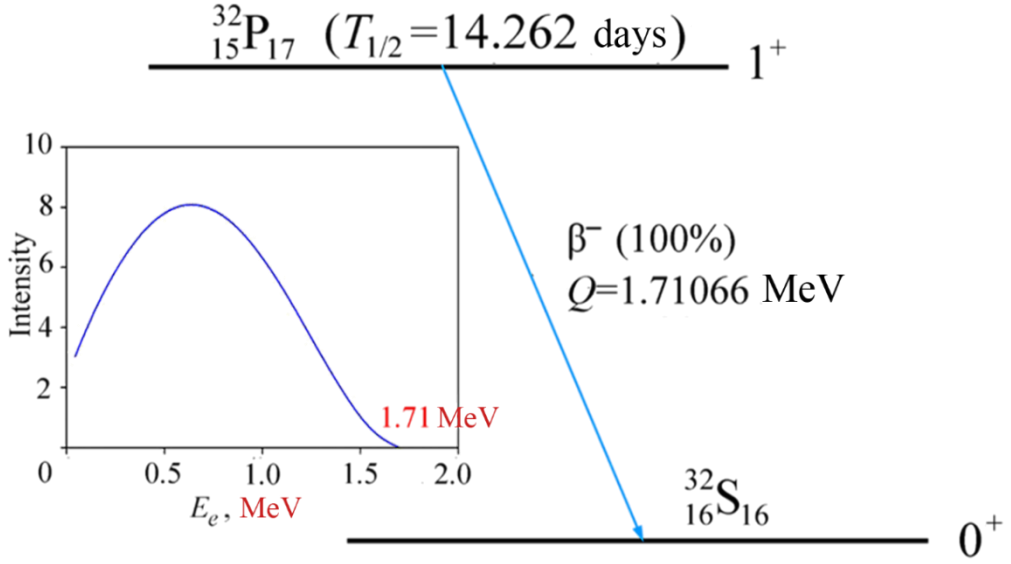

The figure shows the decay scheme of radioactive phosphorus-32, used by de Hevesy. The neutron flux from the neutron generator is directed to the target - stable ^{31}P. As a result of neutron capture, radioactive ^{32}P is formed in an excited state, which quickly passes into the ground state due to the emission of a gamma quantum with an energy of about 17 keV. In the ground state, phosphorus has spin 1 and positive spatial parity[9]. This state is unstable, phosphorus-32 is radioactive, since as a result of radioactive transformation - beta-minus decay - the energy of the nucleus decreases. The result of the decay is the daughter nucleus sulfur-32, an electron and an electron antineutrino. The distribution of the number of emitted electrons versus energy is shown in the inset.

Since the maximum mean free path of electrons in tissues is only 7 mm, de Hevesy obtained tissue sections and studied their emission of electrons. Rats were selected as experimental animals.

The scientist fed the rats with sodium phosphate. Part ^{31}P was replaced with radioactive ^{32}P. Investigated the excretion of ^{32}P in urine and feces, accumulation in internal organs and in offspring. “The most significant result obtained in studies using isotope indicators is, of course, the discovery of the dynamic state of the body's components. The molecules that make up plants and animal organisms are constantly regenerated ”(from the Nobel Lecture, 1944).

Studies have shown that the distribution of radioactive phosphorus in the body between individual tissues is determined by:

- the amount of phosphorus in a given tissue in an exchangeable form;
- the intensity of its exchange;
- by the nature of the tissue: rapidly growing tumor tissues perceive more 32P than normal ones.

[9]Spatial parity is a property of the state of an atomic nucleus relative to reflection in a mirror. It can be either positive (the state does not change) or negative (the state changes sign to the opposite). Conserved in strong nuclear interactions.

The highest concentrations of radioactive phosphorus are found in the bone marrow, lymph nodes, spleen and liver.

The accumulation of radioactive phosphorus in tumor tissues makes it attractive for the treatment of oncological diseases by irradiation with short-range electrons.

However, for diagnostic purposes, radioactive phosphorus is less suitable. For registration of radiation from the place of metabolic disturbance, it is necessary that the radiation passes well through biological tissues. Gamma radiation sources are more suitable for this role. For registration of gamma radiation

For this purpose, the American electrician and biophysicist H. Angers (1920–2005) invented a gamma camera. It was necessary to solve two problems:

a) determine the direction of emission of gamma quanta;

b) convert gamma radiation into electrical impulses.

For solving problem a) collimator is used.

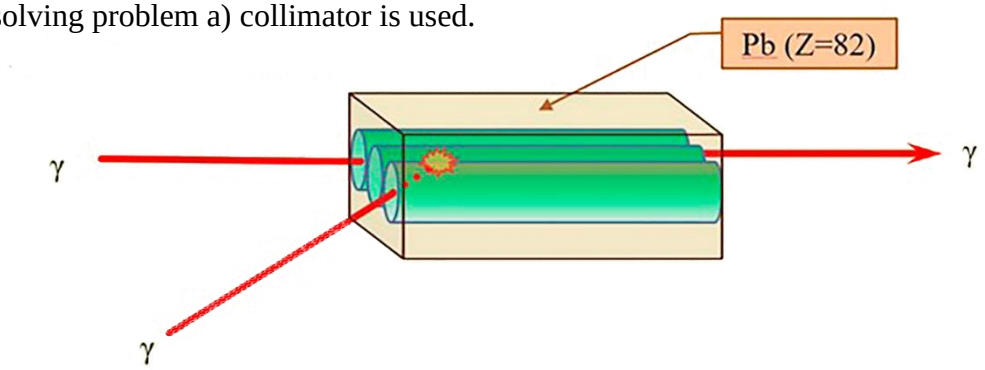

The gamma camera element (collimator) shown in the figure consists of many tubes. Gamma radiation passes through such a collimator only when directed along the axis. Lead is used as a material, as it has a high absorbency.

To solve problem b), a scintillator is used (for example, Tl-activated NaI crystals). They convert invisible gamma rays into flashes of light, which are then converted into electrical impulses by a photomultiplier tube.

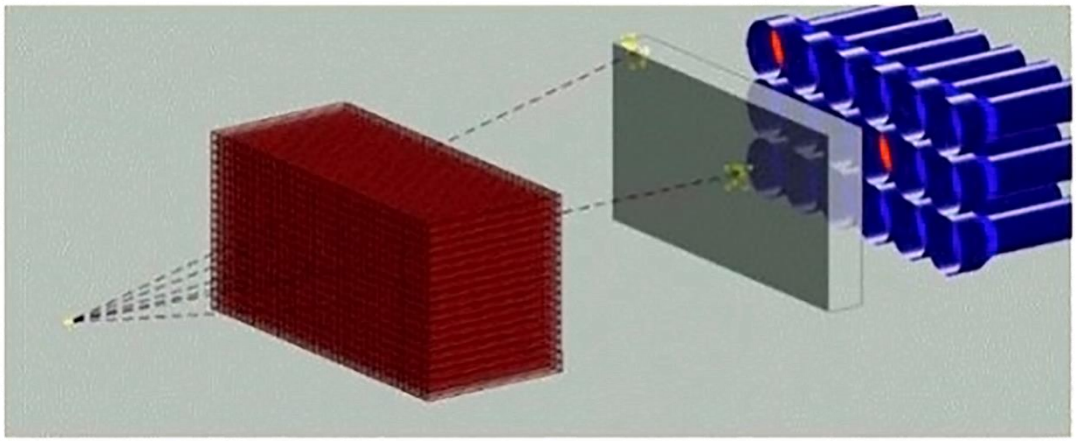

The figure shows how gamma quanta pass through the collimator (brown), cause a flash in the scintillator (gray) and turn into an electrical pulse in the photomultiplier tubes (blue).

But the resolution of such a gamma camera is 6–12 mm, and the size of the left ventricular muscles is 8–12 mm. Therefore, an additional imaging device is required - a computed tomography (CT)[10] scanner or magnetic resonance imaging (MRI)[11] scanner.

Let us consider examples of the use of nuclear physics technologies in the diagnostics and treatment of diseases.

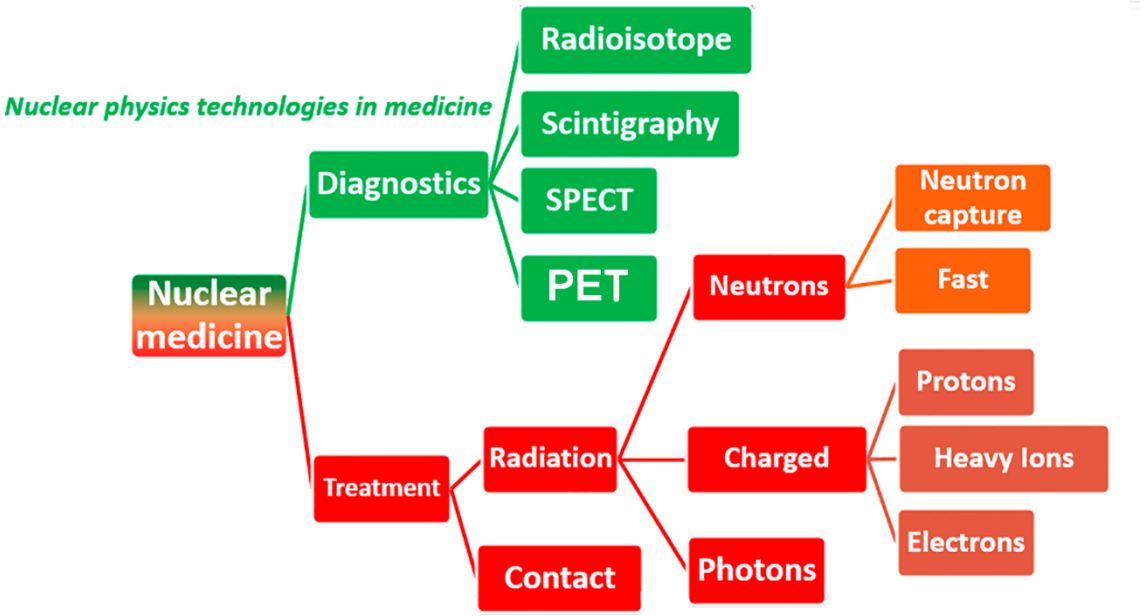

Let's consider methods of treatment. They include several groups. First, by the location of the source of ionizing radiation. They can be located directly next to the affected organ, then we are talking about contact (brachy) therapy. The source may be outside the affected organ, then one speaks about radiation therapy. The radiation particles themselves may not have a rest mass (photon therapy) or be massive (neutron or charged particle therapy). Neutron therapy is penetrating deep into the tissue. Its effect depends on the speed of the neutrons. Slow thermal neutrons with an energy of 0.025 eV are easily captured by nuclides. As the speed of neutrons increases, the probability of their capture by nuclei rapidly decreases. With regard to charged particle therapy, its effect is highly dependent on the mass of the particles. Protons and heavy ions form beams that

[10]Computed tomography scanner - X-ray equipment in combination with software, allowing non-destructive methods to obtain layer-by-layer images of the objects under study at different angles and to perform a three-dimensional reconstruction of their internal structure. CT developers A. Cormack (Great Britain) and G. Hounsfield (USA) were awarded the Nobel Prize in Medicine for 1979.

[11]Magnetic resonance imaging scanner is a hardware and software complex that uses the magnetic resonance method to obtain a layer-by-layer image of the object under study at different angles and allows for a three-dimensional reconstruction of its internal structure. Unlike computed tomography, it does not create a radiation load on the studied organism. MRI developers P. Lauterbur (USA) and P. Mansfield (Great Britain) were awarded the Nobel Prize in Medicine for 2003.

diverge slightly when passing through matter. At the same time, the electron beams begin to diverge at a small depth.

Let's take a closer look at some of the above methods.

1) Neutron therapy.

1.1. Neutron capture therapy. This method is based on the synthesis of artificial radioactive elements under the influence of neutrons, the foundations of which were laid by E. Fermi.

Example. Neutron-boron capture therapy (∽ 1000 people treated).

$$n + {}^{10}_{5}B_5 \rightarrow {}^{11}_{5}B^{*}_{6} \rightarrow {}^{7}_{3}Li_4 + \alpha$$

The advantage of boron is the very high probability of capturing a neutron with the formation of an excited state and subsequent decay into an alpha particle and lithium. The probability of the process is the higher, the lower the energy of the incident neutrons. Thus, a method requires an effective neutron moderation or a source that allows the initial production of low-energy neutrons.

Sources of neutrons:

- nuclear reactor (En = 0–10 MeV, 2 MeV). In this case, a moderator is needed; $\bar{E}_n$ ≈0.025 eV;
- accelerators: ^{7}Li + p → ^{7}Be + n (–1.6 MeV); ^{9}Be + p → ^{9}B + n (- 1.851 MeV). Both reactions are endothermic, that is, for their course, energy supply from the outside is required, that is, the acceleration of protons. For the reaction to proceed in the first case, protons with an energy of 1.6 MeV or more are required, in the second case, 1.851 MeV or more. An accelerator with a controlled proton beam energy makes it possible to obtain neutron fluxes of any required energy from zero and above. It is important that the accelerator allows fine tuning of the proton energy. The advantages of the method being developed in the Russian Federation (G.I.Budker Institute of Nuclear Physics, Siberian Branch of the Russian Academy of Sciences) are the compactness of the installation, less stringent requirements for radiation protection, and the ability to obtain monochromatic neutrons.

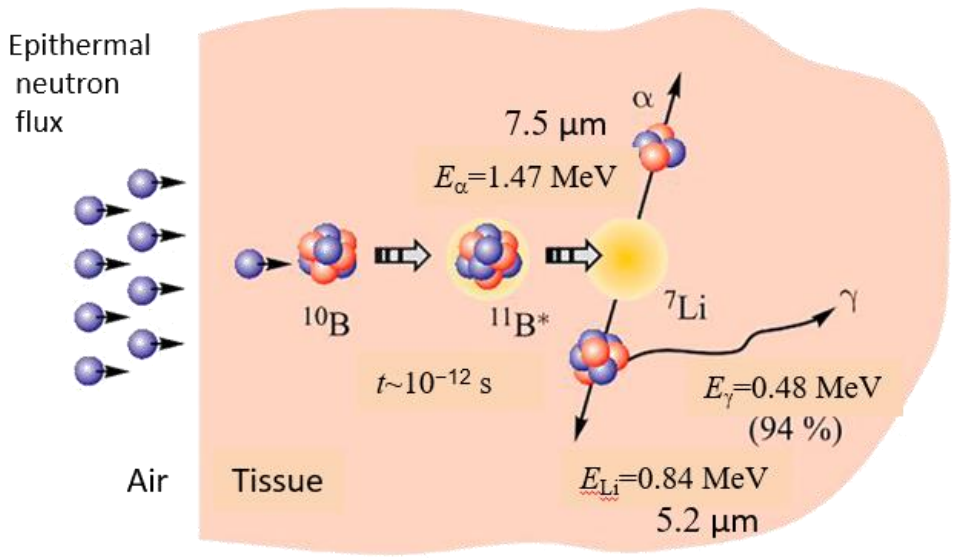

The figure above illustrates the process of boron neutron capture therapy of a malignant tumor. Boron-10 is included in the composition of a pharmaceutical product that delivers to the affected tissue. The main task is to provide a high concentration of boron in the tumor area. The neutron beam from the reactor or accelerator is directed to the place of high boron concentration. It is necessary to adjust the beam energy so that the neutrons stop at the right place. The capture of a neutron creates boron-11 in an excited state, the discharge of which leads, after 10^{-12} s, to the emission of an alpha particle with an energy of 1.47 MeV and Li-7 in an excited state. The latter passes into the ground state with the emission of a gamma quantum with an energy of 0.48 MeV. The range of alpha particles and Li-7 in the tissues is very small, therefore, only the nearby tumor tissues are destroyed. Neighboring healthy tissues are practically not damaged. The desired neutron flux is 10^9 cm $^{-2}$s $^{-1}$.

It should be remembered that along with the interaction of neutrons with boron, there are also background processes with the participation of thermal neutrons:

- ^{14}N (n, p) ^{14}C;
- ^{1}H (n,γ) ^{2}H.

Radiopharmaceuticals have been synthesised that create a concentration of ^{10}B in tumor tissue 3.5 times higher than in healthy tissue, therefore:

- background radiation contribution is acceptably small;
- selective defeat of the cancerous tumor is achieved.

One of the most dangerous malignant tumors is brain glioblastoma. The incidence of this disease is 1 person / 20,000 per year; mortality within 6 months is 100%. Traditional treatments increase survival by 1 year.

Prof. H. Hatanaka (Japan, 1968) performed intraoperative[12]irradiation of 200 patients with a neutron beam from a reactor. The survival rate of patients at stages 3-4 of the oncological process reached 58%. Unfortunately, treatment procedures were discontinued due to the high radiation doses received by the medical staff. However, the method looks very promising. Now neutron boron capture therapy is used in Finland. In the Russian Federation, a clinic is being created on the basis of the Novosibirsk State University, using an accelerator developed at the INP named after Budker as a source of neutrons.

1.2. Fast neutron therapy. This method dates back to the first neutron detection experiments conducted by J. Chadwick and the Joliot-Curies. Only instead of paraffin, the patient's body is

[12] Intraoperative radiation therapy - irradiation of malignant neoplasms in conditions of an open surgical wound and maximum protection of the surrounding organs and tissues - allows high single doses of ionizing radiation to be delivered during surgery directly to the tumor or to the area of its bed.

placed in the path of fast neutrons. Recall that when researchers placed a hydrogen-containing barrier made of paraffin or cellophane between the fast neutron source and the ionization chamber, the ionization chamber registered an increase in the degree of ionization. The reason is that due to the practically equal masses of protons and neutrons, the incident neutron can stop after the first collision, giving all its energy to hydrogen nuclei (protons), which are abundant in biological tissues.

Let us cosider the mechanism of the damaging effect of ionizing radiation, leading to the death of the tumor.

A. The main distinguishing feature of cancer tumors is the ability to divide quickly. This ability can be destroyed by damaging the DNA molecule so that it is not capable of self-healing. Studies show that for this it must be torn apart in several places. In the case when a neutron transfers its energy to a proton, the proton penetrating inside the tumor ionizes the molecules, generating around itself a dense cloud of ionization products - electrons. The latter resemble buckshot, which cuts everything in its path. Including break in several places the DNA molecules of the tumor.

B. Heavy protons and high-energy electrons are capable of breaking molecules apart, forming free radicals[13]. Free radicals are chemically very aggressive and disrupt normal biochemical reactions in the tumor, which also leads to its death.

It should be noted that nuclear medicine deals with such a complex system as the human body. Therefore, it is very difficult to predict a priori the efficacy and safety of a particular treatment method. Practice and the doctor's intuition are critical. The fast neutron method is no exception. It went through a difficult path from initial enthusiasm to complete rejection and, as a result, the definition of indications for its use. R. Stone (USA, 1940s, University of California Clinic), who first used fast neutron therapy, found that tumor regression was achieved, but radiation damage to surrounding tissues was too great. Therefore, fast neutron therapy was abandoned. However, in the 1970s at Hammersmitt Hospital (England) it was found that:

- with neutron irradiation, a more pronounced suppression of the processes of post-radiation cell recovery is observed than with other methods of radiation therapy;
- the radiosensitivity of cells to neutron irradiation slightly differs in different phases of the cell cycle (this is essential, the radiosensitivity of cancer cells is not a constant value and this is one of the problems of the effectiveness of radiation therapy);
- the survival of the irradiated cells weakly depends on the concentration of oxygen in them (studies have shown that the lack of oxygen, characteristic of fast-growing tumor tissues, as a rule, increases their survival);

[13] Free radicals are particles containing one or more unpaired electrons on the outer electron shell.

- the values of the biological effectiveness of radiation used earlier were underestimated, which led to an overdose.

These findings have led to a renaissance in fast neutron therapy. One example is

Washington State University Clinic (Seattle, USA). To obtain fast neutrons, the endothermic reaction of knocking out neutrons from Be nuclei by protons is used (the so-called pn-reaction):

$$^{9}Be + p \rightarrow {}^{9}B + n$$

The figure shows a neutron therapy unit. The patient is placed on a table around which a gantry rotates - a device that allows the beam to be directed at different angles to the horizontal plane. The proton beam is supplied by a system of magnets through a proton guide to a beryllium target. After collimation, the neutron beam emitted from the target is directed to the patient.

To date, fast neutron therapy has been used to treat more than 40,000 patients. It turned out that the greatest efficiency is achieved with cancer of the salivary glands. In this case, local improvement is achieved in more than 50% of cases, compared with about 20% with other methods. However, this does not lead to a noticeable increase in the overall survival of patients, which is associated with the fact that neutron therapy methods are used, as a rule, in the late stages of the disease, when metastases appear in other organs.

2) Proton and ion therapy.

The basis for the medical application of beams of protons and heavy ions (in particular, carbon ions - carbon therapy) is an increase in the probability of interaction of a charged particle with a matter (including biological tissue) as the velocity of this particle decreases. As a consequence, the main loss of energy occurs at the very end of the path in the matter, literally before the very stop. As long as the particle is moving rapidly, it hardly interacts with organs on its way and, therefore, does not damage them. This minimizes tissue destruction along the trajectory of the beam, as well as, if the energy is correctly calculated, behind the tumor. This dependence of energy loss per unit path length is called the Bragg curve.

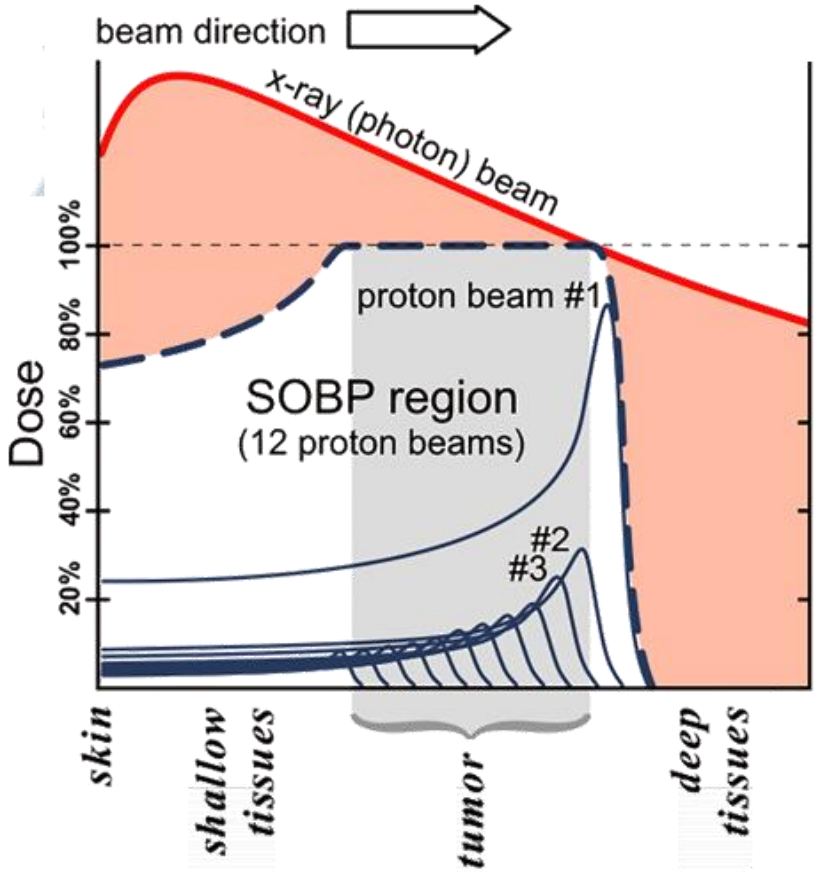

The ordinate represents the radiation dose per path unit (in relative units) for various irradiation schemes. The abscissa shows the depth to which the beam penetrates in the body. Light brown area - the distribution of the relative dose for X-ray irradiation. It can be seen that the maximum radiation dose is concentrated near the body surface, where there is still no tumor (gray area). Moreover, a significant dose of radiation goes to tissues located deeper than the tumor. Naturally, with X-ray irradiation, damage to healthy tissues can lead to both immediate and long-term negative consequences (including the appearance of malignant neoplasms). When irradiated with a monochromatic proton beam (proton beam # 1), the curve of the absorbed dose per unit path corresponds to the Bragg curve (sharp peak at the end of the proton path). In the case when it is

necessary to irradiate tissues at different depths, a series of beams of different energies and intensities is used (beam # 2, # 3 ...). In this case, a modified Bragg curve is formed (bold dashed line, SOBP – Spread-Out Bragg Peak). The distribution of the absorbed dose in depth in this case is abruptly cut off behind the tumor, but the tissues lying in front of the tumor receive a more noticeable dose than with a single Bragg peak.

The first article on the possibility of using proton therapy for the treatment of cancerous tumors was published by the American physicist R.R.Wilson in 1946. Since 1954, the first centers based on research accelerators began operating in the USA and Sweden. Since 1961, the systematic treatment of cancer patients with the use of proton therapy began at Harvard. In Russia, the first experiments with the medical application of proton beams began in 1968 at the Joint Institute for Nuclear Research (Dubna), then in 1969 a proton therapy center was opened at the Institute for Theoretical and Experimental Physics (Moscow). Currently, there are more than 80 proton therapy centers in the world, including 5 in Russia.

The proton therapy method is most effective in the treatment of dense, complex tumors with a clear edge without metastasis, close to vital organs:

- tumors of the head and neck,
- brain tumors
- retina,
- prostate cancer,
- lungs,
- esophagus,
- kidneys.

Accuracy ∽0.5 mm. The irradiation process lasts 1–3 minutes. However, the cost of a course of treatment is high. In the United States, it is about $ 100,000. The price of a course of treatment in the only commercial center of the International Institute named after S. Berezin (MIBS, St. Petersburg) about 2.5 million rubles. In addition, since 2019, the second clinical center for proton therapy of the FMBA of Russia in Dimitrovgrad has been operating in Russia. Another center is planned to be built within the framework of the Multidisciplinary Medical Complex in the Leningrad Region. The rest of the Russian centers are based on research accelerators.

Accelerators used for proton therapy must have a beam energy sufficient to penetrate the body to a depth of 0 to 30 cm. For this, the range of proton energies in the beam must be from 70 to 250 MeV. Structurally, hardware complexes for proton therapy include a cyclotron, which provides a proton beam with the required energy range and high accuracy of adjusting the energy and beam profile, a proton guide that provides a proton beam to the patient, a complex of X-ray equipment (CT) that allows to accurately determine the treatment field. In this case, the system for bringing the

beam to the patient can consist both of a beam fixed in the direction of the beam (in this case, the irradiation of various zones is provided by changing the position of the patient), and also include a complex rotary mechanism that allows the patient to be irradiated from different directions (a rotary device is called a gantry). As an example, the figure shows the equipment of a treatment room for proton therapy at MIBS (St. Petersburg).

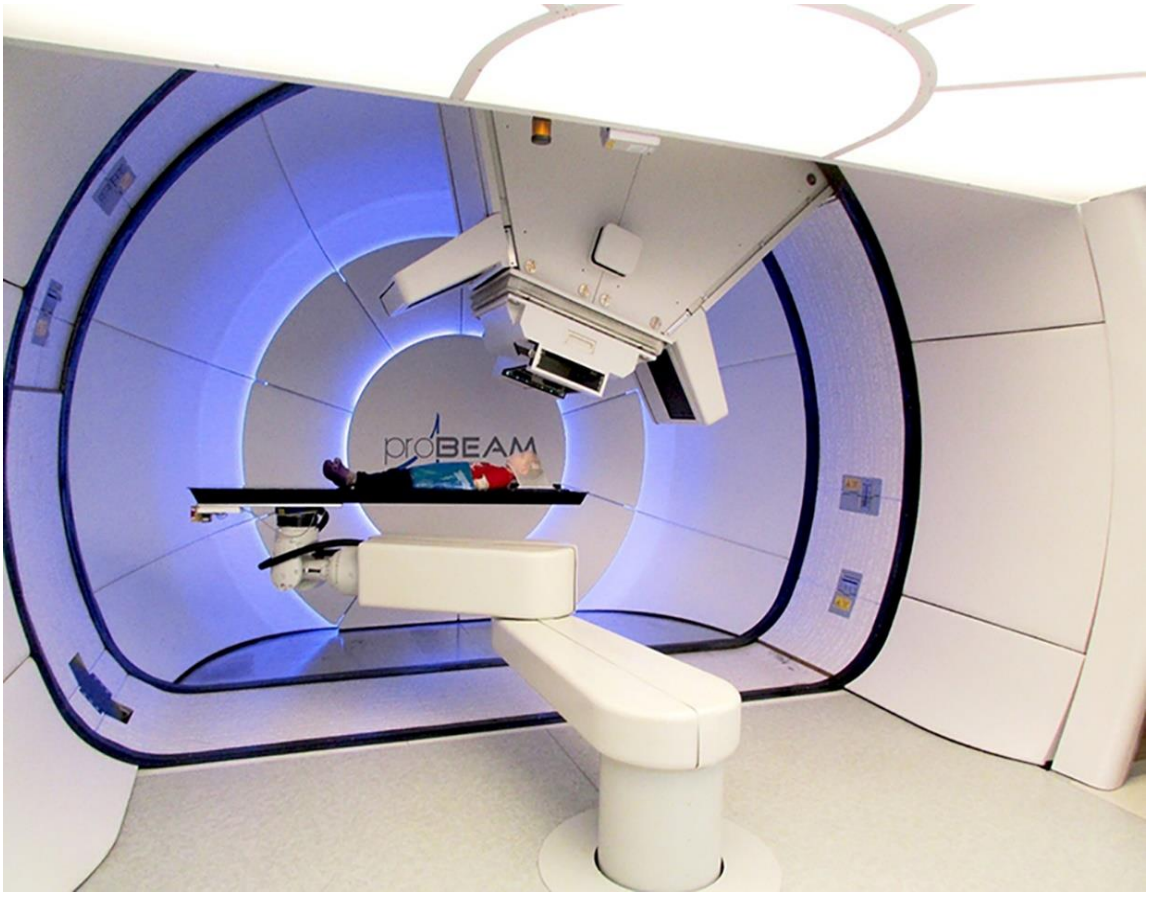

A further development of the proton therapy method is heavy ion therapy. The advantage of the method is the great sharpness of the Bragg peak. As a result, the radiation doses received by tissues outside the treatment field are reduced. Thus, it is possible to increase the radiation dose directed to a cancerous tumor without fear of irradiation of healthy tissues. This, in turn, makes the treatment more effective.

The table shows the number of carbon therapy centers built and under construction (in brackets) in different countries.

Country	Japan	Germany	PRC	Austria	Italy
Accelerators	5 (1)	2 (1)	2	1	1

3) Gamma Knife.

Let us return to the figure showing the distribution of the intensity of the absorbed radiation depending on the depth of the absorber (biological tissue). As can be seen from the figure, when using quanta of the electromagnetic field (in the figure - photons), the maximum of the absorbed energy is located near the surface of the body. Is it possible to use photon irradiation to treat deeply located tumors, while avoiding overexposure of superficial tissues? The answer to this question was the creation in Sweden in 1968 of an installation called the gamma knife.

Consider ^{60}Co for example.

This radioactive nucleus has a half-life of approximately 5.2 years. The decay scheme is as follows:

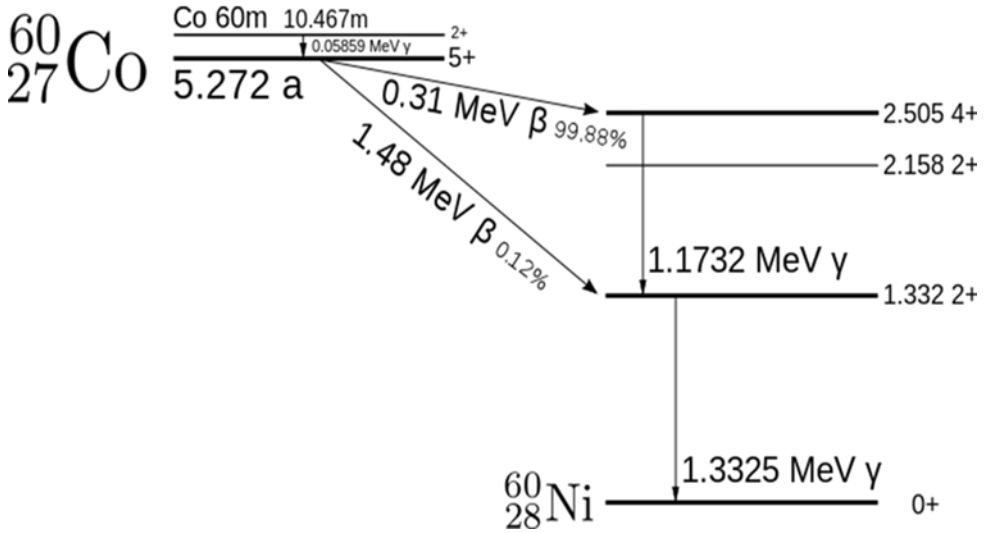

After a beta-decay of ^{60}Co the daughter nucleus ^{60}Ni decays from the excited to ground state by emission of two gamma quanta with energies of 1.1732 MeV and 1.3325 MeV. These two gamma quanta are what are needed to irradiate a sick organism! It is necessary to take ^{60}Co and to use the gamma quanta emitted from the ampoule with these nuclei. To get radioactive ^{60}Co E. Fermi's method with neutrons from neutron generator is used:

$$n + {}^{59}Co \rightarrow {}^{60}Co + \gamma$$

Deposits of stable cobalt are often found together with deposits of silver (for example, in the Czech Republic).

How to obtain high-energy gamma radiation was known long before 1968. In 1968, the last and most important step was taken to protect healthy tissues from overexposure.

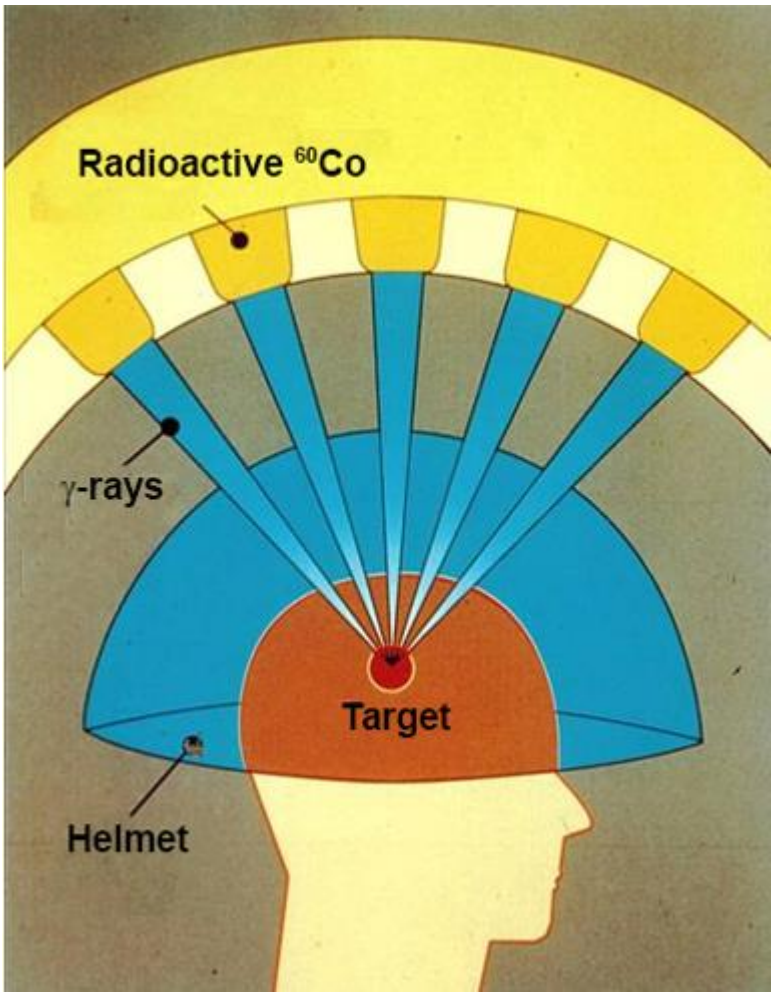

Swedish neurosurgeon Lars Leksell (1907-1986) in 1951 proposed to concentrate several multidirectional beams from radioactive sources at one point (focal point) and thereby achieve the effect of multiple amplification of radiation exposure at this point. This approach has been called radiosurgery. Initially, it was planned to use X-ray sources, but gamma-ray sources are much more compact. The sources (there are about 200 of them in total, the activity of each is about 1 TBq) are placed in a lead casing with collimation holes. The holes are arranged in such a way that all the rays converge at one point. Constant dose surfaces are close to spherical. To fix the patient's head in a certain position, a special helmet is put on the head, fixed on the operating table. The positioning accuracy of the irradiated area is approximately 0.5 mm. The duration of one fraction of irradiation is from 10 min. up to 4 hours. Treatment can be carried out simultaneously (radiosurgery) or within 3-5 days. Splitting the total dose into several fractions often improves treatment results, since at some periods of their development, cancer cells have increased radioresistance. In addition, the reduction in radiation exposure delivered at the same time facilitates the tolerance of radiation therapy. Recurrences of metastases after gamma knife radiosurgery are almost 3 times less common than after linear accelerator radiosurgery.

The picture below shows the installation of the latest generation of gamma knife. Cobalt springs are located behind retractable curtains.

The main types of diseases that are treated with the gamma knife:

- Brain tumors (<3–3.5 cm).
- Vascular coagulation after hemorrhagic stroke.
- Trigeminal neuralgia.

4) Along with the methods of external radiation therapy, when the source is outside the patient's body, methods of interstitial radiation therapy have become widespread, when the source of ionizing radiation is placed in the immediate vicinity of the tumor inside the patient's body (brachytherapy).

Brachytherapy is used to treat tumors of the cervix, uterus, prostate, vagina, esophagus, rectum, tongue. The advantage of brachytherapy is that the tumor is irradiated 40 times more intensely than with conventional radiation therapy, and the surrounding cells are not affected.

There are many types of brachytherapy.

They differ in localization:

- intracavitary (gynecology, proctology);
- interstitial (prostate);
- intraluminal (esophagus, bronchi);
- superficial (application);
- intravascular.

According to the method of application, brachytherapy is distinguished:

- manual - installation and removal of the emitting element is done manually.
- automated - automated remote sequential loading of the source. The source is in a special container and during the procedure is automatically delivered to the planned point of the applicator through the supply channels, and then returned to the storage of the device.

Let us dwell briefly on the diagnostic capabilities of nuclear medicine.

Positron emission tomography (PET) is the most perfect method for tracking functional changes in metabolic processes in the body, as well as localizing tumors. The idea is to inject radiochemical into the body, which include radionuclides that emit positrons. If this drug has an affinity[14] to some areas of cancer cells, then after its introduction into the blood, it reaches the cancer cells with the bloodstream and accumulates in them. Annihilation gamma quanta with an energy of 511 keV escaping from the tumor in opposite directions can be registered using two oppositely located detectors, tuned for signal coincidence. Then the tumor is on a straight line passing through both detectors. By rotating a pair of detectors around the tumor site or using multiple opposing pairs of detectors, it is possible to pinpoint the tumor at the intersection of the lines connecting the detectors. In a similar way, one can find out the functional state of the internal organs (for example, the heart) by the picture of the accumulation of the radiopharmaceutical. The choice of the chemical is decisive.

A PET complex is shown in the figure below

[14]Affinity is the strength of interaction between individual sections of macromolecules, which determines their mutual affinity. Affinity is based on spatial correspondence (complementarity) of interacting areas.

One of the most common radiopharmaceuticals is ^{18}F-fluorodeoxyglucose (the OH group in glucose is replaced by ^{18}F, which undergoes β+ (positron) decay to ^{18}O with a half-life of $T_{1/2}$ = 109.8 min). Glucose is heavily consumed by rapidly growing cancer cells. Therefore, after injection of this radiopharmaceutical into the blood after 60-90 minutes, a noticeable amount of it will accumulate in the cancer cells. At the same time, the decay product of ^{18}F - oxygen is not toxic and does not cause negative consequences. From the picture of the accumulation of fluorodeoxyglucose in the heart muscle under stress and without, one can judge the functional state of the heart, which is used in cardiology. To obtain ^{18}F, as a rule, the pn reaction on ^{18}O nuclei is used:

$$^{18}_{8}\mathrm{O}\left(p,n\right)^{18}_{9}\mathrm{F}$$

Naturally, to obtain ^{18}F, the proton accelerator must be placed next to the PET facility.

Not in all cases ^{18}F fluorodeoxyglucose can be used for the diagnosis of oncological diseases. For example, the brain consumes glucose intensively during work, so the accumulation of this radiopharmaceutical in brain tumors is almost impossible to notice. More effective is ^{11}C-methionine. Methionine is an essential amino acid accumulated by rapidly growing cells.

^{11}C decays with a half-life of 20.3 minutes:

$$^{11}_{6}\mathrm{C} \rightarrow {}^{11}_{5}\mathrm{B}+\mathrm{e}^{+}+\nu_{e}+0.96\ \text{МэВ}$$

and the location of the tumor can be determined using PET.

Naturally, such a short-lived isotope must be produced in the immediate vicinity of the diagnostic site. For this, an accelerator (usually a cyclotron) and a reaction are used:

$$^{10}_{5}\mathrm{B}\left(d,n\right)^{11}_{6}\mathrm{C}$$

One of the most common oncological diseases in men is prostate cancer (PCa), and even after treatment, after 10 years with a probability of 27–53%, there is a relapse with metastases. It is becoming clear how important early diagnosis of this disease is.

The standard screening method is based on the determination of the serum PSA level in the blood. The norm is 2.5 ng / ml. If PSA is <4 ng / ml, the chance of cancer is 15%; if PSA <10 ng / ml - 25%; if PSA> 10 ng / ml - 50%. But the reliability of the method is low. Even if PSA is normal, this does not guarantee the absence of cancer.

In prostate cancer, prostate specific membrane antigen (PSMA) molecules are concentrated on the surface of cancer cells - 10 times more than on healthy ones. A chemical agent that binds to PSMA was found. This agent, labeled with the ^{68}Ga radionuclide, decays with the emission of positrons:

$$^{68}\mathrm{Ga} \rightarrow {}^{68}\mathrm{Zn} + \mathrm{e}^{+} + \nu_{e}.$$

It was named ^{68}Ga-PSMA. The half-life of ^{68}Ga is about 68 minutes, which is acceptable for diagnostics, but requires obtaining this isotope immediately before the study. Fortunately, no accelerator is required to produce ^{68}Ga. It is enough to use ^{68}Ge, which turns into ^{68}Ga in the process of electron capture

$$^{68}\mathrm{Ge} + e^{-} \rightarrow {}^{68}\mathrm{Ga} + \nu_e$$

with a half-life of 271 days. Thus, ^{68}Ge can be produced at a cyclotron far from a hospital, and then ^{68}Ga can be obtained from it at the research site. ^{68}Ga-PSMA is highly effective in the diagnosis of cancer. Cancer can be detected with PSA> 0.2 ng / ml. At the same time, the accuracy is 86%.

Summarizing what has been said about nuclear medicine, we can conclude that over the past few decades, nuclear physics has become one of the most important components of the struggle for human health.

LECTURE 7

NUCLEAR REACTIONS

7.1. General form of nuclear reactions

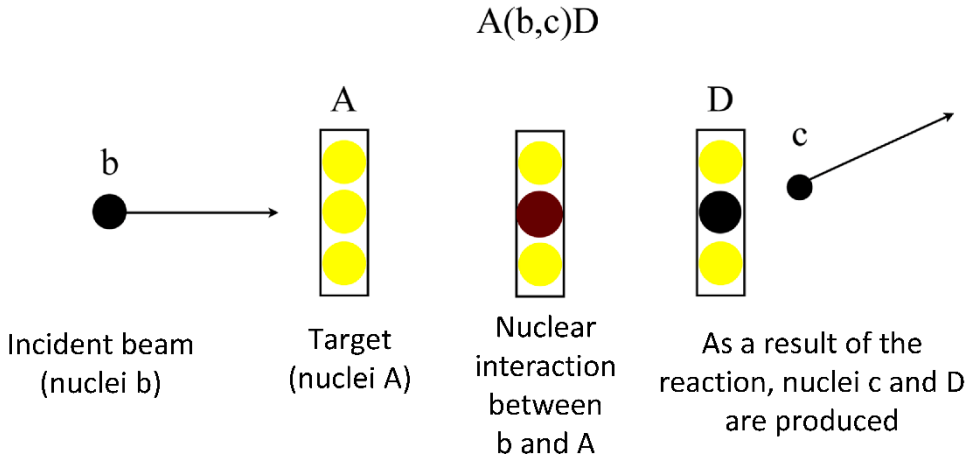

7.2. Conservation laws in nuclear reactions

1) Conservation of mass-energy;

$$(E_A + M_A c^2) + (E_b + M_b c^2) = (E_c + M_c c^2) + (E_D + M_D c^2);$$

$$Q = (M_A + M_b - M_c - M_D)c^2 = E_c + E_D - E_A - E_b$$

2) Conservation of charge;

3) Conservation of the number of heavy particles (baryons);

4) Conservation of angular momentum;

5) Conservation of angular momentum (taking into account the spins of particles);

6) Conservation of parity;

7) Conservation of isospin in strong interactions.

7.3. Nuclear reactions mechanisms

Scattering is a process without changing the composition of particles.

Elastic scattering does not lead to particle excitation.

Inelastic scattering is accompanied by particle excitation.

Reaction is a process with a change in the composition of particles.

The long mean free path of a nucleon in the nucleus makes possible a single interaction of the incident nucleon with nucleons of the nucleus - a *direct nuclear reaction*. The "jamming" of an incident nucleon in a nucleus followed by the emission of other nucleons is a reaction through a *compound nucleus* (figure below).

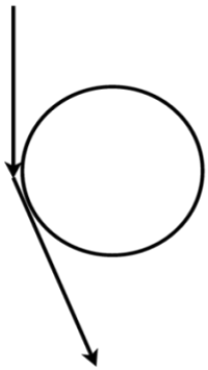

Potential elastic and inelastic scattering
A (b, b) A
A (b, b ') A*

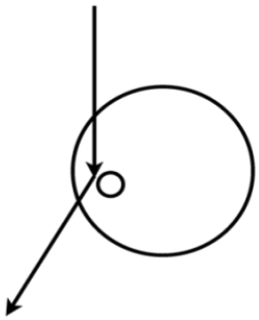

Direct reactions
A(d,p)D* A(p,d)D*

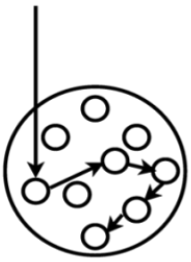

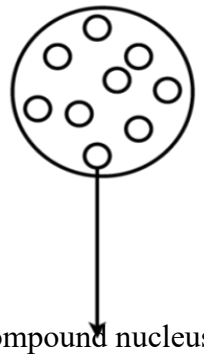

Creation and decay of the compound nucleus
A + b →F * → c + D

a) Elastic scattering.

The optical potential V ($\vec{r}$) between the incident particle and the target nucleus can be represented as the sum of the components of the interactions V (| $\vec{r}$ - $\overrightarrow{r'}$|) of the incident particle with individual nucleons of the scattering nucleus (the density of nuclear matter is ρ_m (r)).

$$V(r) = \int \rho_m(r')V(r-r')d^3r'.$$

Due to the short-range nature of nuclear forces, the potential repeats the shape of the nucleus:

$$V(r) = \frac{V_0}{1 + exp\left(\frac{r-R}{a}\right)}$$

− Woods-Saxon potential (R is the radius of the nucleus, a is the diffusion parameter).

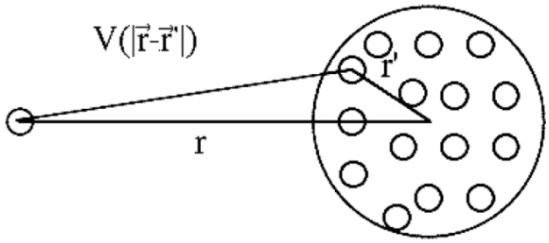

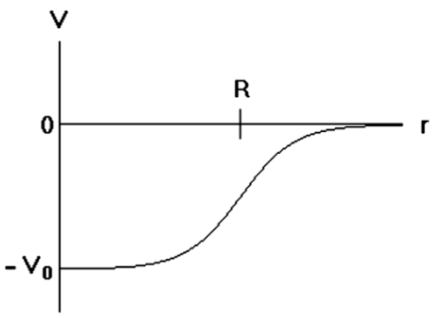

The nuclear potential acts on the incident particles as a lens, changing their direction. At certain energies, the phases of various multiply reflected waves suppress the incident radiation and maxima appear in the cross section (fig. below).

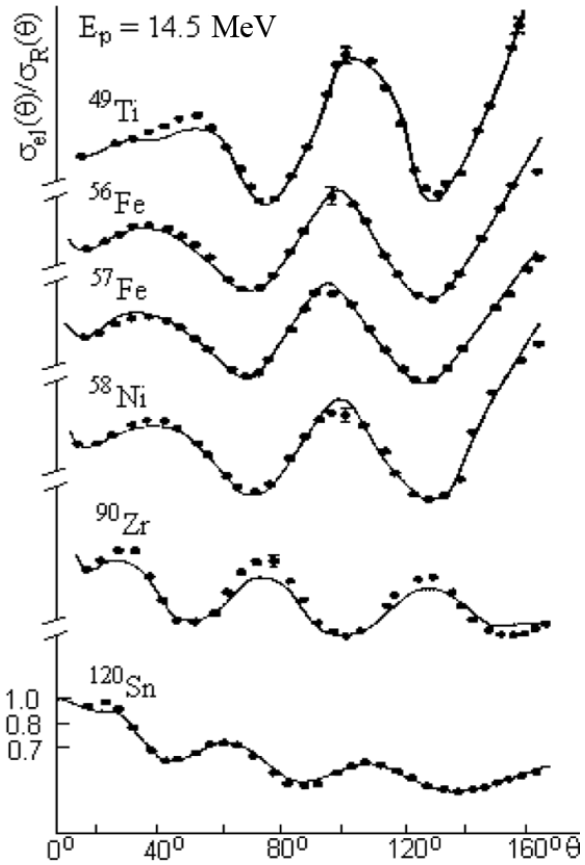

b) Inelastic scattering.

The appearance of inelastic channels weakens the incident wave. To take this circumstance into account, a complex term (a lens with refraction and absorption) should be introduced into the potential of the Schrödinger equation.

- The imaginary part mainly acts on the nuclear surface
- As in the shell model, it is necessary to take into account the spin-orbit interaction, which depends on the derivative of the potential

c) Direct nuclear reactions. Angular distributions in (*p*,*d*) and (*d*,*p*) nuclear reactions.

From the conservation law for the momenta of the neutron, proton and deuteron - (dp) the stripping reaction:

$$k_n^2 = k_d^2 + k_p^2 - 2k_d k_p cos\vartheta.$$

In the case of the capture of a neutron with an impact parameter R, the orbital momentum transferred to the nucleus will be:

$$l_n\hbar = \vec{r} \times \vec{p} = Rk_n\hbar;$$

$$l_n = Rk_n.$$

Knowing the angular momentum and parity of the ground state of the target, we can estimate the angular momenta and parity of the excited states of the residual nucleus (see fig. below).

$$|(|J_A - l_n| - 1/2)| \leq J_{B^*} \leq J_A + l_n + 1/2\,; \quad \pi_A \cdot \pi_{B^*} = (-1)^l.$$

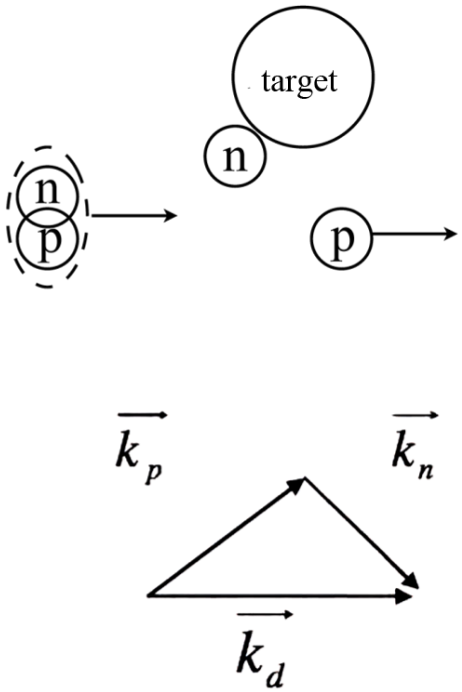

Experimental angular distributions for various states of the final ^{59}Ni nucleus excited in the ^{58}Ni (d, p) ^{59}Ni reaction at an energy of E_d = 15 MeV, and the results of calculations using the distorted wave approximation. All four cases differ in the transfer of the orbital angular momentum Δl.

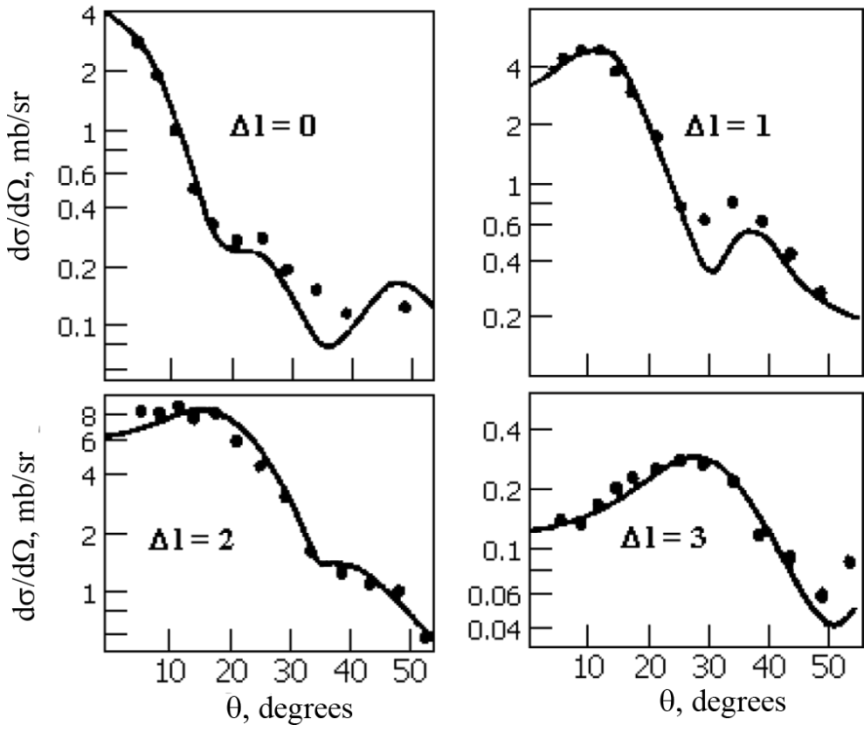

d) Compound nuclei (fig. below).

- When nuclei collide, a larger compound nucleus is formed, which is a highly excited state resulting from the fusion of nuclei.
- After a short time, the compound nucleus decays.
- At the stage of a compound nucleus, information about the type of incident nuclei (or particles) is completely lost.
- The cross section of the process can be represented in the form of two independent factors depending on the initial and final states.

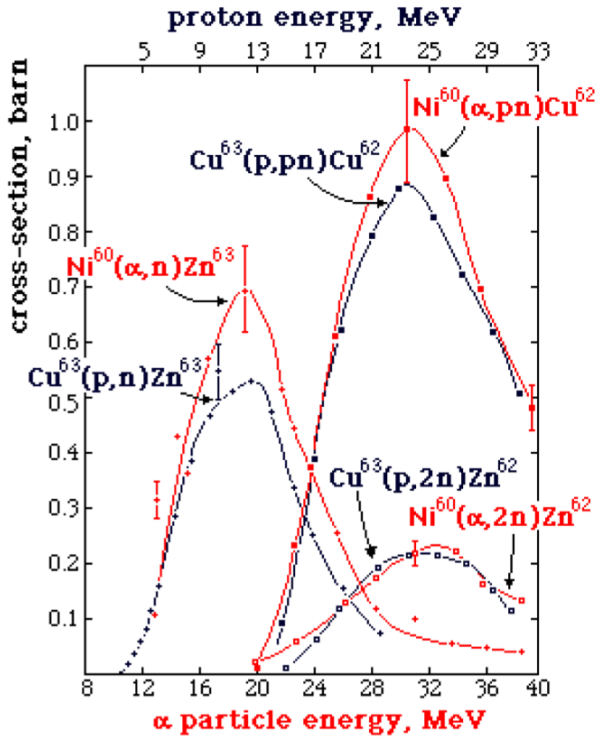

As the energy of the incident particles increases, the composition and number of particles emitted from the compound nucleus change. An increase in the multiplicity of emitted particles indicates a multistage energy transfer from the incident particle (figs. below).

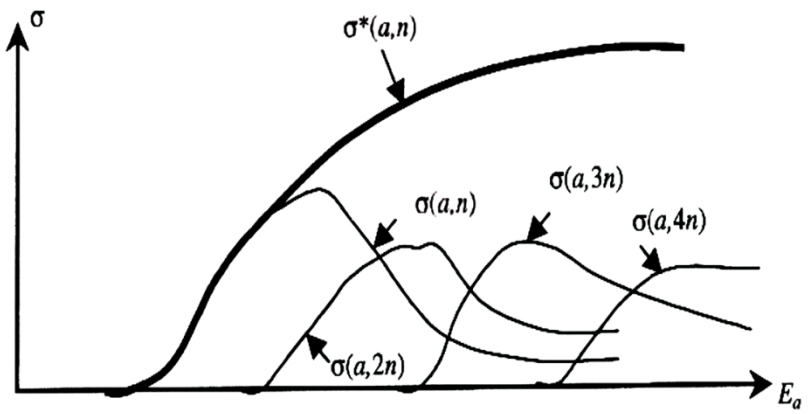

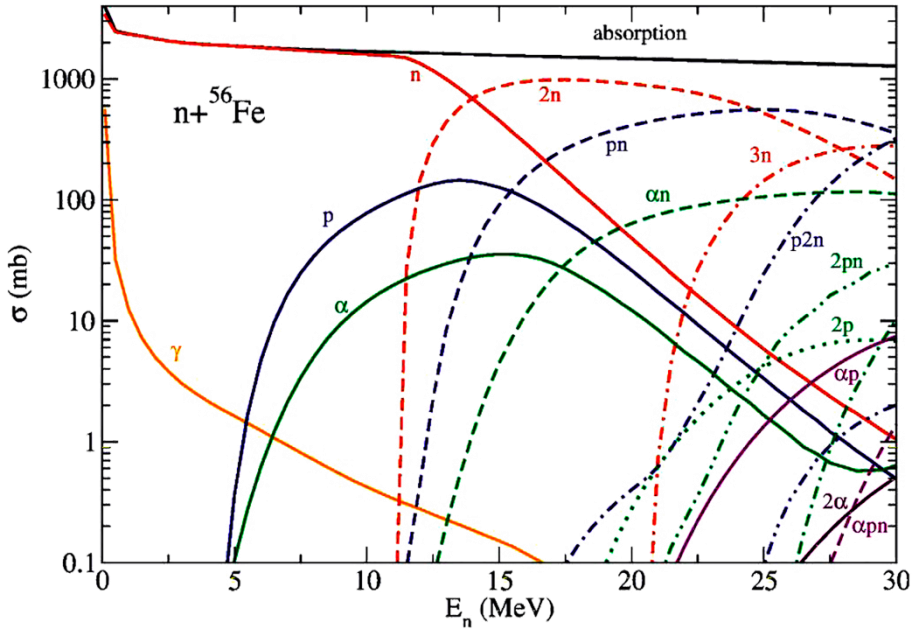

Fig. below shows angular distributions of 3.3 MeV protons from reactions (α, p) - upper curve and (p, p‘) - lower curve. In both cases, the same compound ^{59}Co nucleus is excited with the same excitation energy. It can be seen that the anisotropy in the case of the reaction caused by α -particles with an energy of 20.7 MeV is greater than in the case of using protons with an energy of 16.33 MeV. The cause of the anisotropy is the rotation of the compound nucleus around the axis perpendicular to the direction of the incident particle.

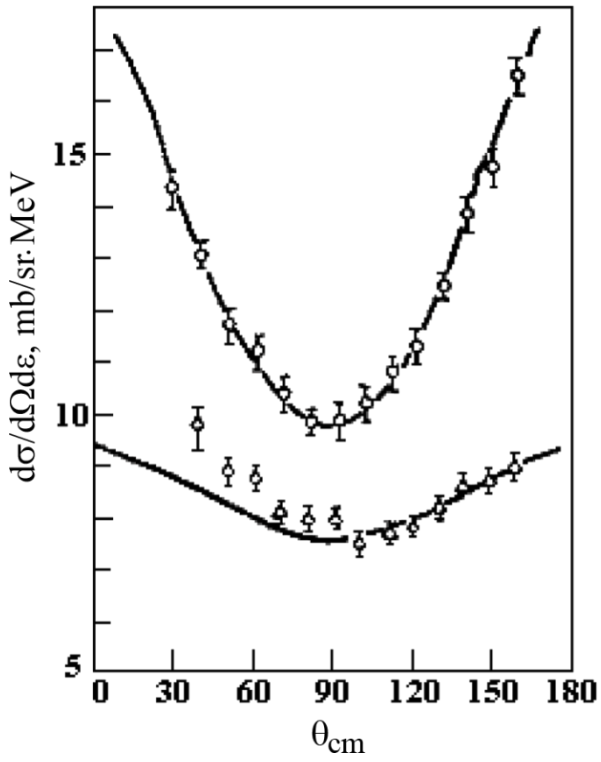

NUCLEOSYNTHESIS

The stages of the evolution of the Universe are shown below.

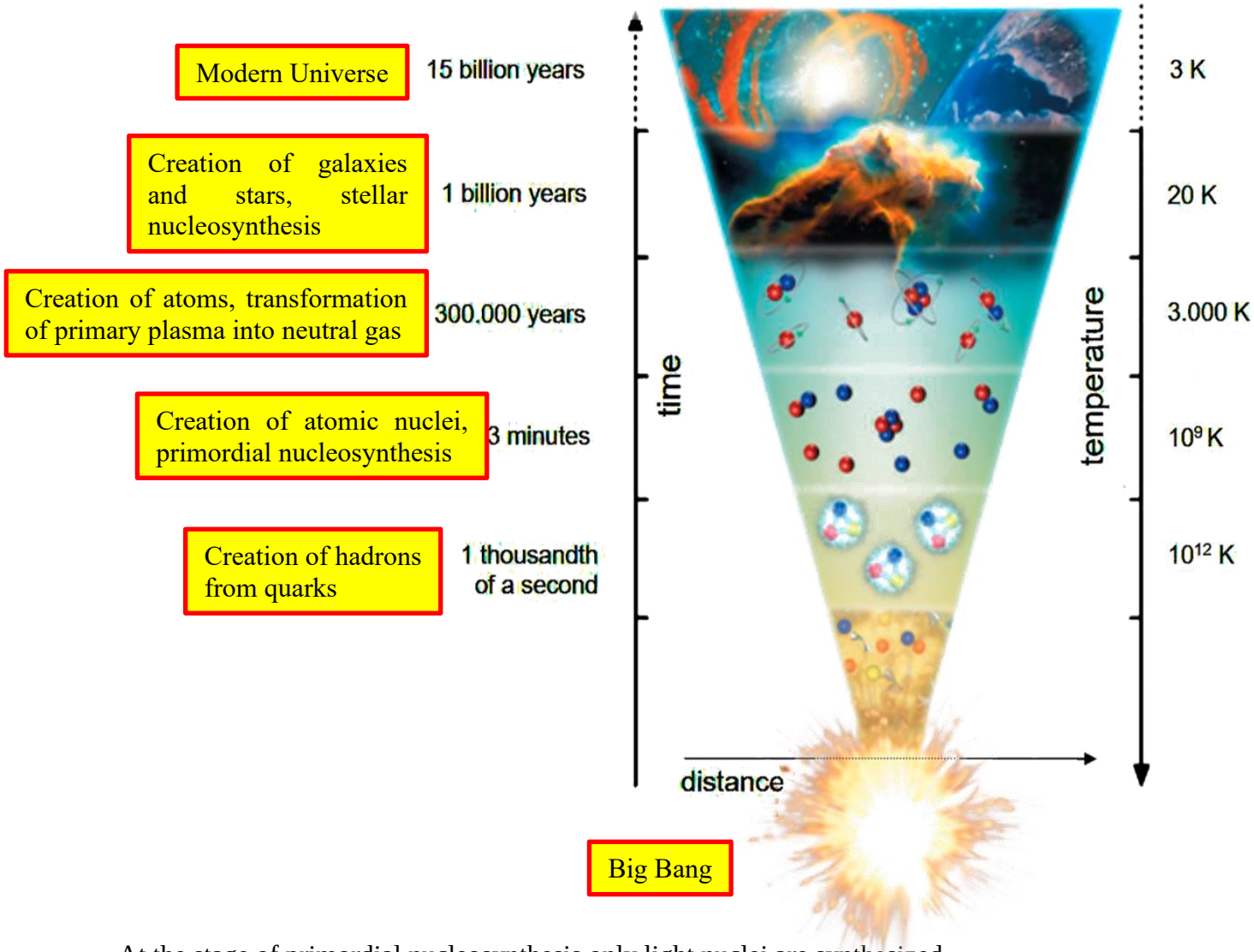

At the stage of primordial nucleosynthesis only light nuclei are synthesized.

Temperature decrease and increase in the size of the Universe stopped the fusion process on stable ^{7}Li.

7.4. Reactions of primordial nucleosynthesis

The first (1-3) minutes of the Universe are shown in the fig. below.

At a temperature T> 10^{10} K, neutrons and protons pass into each other as a result of the reactions:

$$p + e^- \rightarrow n + \nu_e; n + e^+ \rightarrow p + \tilde{\nu}_e.$$

The necessary e^+ and e^- are formed due to the high temperature of γ-quanta in the reaction

$$e^+ + e^- \leftrightarrow \gamma + \gamma. \qquad (*)$$

At this stage $N_n/N_p = 1/5$.

At T $<10^{10}$ K (*) stops and N_n decreases (process 1) to 1/6 of N_p.

When the Universe cools down to T $<10^9$ K, the kinetic energy of thermal motion becomes insufficient for the destruction of ^{2}H deuterons and their accumulation begins (process 2). Processes (3-6, 9, 11) lead to the formation of ^{4}He, and (7, 10, 12) — ^{7}Li. Cooling of the Universe and its expansion cut off the chain of primary nucleosynthesis. Since at the beginning of primary nucleosynthesis there was one neutron for 6 protons, at the end there is one alpha particle for every 10 protons, which is confirmed by astronomical data. The process of formation of nuclei of greater mass occurs in stars.

1. $n \rightarrow {}^1H + e^- + \tilde{\nu}_e$;
2. ${}^1H + n \rightarrow {}^2H + \gamma$;
3. ${}^2H + {}^1H \rightarrow {}^3He + \gamma$;
4. ${}^2H + {}^2H \rightarrow {}^3He + n$;
5. ${}^2H + {}^2H \rightarrow {}^3H + 1H$;
6. ${}^2H + {}^3H \rightarrow {}^4He + n$;
7. ${}^3H + {}^4He \rightarrow {}^7Li + \gamma$;
8. ${}^3He + n \rightarrow {}^3H + {}^1H$;
9. ${}^3He + {}^2H \rightarrow {}^4He + {}^1H$;
10. ${}^3He + {}^4He \rightarrow {}^7Be + \gamma$;
11. ${}^7Li + {}^1H \rightarrow {}^4He + {}^4He$;
12. ${}^7Be + n \rightarrow {}^7Li + {}^1H$.

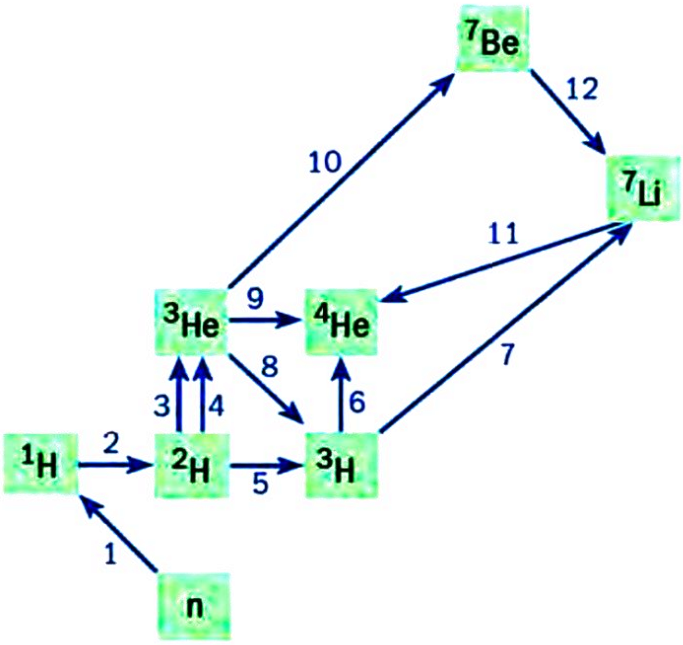

7.5. Thermonuclear reactions in stars

a) CNO-cycle.

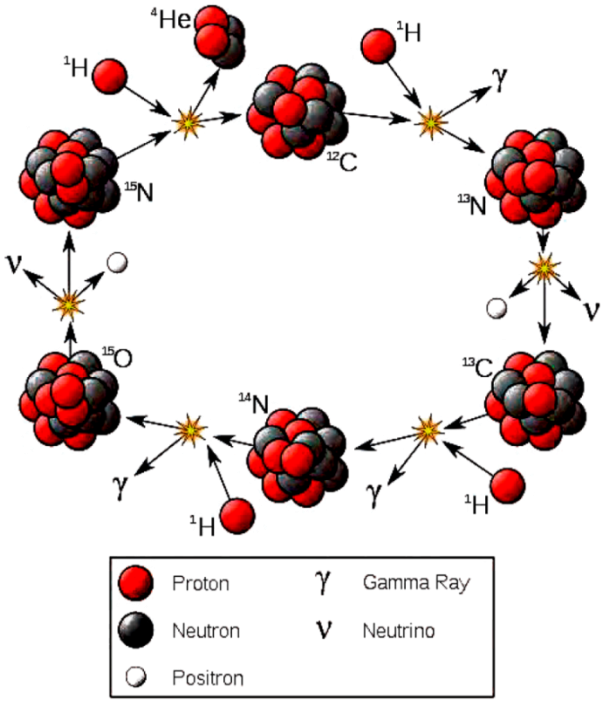

CNO cycle (fig. above): the process of converting 4 protons into an alpha particle, 2 positrons and 2 electron neutrinos with the participation of ^{12}C (acting as a catalyst). The CNO cycle is an example of thermonuclear fusion occurring in stars. Due to the large height of the Coulomb barrier between the proton and carbon, it is leading at T> $17x10^6$ K. The source of energy is gravitational compression, therefore, it occurs at a star mass> 1.3 solar masses. The CNO cycle is possible if the core of the star contains carbon formed in the previous stages of stellar nucleosynthesis. In the cycle, the ^{12}C nucleus and four protons are converted into ^{12}C and an α-particle

The energy yield in the $4p \rightarrow {}^4He$ reaction is 26.7 MeV. About 25 MeV goes to heating the star, and the rest is carried away by neutrinos.

b) pp-cycle.

In cold stars, the hydrogen combustion cycle is more important - the pp cycle (fig. below).

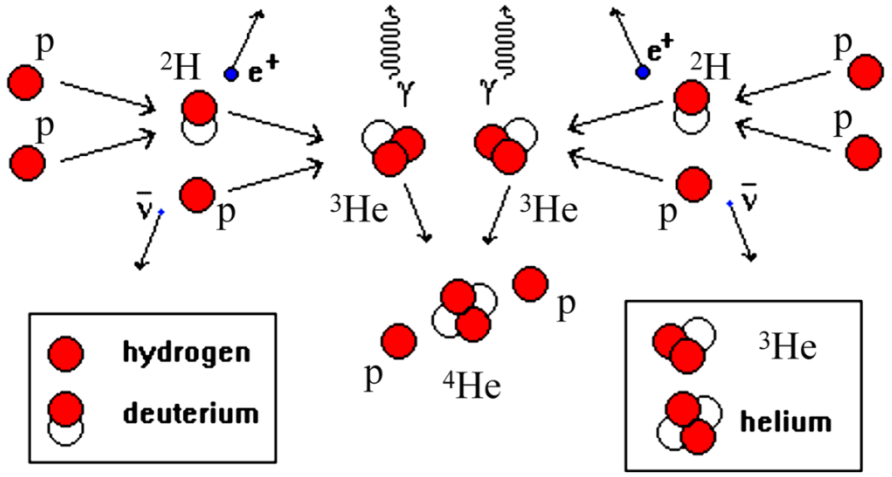

The pp cycle proceeds more slowly than the CNO cycle, but at a lower temperature ⇒ less mass of the star. Thermonuclear fusion process. The main source of solar energy. The energy yield in the $4p \rightarrow {}^4He$ reaction is 26.7 MeV (as in the CNO cycle)

To calculate the reaction rates, it is necessary to know:

a) the temperature distribution inside the Sun;

b) effective cross sections for the indicated reactions up to energies of the order of $14 \cdot 10^6$ K (several keV).

7.6. Star nucleosynthesis

Nucleosynthesis of elements more massive than helium occurs predominantly in stars. The specific binding energy in elements up to Fe increases with an increase in the mass number; therefore, fusion reactions are accompanied by the release of energy. As the charge of the nuclei participating in the fusion increases, the height of the Coulomb barrier increases, so higher temperatures are required. The source of energy is the energy of gravitational compression.

In the core of the star, hydrogen is converted to helium.

The next stage is the beginning of the reaction of the triple alpha process:

$$^4He + ^4He + ^4He \rightarrow ^8Be + ^4He \rightarrow ^{12}C^* \rightarrow ^{12}C + \gamma \text{ (7.37 MeV are released).}$$

For this reaction to occur, a temperature of ~ 10^9 K and a density of ~ 10^4 g / cm^3 are required, which are reached during the gravitational compression of the core. The lifetime of ^{8}Be is ~ 10^{-16} s, but the fusion reaction has time to occur before the decay of ^{8}Be due to the high probability of the formation of a carbon nucleus in this reaction in an excited state of 7.65 MeV (resonance reaction).

As ^{12}C accumulates, the process begins:

$$^{12}C + ^4He \rightarrow ^{16}O + \gamma \text{ (7.16 MeV).}$$

The sequential addition of ^{4}He leads to the formation of ^{20}Ne, ^{24}Mg, ^{28}Si, ^{32}S in exothermic reactions.

At a temperature of ~ 10^9 K and a density of 10^5 g / cm^3, the process of fusion of carbon nuclei begins:

$$^{12}C + ^{12}C \rightarrow ^{20}Ne + ^4He \text{ (4.62 MeV).}$$

The next process is the fusion of oxygen nuclei: $^{16}O + ^{16}O \rightarrow ^{28}Si + ^4He$ (9.59 MeV).

The origin of the elements beyond Fe. The formation due to the interaction of charged particles is suppressed (Coulomb barrier). Solution: add neutrons.

Reactions giving neutrons for the process (nuclides from the CNO cycle).

Process A.

$^{12}C+p\rightarrow ^{13}N+\gamma$ (1.94 MeV);

$^{13}N \rightarrow ^{13}C+e^{+}+\nu_e$ (1.2 MeV, $T_{1/2}$ =10 min.);

$^{13}C+\alpha\rightarrow ^{16}O+n$ (2.22 MeV).

Process B.

$^{14}N+ \alpha \rightarrow ^{18}F+\gamma$;

$^{18}F \rightarrow ^{18}O+e^{+}+\nu_e$ ($T_{1/2}$ =109.7 min.);

$^{18}O+ \alpha \rightarrow ^{22}Ne+\gamma$;

$^{22}N+\alpha\rightarrow ^{25}Mg+n$.

1. *s-process* (slow process). The process of slow radiative neutron capture (n, γ) -reaction. The neutron must be captured by the nucleus before the beta decay of the nucleus occurs, that is, the reaction on stable and long-lived nuclei. Nuclides are formed along the valley of stability.

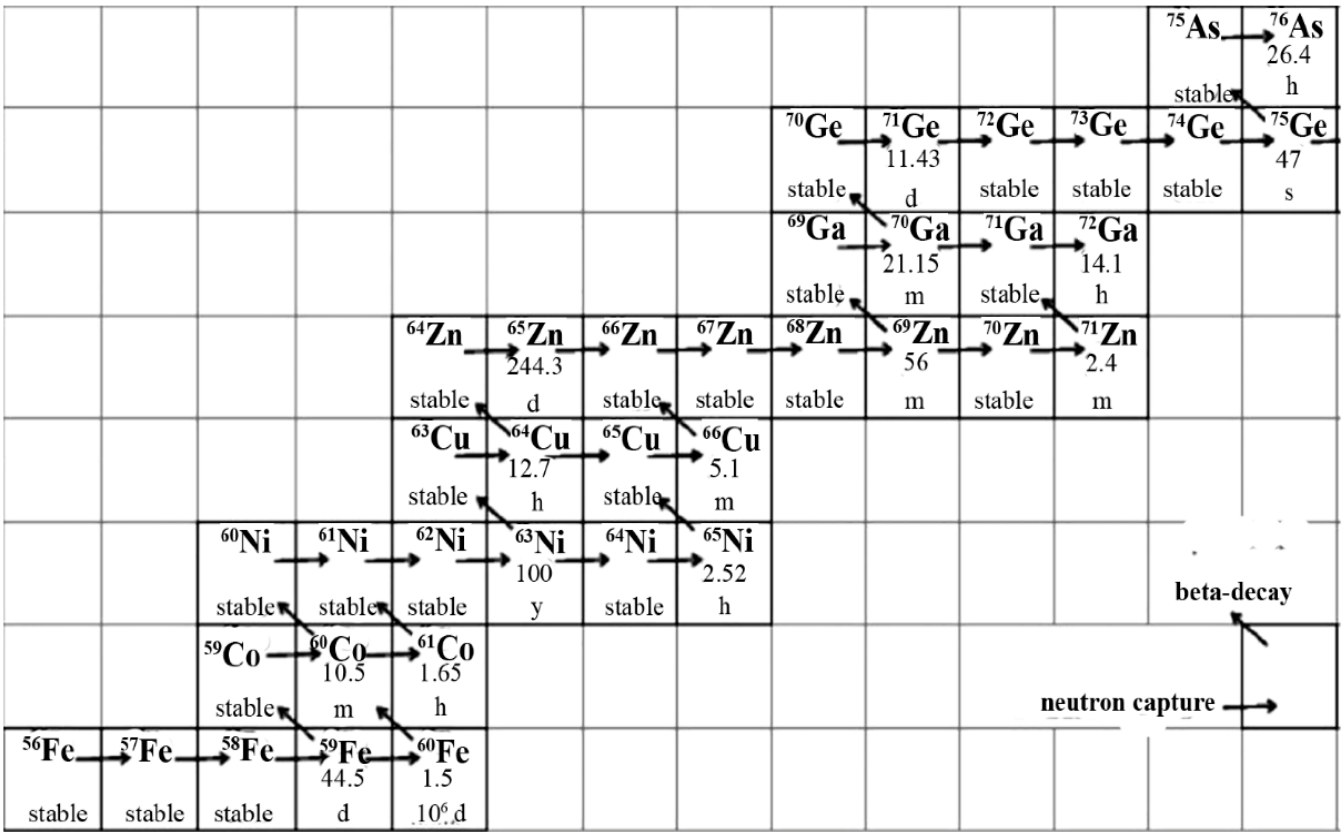

2. *r-process* (rapid process, fig. below). Unstable neutron-excess nuclides (nuclei heavier than ^{209}Bi) are formed, which are below the valley of stability.

As a result of neutron capture, an unstable nuclide is formed, which also captures a neutron, etc. The neutron flux density must be large enough to have time to interact with an unstable nuclide before its decay.

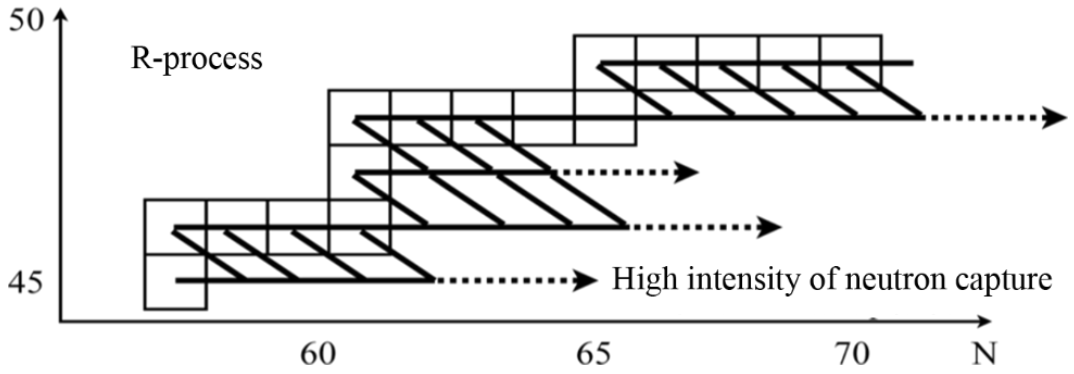

3. *p-process* (proton process). Formation of stable proton-excess nuclides that cannot be obtained in *s*- and *r*-processes (lie above the valley of stability). Examples: proton capture reactions (p, n), (p, γ) and photodisintegration reactions (γ, n), (γ, 2n).

4. *rp-process* (rapid proton process, fig. below). Formation of unstable proton-excess nuclides, for example, in (p, γ) and (p, n) reactions. To overcome the Coulomb barrier $T > 10^9$ K.

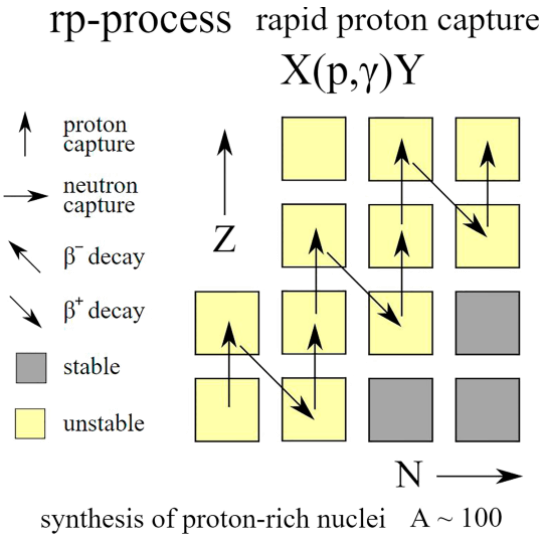

7.7. Origin of elements in the Universe

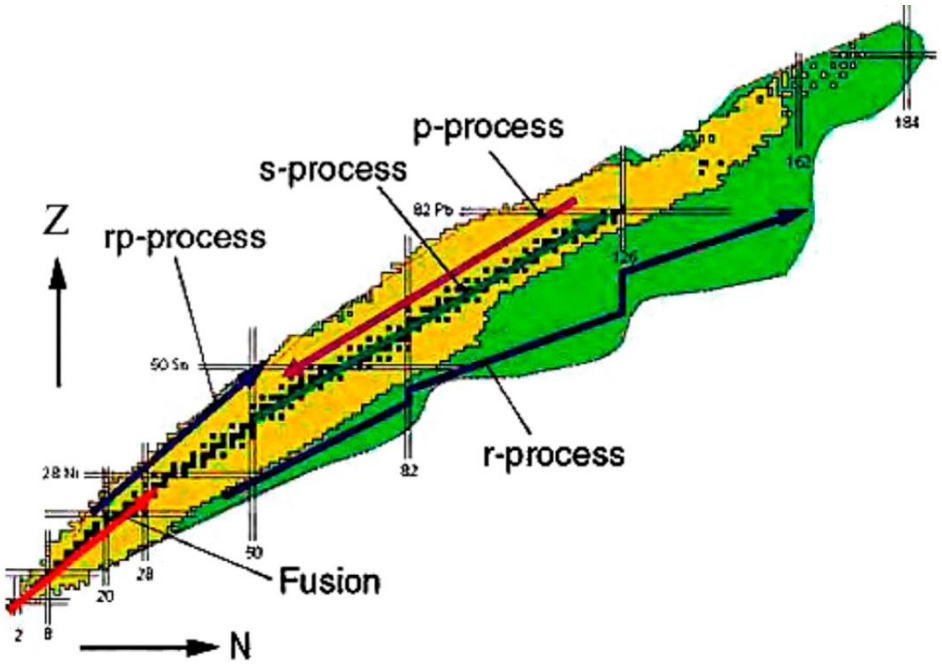

1. The region of small N and Z (Fusion) —reactions of thermonuclear nucleosynthesis: primordial and stellar.
2. Elements heavier than Fe along the stability track are a slow neutron capture process (*s*-process).

3. Unstable elements heavier than Fe below the valley of stability - the process of fast neutron capture (*r*-process).
4. Stable elements are heavier than Fe at the upper boundary of the valley of stability - the process of proton capture (*p*-process).
5. Unstable elements heavier than Fe above the valley of stability — a fast process of proton capture (*rp*-process).

LECTURE 8

ELEMENTARY PARTICLES

8.1. CPT symmetry

Spatial (P) parity.

The transition from the selected coordinate system to the system corresponding to the mirror reflection of all coordinate axes leads to the transformation of the wave function:

$$\hat{P}\Psi(r) = \Psi(-r) = p\Psi(r);$$

$$\hat{P}\hat{P}\Psi(r) = p^2\Psi(r) = \Psi(r); p = \pm 1.$$

If the Hamiltonian of the system commutes with the operator of spatial reflection, the parity of the system is a "good quantum number," that is, conserved.

Transformation of true vectors: $\hat{P}(\vec{r}) = -\vec{r}$; $\hat{P}(\vec{p}) = -\vec{p}$.

Transformation of axial vectors: $\hat{P}(\vec{J}) = -\vec{J}$.

In strong and electromagnetic interactions, the *P*-parity is preserved, the weak interaction breaks the spatial symmetry:

$$\left[\hat{H}_{\text{weak}}, \hat{P}\right] = \hat{H}_{\text{weak}}\hat{P} - \hat{P}\hat{H}_{\text{weak}} \neq 0.$$

Charge (C) parity.

Turns a particle into an antiparticle.

$$\hat{C}Q \to -Q; \quad \hat{C}|\text{particle}\rangle \to |\text{antiparticle}\rangle.$$

For truly neutral particles and systems, the wave function can be an eigenfunction of the C-parity operator.

$$\hat{C}|\Psi\rangle = \lambda_C|\Psi\rangle.$$

Positive *C*-parity particles: π^0 meson, η meson.

Negative *C*-parity particle: γ.

C-parity is conserved in strong and electromagnetic interactions.

CP parity.

In the case of weak interaction *C* and *P* parities are not conserved, but the combined *CP* parity is usually conserved. However, for some particles (K^0-mesons, mass 497.7 MeV and B-mesons, mass 5279 MeV) this is also incorrect. Combined parity of 2-pion and 3-pion systems is:

$$\hat{C}\hat{P}|\pi^+\pi^-\rangle_{l=0} = +|\pi^+\pi^-\rangle_{l=0}, \qquad \hat{C}\hat{P}|\pi^0\,\pi^+\pi^-\rangle_{l=0} = -|\pi^0\pi^+\pi^-\rangle_{l=0}.$$

For the case of K-mesons, only their linear combinations have a certain CP – parity:

$$\hat{C}|K^0\rangle = |\overline{K}^0\rangle; \hat{C}|\overline{K}^0\rangle = |K^0\rangle; \hat{P}|K^0\rangle = -|K^0\rangle;$$

Hence:

$\hat{C}\hat{P}(|K^0\rangle - |\bar{K}^0\rangle) = +(|K^0\rangle - |\bar{K}^0\rangle) \equiv +|K_1^0\rangle;\ \hat{C}\hat{P}(|K^0\rangle + |\bar{K}^0\rangle) = -(|K^0\rangle + |\bar{K}^0\rangle) \equiv -|K_2^0\rangle.$

K^0 -meson consists of two components: short-living $K_S^0$and long-living K_L^0. K_L^0 decays into three pions with mean lifetime $\tau(K_L^0) \cong 5 \cdot 10^{-8}$ s. K_S^0 decays into ttwo pions with mean lifetime $\tau(K_S^0) \cong 10^{-10}$ s.

CP violation and CPT symmetry.

Provided CP is conserved the decays $K_S^0 \to 2\pi$ mean that $K_S^0 = K_1^0$; the decays $K_L^0 \to 3\pi$ mean that $K_L^0 = K_2^0$. However, there is a small probability of the decay of the long-lived state of the K meson into 2 pions, which is a violation of CP parity:

$$\frac{\Gamma(K_L^0 \to 2\pi)}{\Gamma(K_L^0 \to \text{all})} \approx 2 \cdot 10^{-3}.$$

The relativistic field theory proves that the picture of the world obtained by successive reflection of the spatial axes (P), replacing a particle with an antiparticle (C) and reflecting the time axis (T) leads to a picture identical to the original state. This is the CPT theorem. Any Hamiltonian commutes with the product of CPT operators. The consequence is the equality of masses and lifetimes of particles and antiparticles.

8.2. Quarks

- In 1964, M.Gell-Mann proposed a model for describing all known hadrons as a set of the minimum number of more fundamental particles – quarks. Quarks have a fractional charge proportional to $\frac{1}{3}e$. Quarks are fermions – spin is equal to ½. Like leptons, quarks have three generations.

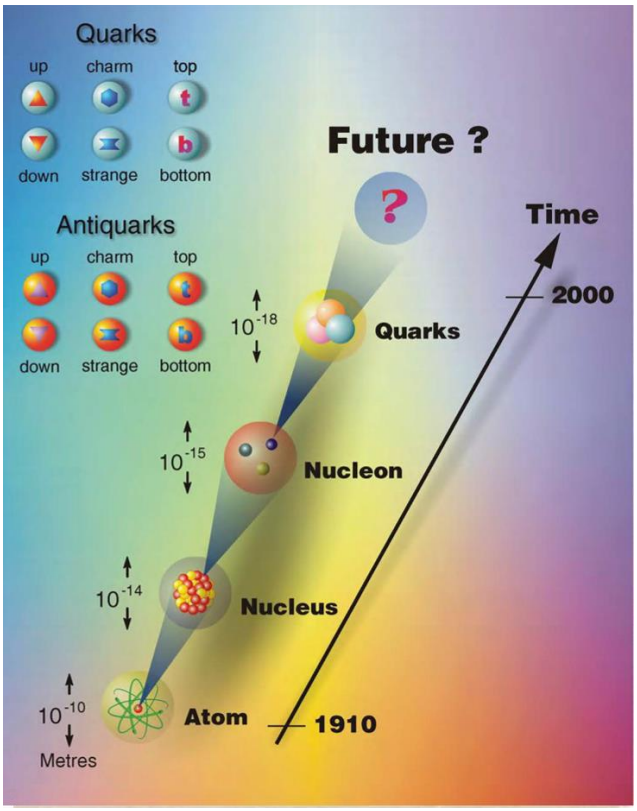

Quark flavor	Symbol	Mass, MeV/c^2	Spin	Charge	I Isospin	I_3 Isospin projection
Up	u	2.16(50)	$\frac{1}{2}$	$+\frac{2}{3}$	$\frac{1}{2}$	$+\frac{1}{2}$
Down	d	4.67(50)	$\frac{1}{2}$	$-\frac{1}{3}$	$\frac{1}{2}$	$-\frac{1}{2}$
Strange	s	93(11)	$\frac{1}{2}$	$-\frac{1}{3}$	0	0
Charm	c	1270(20)	$\frac{1}{2}$	$+\frac{2}{3}$	0	0
Bottom	b	4180(30)	$\frac{1}{2}$	$-\frac{1}{3}$	0	0
Top	t	172.76(30)·10^3	$\frac{1}{2}$	$+\frac{2}{3}$	0	0

The strange quark s is assigned a new additive quantum number - strangeness (S), equal to (-1) for the s-quark and (+1) for the s-antiquark. Strangeness persists in strong and electromagnetic interactions but does not persist in weak interactions.

8.3. Mesons

Nonet of Pseudoscalar Mesons (J=0).

The quark structure of mesons (L = 0) has the form $q_j\bar{q}_j$ (the subscript denotes the flavor of quarks). Spin-parity of mesons in the nonet is 0^{-}. Quark spins in nonet are antiparallel.

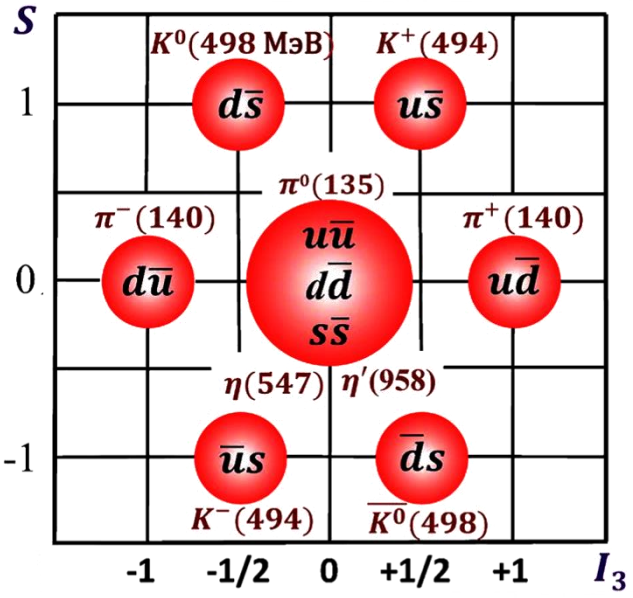

In the fig. above abscissa axes is third isospin projection; the ordinate is the strangeness of mesons; numbers in brackets near the symbols of mesons are their masses (MeV).

Mesons with zero isospin projection:

$\pi^0 = \frac{d\bar{d}-u\bar{u}}{\sqrt{2}}$; $\eta' = \frac{d\bar{d}+u\bar{u}-2s\bar{s}}{\sqrt{6}}$; $\eta_0 = \frac{d\bar{d}+u\bar{u}+s\bar{s}}{\sqrt{3}}$.

π^0 has isospin 1 and is included in the isospin triplet of pi-mesons.

η mesons have isospin 0 and hidden strangeness.

8.4. Baryons

a) *Octet of baryons* (*J*=1/2).

The quark structure of baryons has the form: $q_iq_jq_k$ In the fig. below: abscissa axis is a third isospin projection; the ordinate axis is strangeness; numbers near baryons is their mass (MeV).

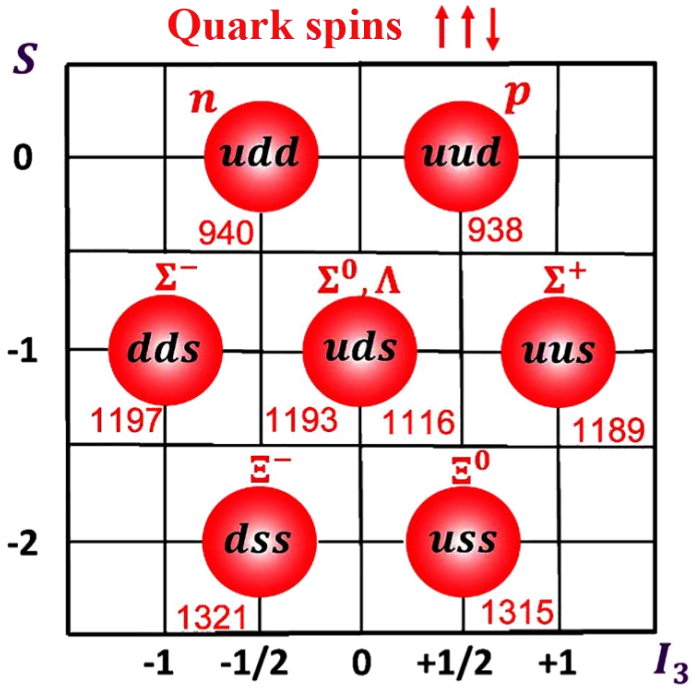

Baryons containing strange (s) quarks are called hyperons. In the octet under consideration, hyperons are all particles, except for the proton and neutron. Σ^0 and Λ hyperons have the same strangeness and third isospin projection, but different isospin values. Σ hyperon enters into an isospin triplet (together with Σ^- and Σ^+) with isospin 1, Λ enters into an isospin singlet with isospin 0.

Quark structure of proton and neutron (arrows mean direction of spin):

$$p\left(J_Z = \frac{1}{2}\right) = \sqrt{\frac{2}{3}}|u\uparrow u\uparrow d\downarrow\rangle - \frac{1}{\sqrt{3}}|u\uparrow u\downarrow d\uparrow\rangle;$$

$$n\left(J_Z = \frac{1}{2}\right) = \sqrt{\frac{2}{3}}|d\uparrow d\uparrow u\downarrow\rangle - \frac{1}{\sqrt{3}}|d\uparrow d\downarrow u\uparrow\rangle.$$

b) *Decuplet of baryons* (*J*=3/2).

In the decuplet of baryons (J = 3/2), the spins of all quarks are directed in the same direction. There are states with quark structure that are not in the octet: states of three *u* or *d* quarks (I = 3/2, delta resonances) and three *s* quarks (I = 0, omega minus hyperon).

$\Delta^{++}(j_z = 3/2) = |u\uparrow u\uparrow u\uparrow\rangle$; $\Omega^{-}(j_z = 3/2) = |s\uparrow s\uparrow s\uparrow\rangle$.

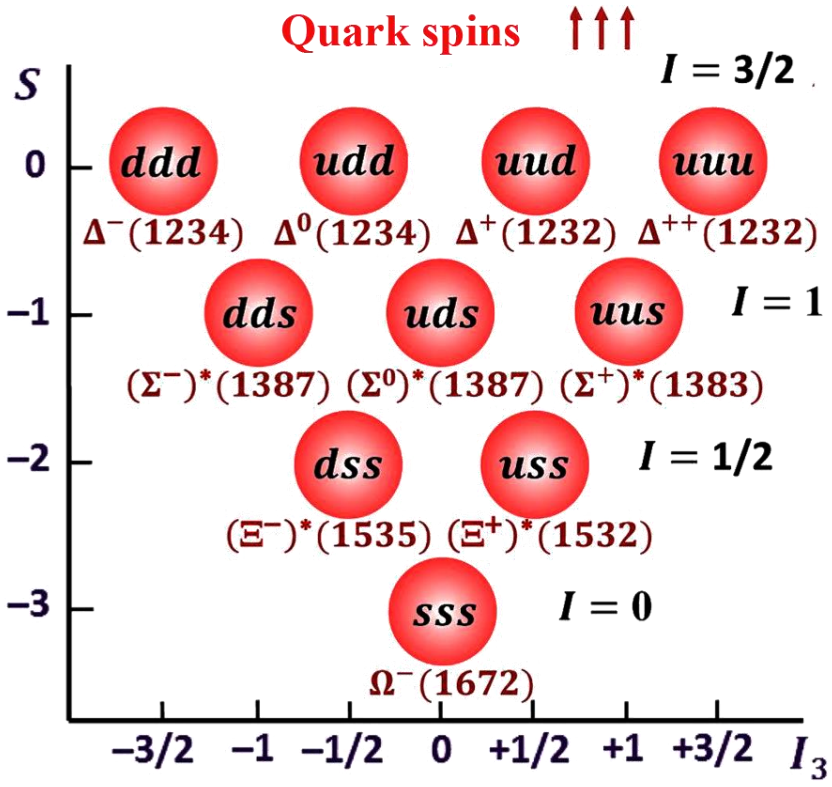

Pauli's principle forbids three fermions (quarks) to be in the same state.

Conclusion: either quarks are distributed over different levels, or there is a new quantum number that makes it possible to distinguish quarks with the same flavors and spins.

8.5. Masses and quark composition of hadrons

The data on hadrons (mesons and baryons) are given in the table below.

The first 6 particles in the table are mesons. Other –baryons.

The decay of π^+ and K^+ mesons into leptons shows that quarks can decay into leptons. Long lifetime means that decay occurs due to weak interaction. Short lifetime of π^0 meson, hence decay occurs due to electromagnetic interaction. Decays of the K^+ -meson, Ω^- and Λ^-hyperons do not conserve strangeness, it leads to long mean lifetime, decay is caused by weak interaction.

Particle	Mass	Lifetime (s)	Major decays
$\pi^+(u\bar{d})$	140	$2.6 \cdot 10^{-8}$	$\mu^+\nu_\mu$ (~100%)
$\pi^0(u\bar{u}, d\bar{d})$,	135	$8.4 \cdot 10^{-17}$	$\gamma\gamma$ (~100%)
$K^+(u\bar{s})$	494	$1.2 \cdot 10^{-8}$	$\mu^+\nu_\mu$ (64%) $\pi^+\pi^0$ (21%)
$K^{*+}(u\bar{s})$	892	$\sim 1.3 \cdot 10^{-23}$	$K^+\pi^0$, $K^\circ\pi^+$ (~100%)
$D^-(d\bar{c})$	1869	$1.0 \cdot 10^{-12}$	Several seen
$B^-(b\bar{u})$	5278	$1.6 \cdot 10^{-12}$	Several seen
p(uud)	938	Stable	None
n(udd)	940	879	$pe^-\bar{\nu}_e$ (100%)
Λ(uds)	1116	$2.6 \cdot 10^{-10}$	$p\pi^-$~ (64%), $n\pi^0$ (36%)
Δ^{++}(uuu)	1232	$\sim 0.6 \cdot 10^{-23}$	$p\pi^+$ (100%)
Ω^-(sss)	1672	$0.8 \cdot 10^{-10}$	ΛK^- (68%) $\Xi^\circ\pi^-$ (24%)
Λ_c^+(udc)	2285	$2.0 \cdot 10^{-13}$	Several seen

8.6. Color charge

a) Quark color.

Color is a new quantum number that allows placing up to three quarks with matching flavors and spin projections at the lower energy level without contradicting the Pauli principle for fermions. Hadrons are built from quarks of different colors and have no colors (colorless):

$$\Omega^-(J_z = 3/2) = |s\uparrow s\uparrow s\uparrow\rangle;$$

$$\Delta^{++}(J_z = 3/2) = |u\uparrow u\uparrow u\uparrow\rangle$$

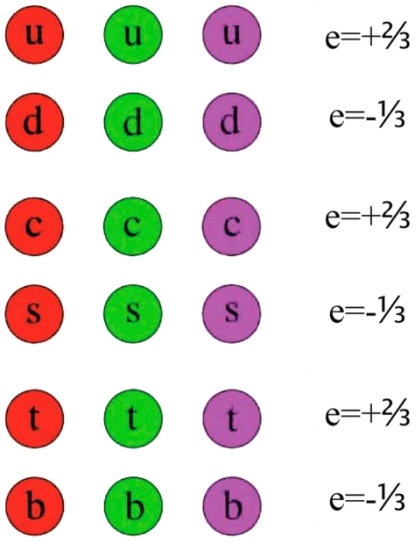

Quark structure of proton is given by expression:

$$p\left(J_Z = \frac{1}{2}\right) =$$

$$= \sqrt{\frac{1}{18}}[2|u\uparrow u\uparrow d\downarrow\rangle + 2|u\uparrow d\downarrow u\uparrow\rangle + 2|d\downarrow u\uparrow u\uparrow\rangle - |u\uparrow u\downarrow d\uparrow\rangle - |u\downarrow u\uparrow d\uparrow\rangle$$

$$- |u\uparrow d\uparrow u\downarrow\rangle - |u\downarrow d\uparrow u\uparrow\rangle - |d\uparrow u\uparrow u\downarrow\rangle - |d\uparrow u\downarrow u\uparrow\rangle]$$

b) Experimental confirmation of quark color.

Annihilation of e^+ e^- pairs into hadrons at high energies $(E = \sqrt{s})$ $e^+ + e^- \to q + \bar{q} \to$ hadrons

$$R(s) = \frac{\sigma(e^+e^- \to \text{hadrons})}{\sigma(e^+e^- \to \mu^+\mu^-)} \sim 3 \sum_i e_i^2,$$

Where 3 corresponds to the number of colors and summation is performed over flavors.

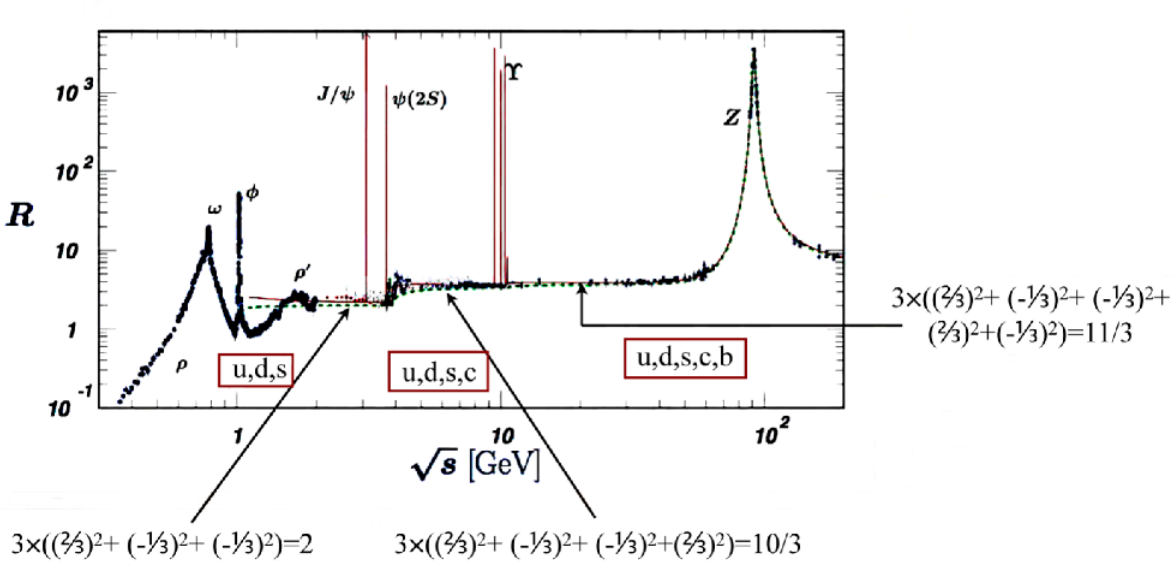

8.7. Gluons. Quantum chromodynamics

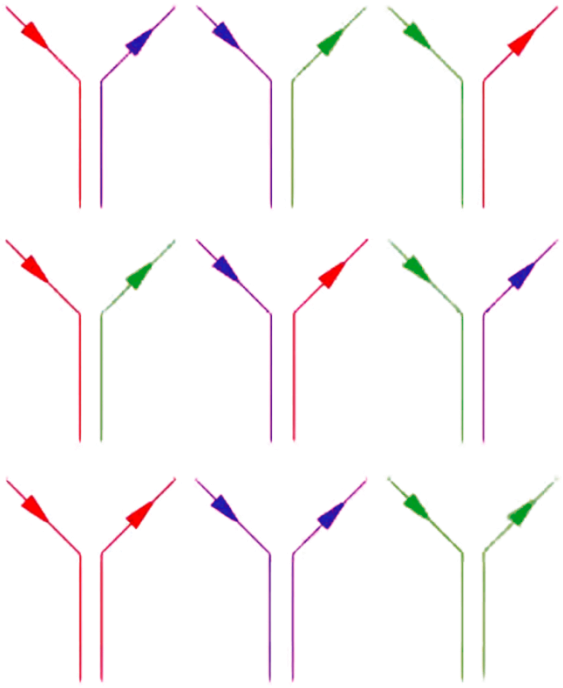

Color is a new type of charge ("color");

Gluons are vector massless bosons, carriers of interactions between color charges;

There are 8 ways to transfer the color of quarks –8 types of gluons (3x3-1 = 8).

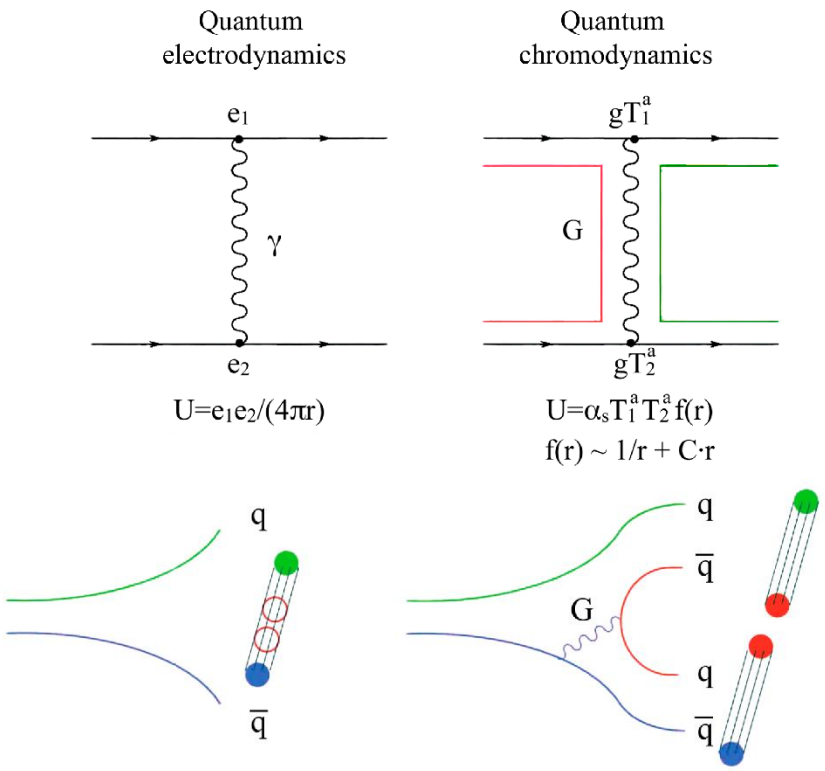

When quarks fly apart over large distances, the “string” that connects the quarks “breaks”, and a new pair is formed at the place of the break — a quark — antiquark.

In quantum chromodynamics, with increasing distance, the color charge does not decrease, but increases – asymptotic freedom.

8.8. Excited states of nucleons and charmonium

a) Nucleon.

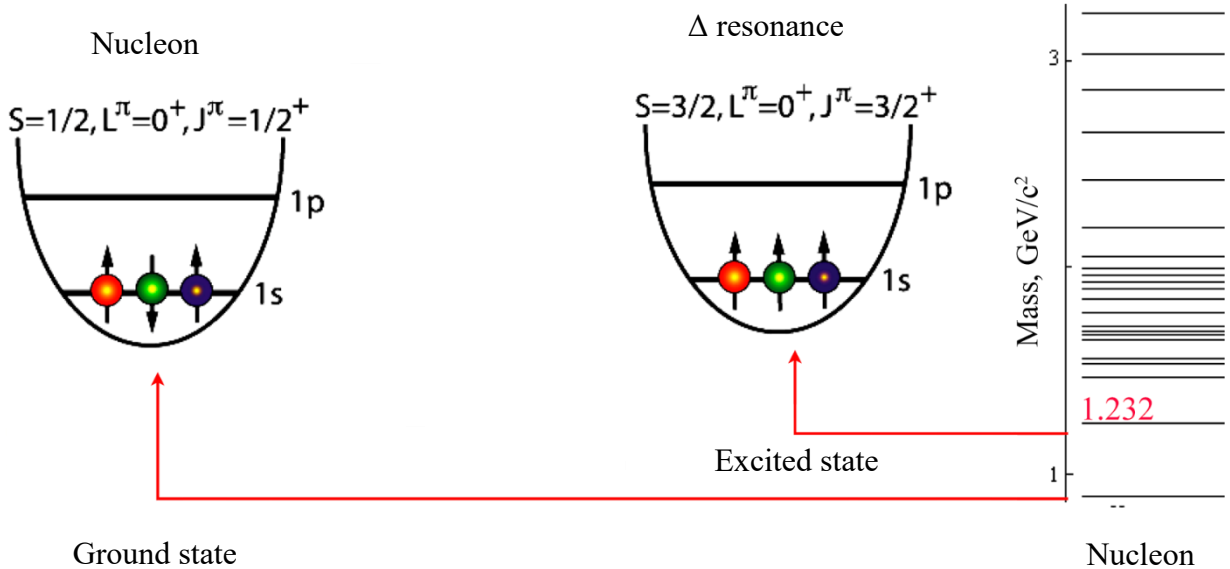

b) Charmonium $\bar{c}c$.

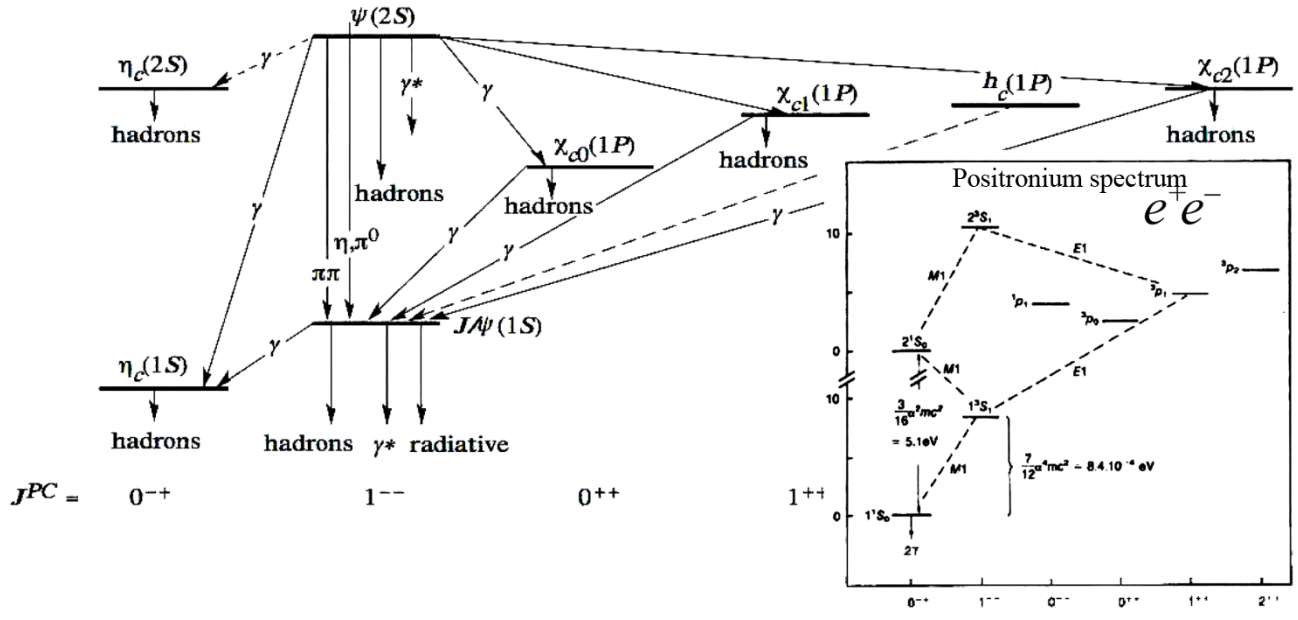

The first discovered bound state of the pair $c\bar{c}$ (charmonium) – particle J/ψ (1974).

The figure shows a part of the discovered states of charmonium, each of which has its own name. The states differ in spin J, spatial parity P, and charge parity C. In parentheses, states S, P have the orbital angular momentum of relative motion L = 0, 1, respectively. The spectrum of charmonium resembles the spectrum of the positronium atom.

The charmonium spectrum can be used to determine the interaction potential $c\bar{c}$.

At small distances, the potential behaves like 1/r, and at large distances (> 10^{-13} cm) as:

$$V(r) = -\frac{4}{3}\cdot\frac{\alpha}{r} + \frac{r}{\beta^2} + \delta.$$

8.9. Pion exchange between nucleons

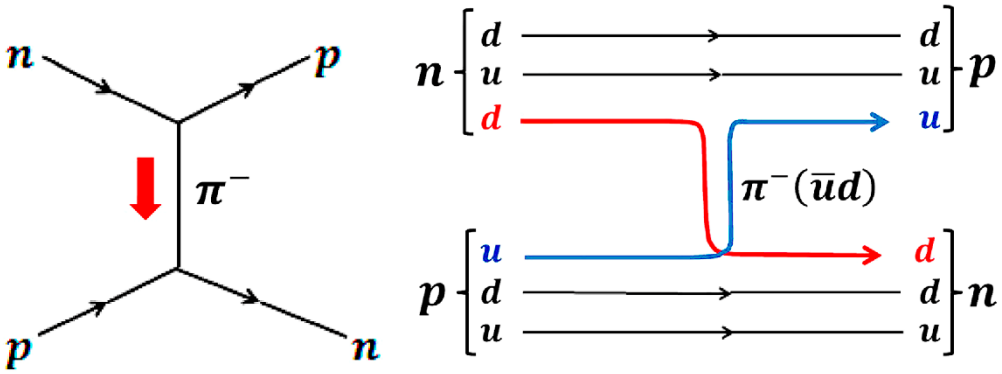

8.10. Weak interaction. *W* and *Z* bosons

W and Z bosons are carriers of weak interaction (intermediate bosons). $S_W = S_Z = 1$

Z^0 mass is 91.2 GeV, W^+ and W^- mass is 80.4 GeV.

Main decay modes:

$W^+ \to e^+\nu_e$, $W^+ \to \mu^+\nu_\mu$;

$Z^0 \to e^+e^-$, $Z^0 \to \mu^+\,\mu^-$.

Discovery of Z^0 (resonance in e^+e^- reaction) is shown in the fig.

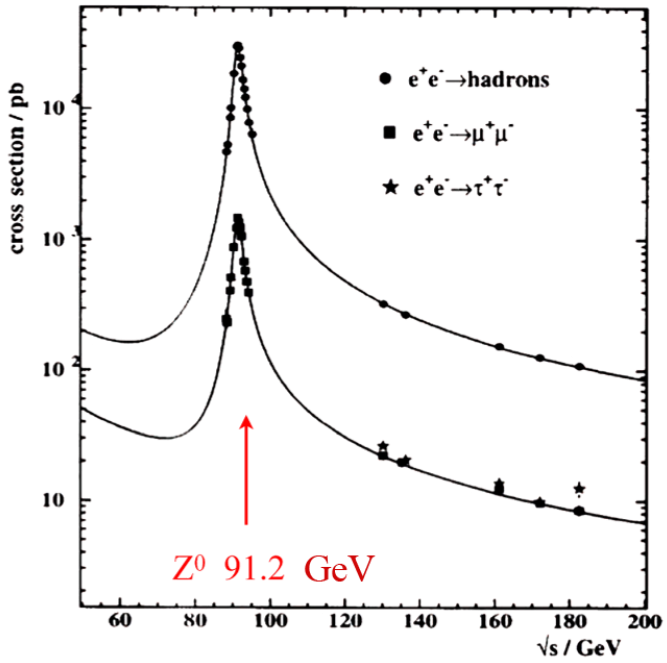

In the process of interaction, a virtual boson is emitted with its subsequent decay or absorption. Due to the large mass of the W and Z^0 bosons, the radius of the weak interaction is small:

$$r_W = \frac{\hbar}{mc} \sim 0.2 \text{ фм}$$

Example: decay of neutron.

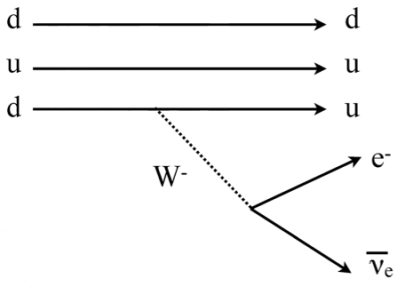

Leptons and quarks participate in weak interactions. In weak decay of quarks with the participation of W bosons, isospin, strangeness, quantum numbers of beauty (b), charm (c) and truthfulness (t) may not be preserved.

The figure shows the processes of virtual decay of quarks (the process develops from bottom to top) with violation of strangeness (a), charm (b) and beauty (c).

Decay of W bosons occurs both into lepton-antilepton and quark-antiquark pairs.

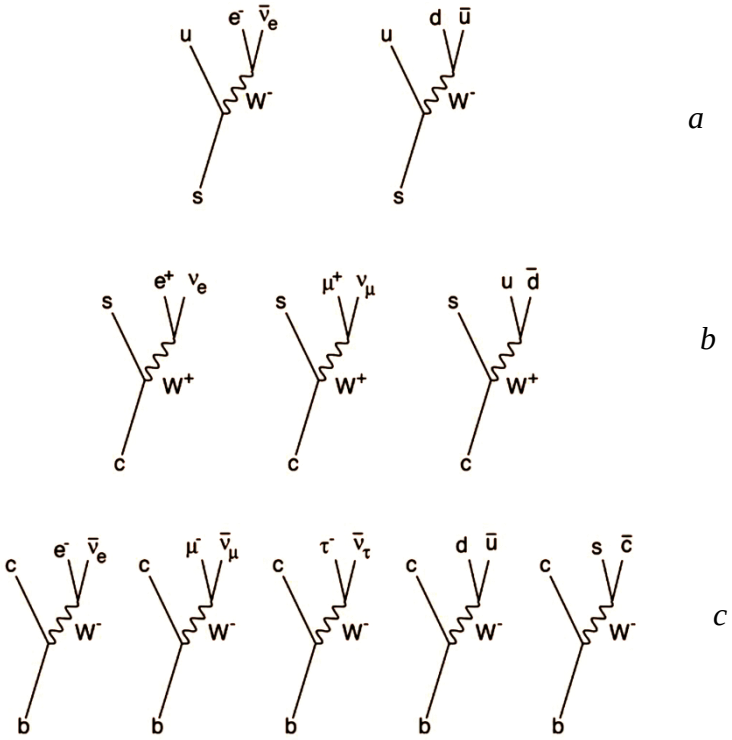

Unlike W bosons, Z^0 do not carry charge (neutral weak currents). Z bosons are one of the reasons for the inelastic scattering of neutrinos by electrons, leading to the ionization of atoms.

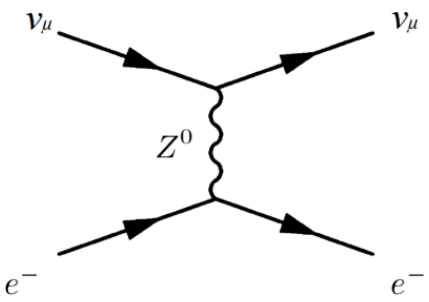

8.11. Spontaneous symmetry breaking

- Gauge theories require the existence of massless vector bosons;
- the theory is not applicable to weak interactions (massive Z and W bosons);
- The theory without gauge invariance leads to irreparable divergences.

Solution: spontaneous symmetry breaking.

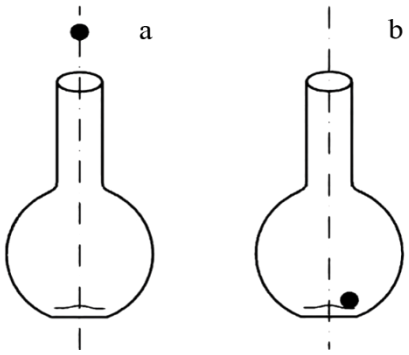

Example of spontaneous symmetry breaking: the Hamiltonian remains completely symmetric, but the ground state breaks symmetry (hidden symmetry).

Hidden symmetry can lead to massive particles.

8.12. Higgs mechanism of mass generation

Consider complex scalar fields (Higgs fields) φ and φ*, requiring scalar mesons H^+ and H^-. We represent them by a combination of real fields φ_1 and φ_2.

$$\phi = \frac{1}{\sqrt{2}}(\phi_1 + i\phi_2);\ \phi^* = \frac{1}{\sqrt{2}}(\phi_1 - i\phi_2).$$

Let the masses of the field quanta be zero, but the motion occurs in a potential of the form:

$$V = -\lambda^2\phi^*\phi + \eta^2\phi^*\phi^2.$$

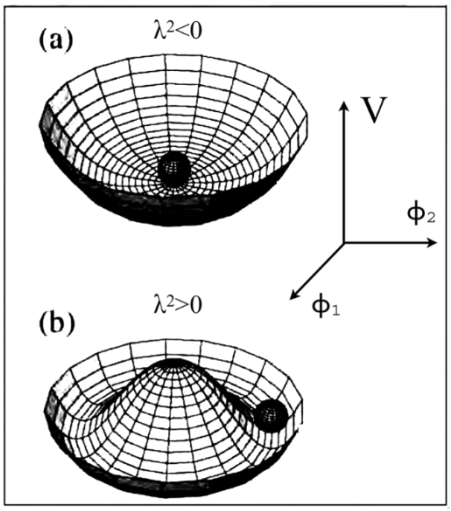

Klein-Fock-Gordon equation:

$$\left[\frac{1}{c^2}\frac{\partial^2}{\partial t^2} - \nabla^2 - \lambda^2 + 2\eta^2(\phi^*\phi)\right]\phi = 0$$

Keeping only linear terms ($\lambda^2 = -u^2$):

$$\left[\frac{1}{c^2}\frac{\partial^2}{\partial t^2} - \nabla^2 + u^2\right]\phi = 0.$$

The condition of the minimum kinetic energy takes place for the case:

$$|\phi_{\min}| = \sqrt{\frac{\lambda^2}{2\eta^2}} = \frac{v}{\sqrt{2}}.$$

Let us choose for the case of the ground state: $\phi = \phi^* = \frac{v}{\sqrt{2}}$.

For small perturbations, we can write (introducing new fields R and Θ):

$$\phi = \frac{1}{\sqrt{2}}(v + R)e^{i\Theta/v} \approx \frac{1}{\sqrt{2}}(v + R + i\Theta);$$

$$\phi^* = \frac{1}{\sqrt{2}}(v + R)e^{-i\Theta/v} \approx \frac{1}{\sqrt{2}}(v + R - i\Theta).$$

Substituting this into the Klein-Fock-Gordon equation:

$$\left[\frac{1}{c^2}\frac{\partial^2}{\partial t^2} - \nabla^2 + 2\lambda^2\right] R(x,t) = 0; \qquad \left[\frac{1}{c^2}\frac{\partial^2}{\partial t^2} - \nabla^2\right] \Theta(x,t) = 0$$

The mass term appears: $m = \frac{\sqrt{2}\lambda\hbar}{c}$

Illustration of Higgs mechanism:

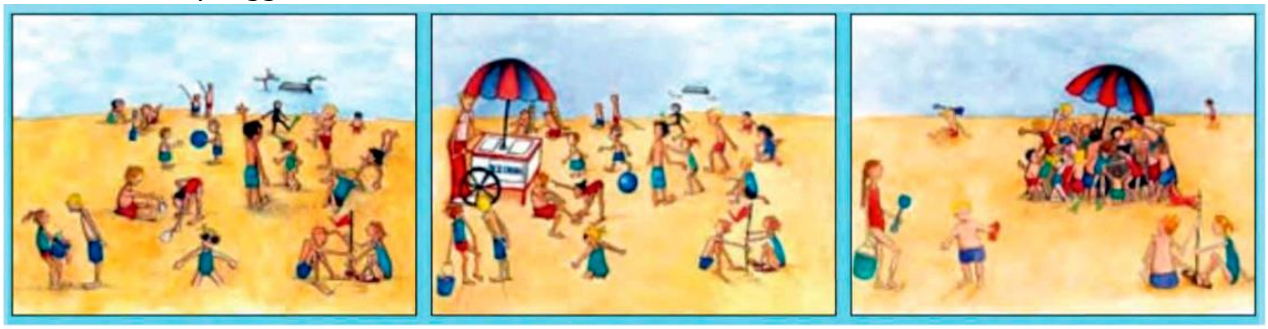

Empty space (beach full of children).

Particle is crossing an area of space (ice cream vendor).

The particle gains mass (children surround the cart and slow down its movement).

At a temperature T »10^{15} K, the Higgs fields exist in the form of individual elementary particles. At T ~ 10^{15} K, a phase transition occurs, and the fields "condense" (a "new vacuum" appears). Due to the violation of symmetry, the field splits into components - a massive spinless particle and a massless particle, which are absorbed by the particles carriers of weak interaction (Z and W bosons), as well as quarks, thus acquiring mass. The photon remains massless.

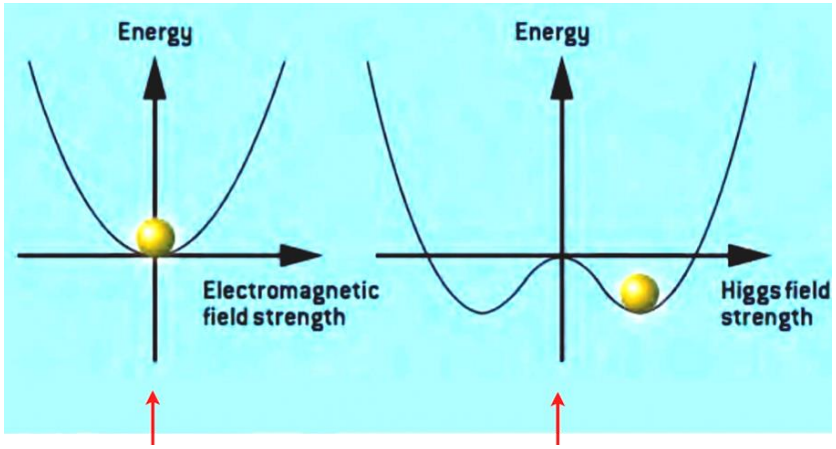

The energy of ordinary (electromagnetic) fields is minimal at zero strength.

Higgs field energy is smallest at nonzero field strength

8.13. Standard model fundamental particles

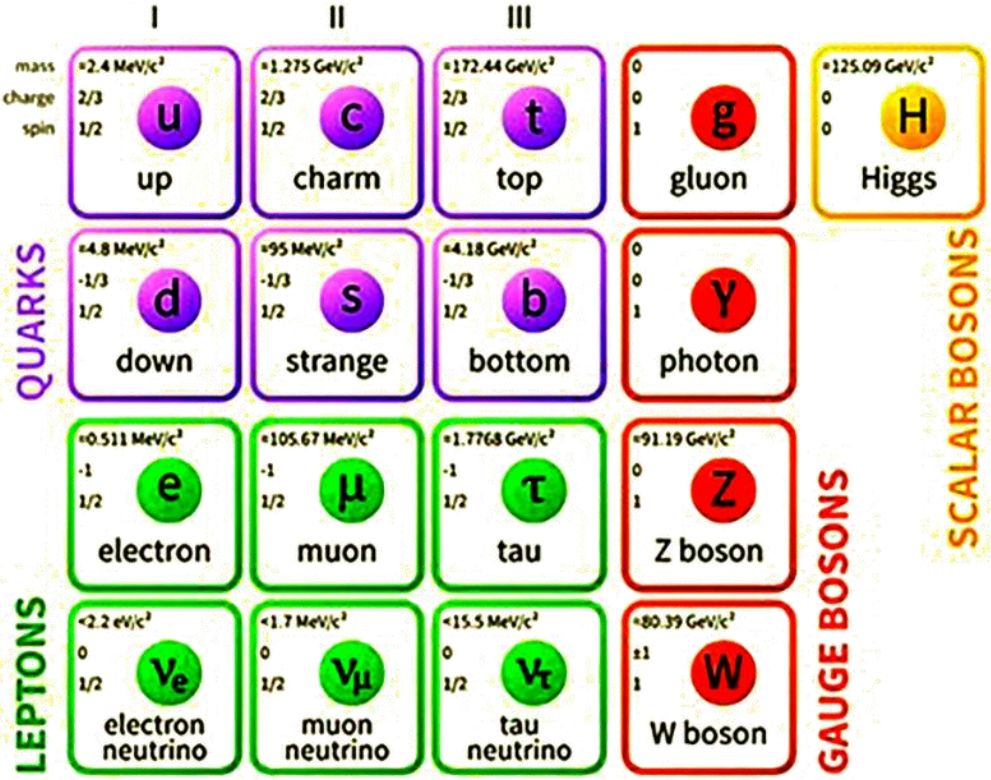

CONCLUSION

This textbook gives overview of nuclear physics in unity with the history of mankind, the fate of culture and specific scientists. The development of nuclear physics, which took place in the 20th century, was accompanied by two world wars, that left an indelible mark on the lives of scientists. Perhaps not a single era and not a single science could so sharply raise the question of the choice of the moral position of the scientist and his responsibility for the results of the research. And this is perhaps the main lesson of the past century.

What's next? Has the creation of the Standard Model of elementary particles really completed the construction of the physical picture of the world, and there is only an in-depth development of particular questions and the search for a practical application of the knowledge gained? This is most likely not the case. In essence, we are returning to the state that was at the beginning of the twentieth century, when Baron Kelvin, in his speech, marked some clouds over the then almost complete physical picture of the world. There are similar clouds now. Their source is astronomical data. According to these data, associated with observations of the motion of galaxies, there is invisible (or, as it is called, dark) matter in the Universe, which manifests itself only through gravitational forces. So far, one can only guess about the nature of such matter. There are extensions to the Standard Model, including new types of elementary particles, which could be the building blocks of the substance of dark matter, but so far such particles have not been experimentally detected. Moreover, observation of the radiation from distant galaxies shows that the Universe is expanding faster and faster, which can be explained by the presence in the world around us of the hidden energy of incredible force (it is called dark energy). The total energy of the processes, the laws of which we have studied, is only a few percent of the total energy of the Universe, about which we cannot say anything. Only now it becomes clear how incomplete our knowledge is and what an abyss of the unknown is before us. Most likely, humanity, without even knowing it, is on the threshold of a new scientific and technological revolution, and these revolutions are to be accomplished by the current generation of scientists.

PROBLEMS

1. Estimate the energy released in the induced fission reaction:
   $n + {}^{235}U \rightarrow {}^{95}Sr + {}^{139}Xe + 2n$
   The kinetic energies of neutrons causing fission of ^{235}U are considered thermal.
2. Determine the excitation energy of a compound nucleus formed during the capture of α-particles with energy $T_\alpha = 7$ MeV by a stationary nucleus of ^{10}B.
3. Determine the upper limit of the age of the Earth, assuming that everything on earth ^{40}Ar was formed from ^{40}K as a result of e-capture. Currently, for every 300 atoms ^{40}Ar accounts for one ^{40}K atom.
4. The mass of neutral ^{16}O atom is 15.9949 a.m.u. (1 a.m.u. = 931.5 MeV). Determine the ^{16}O binding energy per nucleon.
5. What is the maximum kinetic energy of a neutron (in a center of mass system) at which the differential cross section of neutron scattering is isotropic?

LITERATURE

1. B. R. Martin. Nuclear and Particle Physics. Chichester: John Wiley & Sons, Ltd., 2006.- 411 p. ISBN 978-0-470-01999-3.

2. A. Obertelli, H. Sagawa. Modern Nuclear Physics: From Fundamentals to Frontiers. Springer, 2021. – 711 p. ISBN 978-9-811-62288-5.

3. J.-L. Basdevant, J. Rich. Fundamentals in Nuclear Physics: From Nuclear Structure to Cosmology. Springer, 2010.– 532 p. ISBN 978-1-441-91849-9.

4. B. Milner. Nuclear and Particle Physics. Cambridge University Press, 2001. ISBN 978-0-521-79837-2.

5. W. N. Cottingham, D. A. Greenwood. An Introduction to Nuclear Physics. Cambridge University Press, 2001. Online ISBN:9781139164405.

6. A. Das, T. Ferbel. Introduction to Nuclear and Particle Physics. World Scientific Publishing, 2004. – 401 p. ISBN 981-238-744-7.